Journal of the
OPTICAL SOCIETY *of* AMERICA

VOLUME 29 FEBRUARY, 1939 NUMBER 2

X-Ray Photography by Means of Fluorescence X-Radiation

ELMER DERSHEM
Ryerson Physical Laboratory, University of Chicago, Chicago, Illinois
(Received November 11, 1938)

TO show structural detail in very thin objects it is necessary to use soft x-rays. If these x-rays are, in addition, of such wave-length that they are selectively absorbed by one of the elements in the object, the pattern on which particles of this element are placed will be more clearly revealed. The simplest way to secure a beam of x-rays whose wave-lengths are confined to a narrow region is to radiate an element with x-rays of a frequency somewhat higher than the critical absorption frequency of this element. The latter will then emit, almost exclusively, its own characteristic *K* radiation.

A camera was designed and constructed to utilize these principles in the x-ray photography of microtome sections of bone with special reference to the calcium deposits. In Fig. 1, Parts *A* and *B* show two sections of the camera at right angles to each other. The x-rays from any available tube pass through the thin aluminum windows *W* and through the radiator *R*. The fluorescence radiation from the latter passes downward through the specimen to the photographic plate. By releasing the screw with the knurled head *H* and swinging the yoke bearing it to one side, the lower end block carrying the specimen and photographic plate may be removed. The camera may be loaded in a dark room and then supported on a laboratory stand in the proper position before an x-ray tube. Since these very soft x-rays are much absorbed by passage through air the camera should be evacuated with a mechanical oil pump. The outlet tube to the pump is permanently connected to the latter by a rubber hose but may be quickly attached to or detached from the camera

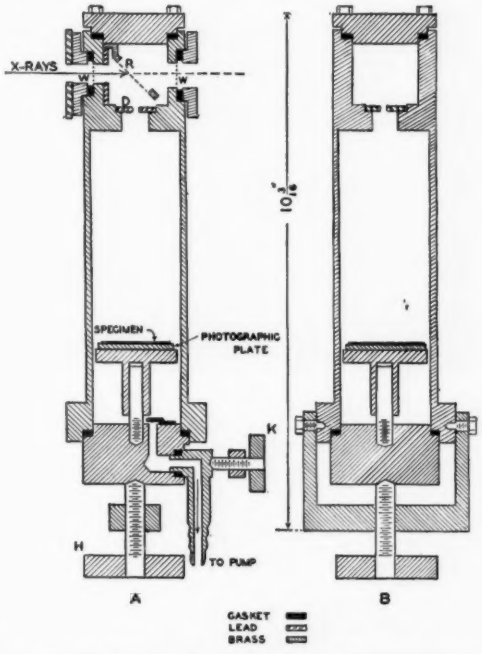

FIG. 1. Cross-sectional drawings of fluorescence x-ray camera.

BOSTON UNIVERSITY
COLLEGE OF LIBERAL ARTS
LIBRARY

to which it is sealed with a few turns of the screw marked *K*.

The *K* absorption limit of calcium is at 3.06A while the weighted average wave-length of the *K* emission lines of scandium is 3.02A. Hence scandium is used as a radiator for optimum absorption by calcium. The radiator was made of thin onion skin paper to which a thin layer of scandium oxide was attached on the side nearest the photographic plate by mixing it with a cement consisting of a thin solution of celluloid dissolved in amyl acetate and acetone.

Figure 2 shows the results obtained with a microtome section, 0.01 mm thick, of the leg bones of a young rat. The exposure time was 40 min. with an x-ray tube current of 10 milliamperes at 40 kv. Better results could probably have been secured with a low voltage tube designed for this purpose, since with high voltage the radiation scattered from the radiator is more penetrating and tends to mask the effects of the longer wave-lengths characteristic of the radiator.

FIG. 2. Microtome section of leg bones of a young rat. Photographed with scandium fluorescence x-radiation.

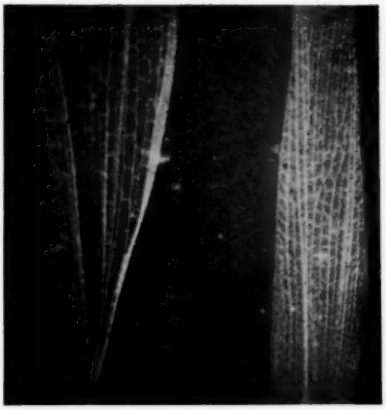

FIG. 3. Grasshopper wings. Photographed with sulphur fluorescence x-radiation.

The same methods may be made to reveal the presence of particles of other elements in thin sections. It may also be used to secure x-rays of varying degrees of softness by a proper choice of radiator.

Figure 3 is an x-ray photograph of the wings of a grasshopper using sulphur as a radiator. The principal line of sulphur radiation has a wave-length of 5.36A. Scandium radiation was found to be entirely too hard for such a thin specimen while that from magnesium, whose principal line is at 9.86A, was found to be too soft.

The microtome section was supplied by Dr. Franklin C. McLean of the Department of Physiology to whom the writer is also deeply indebted for the construction of the camera in the Physiology Department shop.

Laboratory Analysis of the Selective Absorption of Light by Sea Water*

GEORGE L. CLARKE, *Harvard University, Cambridge, Massachusetts*

AND

HARRY R. JAMES, *Hastings College, Hastings, Nebraska*

(Received November 25, 1938)

PRECISE laboratory measurements of the absorption of light by distilled water and by samples of water from a large number of Wisconsin lakes have been carried out by James and Birge[1] (1938) using a tube one meter long and a highly sensitive monochromator covering wavelengths 3650–8000A. Opportunity to make use of the same instrument for similar measurements on samples of sea water presented itself during the summer of 1938 as a part of the limnological program of the Wisconsin Geological and Natural History Survey. The authors are indebted to Dr. E. A. Birge and Dr. C. Juday for creating this opportunity and for their help and valuable suggestions throughout the undertaking.†

The purpose of the present investigation was to establish the general form of the absorption curves for specimens of sea water from various typical areas of the ocean and to analyze the different effects of dissolved and suspended material in the waters of the several regions. In the only previous laboratory measurements of sea water, namely those of Hulburt,[2,3] which were limited to samples from off-shore, and those of Sawyer,[4] which involved coastal water only, an analysis of the sort contemplated was not undertaken. Furthermore, we proposed to compare our absorption values with measurements of light penetration made by lowering a photometer into the water at the same time and place at which our samples were taken. In neither of the former investigations were comparisons made with contemporaneous field measurements.

A special objective in this investigation was to ascertain in what particulars "pure" sea water differs from distilled water in its optical properties. It was proposed to attack this problem by obtaining sea water from the open ocean and removing the particulate matter by passing it through a Berkefeld filter. We define such water as "pure" sea water. The absorption of this water in every part of the spectrum within the range of our instrument may be compared with distilled water. Information would thus be gained as to whether the salts in solution or any other filter-passing material exert an appreciable effect on the general transparency, and particularly whether they have any selective action on light.

A further important object of the present undertaking was to determine to what degree the differences in transparency of various ocean waters are caused by "suspensoids" and to what extent to filter-passing material. Suspensoids are defined as all particulate matter which is removed from the water by a "fine" Berkefeld filter (following James and Birge), and filter-passing material (termed "color" by James and Birge) includes substances in true solution as well as suspended matter too fine to be retained by the filter. This point could be settled by obtaining samples from areas differing sharply in transparency, Berkefeld filtering the water, and then comparing the absorption measurements of the filtrates. Another respect in which oceanic areas differ is in the part of the spectrum to which they are most transparent.[5] The question has always existed as to whether this

---

* From the Woods Hole Oceanographic Institution, Contribution No. 193. From the Limnological Laboratory of the Wisconsin Geological and Natural History Survey. Notes and Reports No. 88.

[1] H. R. James and E. A. Birge, "A Laboratory Study of the Absorption of Light by Lake Waters," Trans. Wis. Acad. of Sci. **31**, 1–154 (1938).

† This investigation was supported by grants from the Wisconsin Alumni Research Foundation, the Brittingham Trust Fund, and the Woods Hole Oceanographic Institution. The authors also wish to acknowledge the assistance of Mr. Dean F. Bumpus in the collection of water samples and the field measurements of light penetration.

[2] E. O. Hulburt, "The Transparency of Ocean Water and the Visibility Curve of the Eye," J. Opt. Soc. Am. and Rev. Sci. Inst. **13**, 553–556 (1926).

[3] E. O. Hulburt, "The Penetration of Ultraviolet Light into Pure Water and Sea Water," J. Opt. Soc. Am. and Rev. Sci. Inst. **17**, 15–22 (1928).

[4] W. R. Sawyer, "The Spectral Absorption of Light by Pure Water and Bay of Fundy Water," Conts. Can. Biol. and Fisheries, n. s. **7**, No. 8, 75–89 (1931).

[5] R. H. Oster and G. L. Clarke, "The Penetration of the Red, Green and Violet Components of Daylight into Atlantic Waters," J. Opt. Soc. Am. **25**, 84–91 (1935).

TABLE I. *Locations from which water samples were obtained.*

SAMPLE NUMBER	STATION NUMBER	LOCATION	LATITUDE	LONGITUDE	DATE COLLECTED 1938	TREATMENT OF WATER AT TIME OF COLLECTION*	LIGHT PENETRATION MEASUREMENT SERIES NO.
1	5	Buzzards Bay‡	41°33′N.	70°42′25″W.	June 22	Unfiltered	(325)†
2	4	Vineyard Sound§	41°30′	70°36′	June 22	Unfiltered	(322)†
3	3	V. S. Whistle Buoy‖	40°17′30″	71°00′	June 25	Unfiltered	
4	3	V. S. Whistle Buoy‖	40°17′30″	71°00′	June 25	Unfiltered	
5	C	Sargasso Sea	35°05′	67°06′	July 10	Unfiltered	473
6	C	Sargasso Sea	35°05′	67°06′	July 10	Unfiltered	
7	B	Continental Slope	39°20′	70°33′	July 14	Unfiltered	476
8	B	Continental Slope	39°20′	70°33′	July 14	Paper filtered	
9	A	Continental Shelf	40°38′	71°38′	July 17	Unfiltered	478
10	A	Continental Shelf	40°38′	71°38′	July 17	Paper filtered	
11	3	V. S. Whistle Buoy¶	40°17′30″	71°00′	July 29	Unfiltered	480
12	3	V. S. Whistle Buoy¶	40°17′30″	71°00′	July 29	Berkefeld filtered	

* 10 cc of $HgCl_2$ was added to each carboy at the time of collection.
† Measurements made four years previous.
‡ Tide in Woods Hole running west.
§ Tide off West Chop running west.
‖ Tide off Gay Head had run west for one hour.
¶ Tide off Gay Head running east.

difference is caused entirely by selective scattering by suspensoids or whether filter-passing material may be effective. That part of the selective absorption due to filter-passing material (other than pure water) will be designated as "color." Many lakes have color in this sense and we wished to learn if the same was true of any samples of sea water. If any such color effect were found in sea water, one would expect it to be slight, since no specimens of sea water appear colored to the naked eye as water samples from lakes often do.

COLLECTION OF WATER SAMPLES

The locations from which water samples were collected (see Table I)* were chosen so as to cover the entire range of transparencies found in the ocean and at the same time to test water masses which are typical of large portions of the sea. At the four most important stations complete series of measurements of the penetration of daylight were made with a submarine photometer at the same time that the water samples were collected. At the other two locations simultaneous field measurements could not be arranged, but the characteristic transparency of the water at these points is known from earlier observations.

The water was dipped up from the surface in all cases and poured into five-gallon glass carboys. For samples one to ten inclusive, a galvanized bucket and tin funnel were used, but a wooden bucket and glass funnel were employed in the collection of samples 11 and 12. To all samples which were left unfiltered at the time of collection 10 cc $HgCl_2$ per carboy were added immediately. This was necessary in order to prevent bacterial action which otherwise would cause significant changes in transparency within a few hours. Samples 8 and 10 were passed through a paper filter as soon as collected and the preservative added immediately afterwards. The carboy containing the freshly collected sample 12 was placed in the ice box on board ship during the three-hour run to the laboratory. The sample was then passed through a specially prepared "fine" Berkefeld filter† and thence directly into another carboy to which the preservative was added. All carboys were landed at Woods Hole and shipped to the University of Wisconsin where the monochromator was in operation.

* The location of Stations 3, 4 and 5 is shown on the map of Fig. 1, reference 6.
[6] G. L. Clarke, "Seasonal Changes in the Intensity of Submarine Illumination off Woods Hole," Ecology **19**, 89–106 (1938).

† A slightly used Berkefeld filter of "fine" porosity was prepared as follows: 5 liters of 10 percent $HgCl_2$ were run through the filter. Then the candle was removed and boiled in 10 percent $NaHCO_3$. The filter was thoroughly rinsed by passing a carboy of distilled water through it. The candle was then dried and the base dipped in paraffin until all metal parts were thoroughly coated inside and out. The apparatus was arranged in such a way that in leaving the filter the water came in contact with nothing but glass. Dust was excluded from the air stream by means of cotton plugs.

Laboratory Measurements of Absorption

A. Procedure

The arrangement of the apparatus‡ and the procedure in the absorption measurements were the same as those described by James and Birge[1] with the exception of the method of lining the brass tube in which the samples were placed. The silver lining used for certain of the measurements of distilled water was obviously out of the question for sea water. For all of the present measurements the inside of the tube was blackened by treatment with ammoniacal copper carbonate and three different materials were tried for a lining coat. The first of these was paraffin, which had been used in the case of the measurements of lake water. On several occasions the absorption of samples of sea water was found to increase at the blue end of the spectrum as it stood in the tube. The same situation was encountered when the tube was lined with glyptal resin. With a lining of ceresin wax, however, no measurable change in the absorption was found to occur even after the water had stood in the tube over night. But as a precaution our tests were always run immediately after placing the water in the tube, beginning with wave-length 3650A. The measurement at 3650A was repeated at the end of the series.

During the time which had elapsed between the collection of the water and the laboratory measurements particulate matter had settled to the bottom of the carboys. It was obvious that since this material had been in suspension in the water when the field observations were made, its effect on absorption should be included in comparing the laboratory measurements with those made at sea. Accordingly, the carboys were shaken up before the water was poured out into the tube. The probable influence of changes in the physical nature of the suspensoids caused by standing and by the preservative, and the possible reaction of the sea water with the glass of the containers are discussed below.

‡ The effective length of the tube was 97 cm. The accuracy of the measurements was approximately as follows: 5 percent for readings where absorption was more than 10 percent per meter, 10 percent for readings where absorption was between 5 percent and 10 percent per meter, 30 percent for readings where absorption was between 1 percent and 3 percent per meter.

The majority of measurements on lake water carried out by James and Birge were made with "settled" water rather than "shaken" water and certain tests were run on the sea water samples after they had been allowed to stand. Since the length of time of settling has a very pronounced effect on the absorption value of sea water even after a week—as is also the case with lake water,[7] —a standard period of forty-eight hours after shaking was adopted for settling. The water was then siphoned into the tube and measured immediately.

In addition to the tests run on the freshly shaken water and on settled water, certain samples were subjected to Berkefeld filtering in the Wisconsin laboratory. The Berkefeld filter used for this purpose was also of the "fine" type and was prepared in similar fashion to the one used in Woods Hole. After the discovery of the possible trouble with the paraffin lining of the tube, the paraffin was removed from the base of the filter and the metal parts were recoated with ceresin.

B. Absorption measurements

The measurements of absorption undertaken in the Wisconsin laboratory are presented graphically in Figs. 1–7. The measurements represented by Figs. 1–4 inclusive were carried out toward the end of the work and are the most reliable, since profit was made of earlier experience. All the curves in these figures are based on measurements with the tube lined with ceresin wax.* In all four cases, however, at least one measurement had been completed on another portion of the unfiltered water using the resin-lined tube. Since the two sets of observations are in substantial agreement, they serve as a check on each other and show that the resin lining was sufficiently reliable in cases in which the tests were run immediately. In the case of Station *C* (sample 5) a third portion of the water was run (in ceresin-lined tube) and this agreed well with

[7] Reference 1, Fig. 19.

* The tube used was slightly less than 1 meter longer than the comparison tube (see reference 1), hence the absorption values given are too low for 1 m by a small amount. Since the correction for these relatively transparent waters is so slight (maximum = 1 percent at 7600A) and becomes less than 0.1 percent at all wave-lengths shorter than 7400A, it has been neglected.

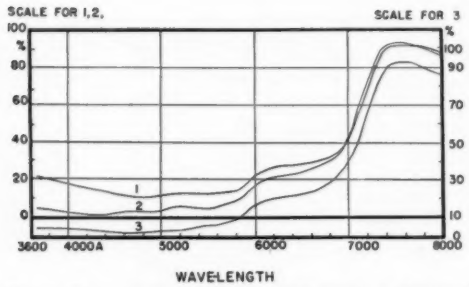

FIG. 1. Sargasso water. Station *C*. Percentage absorption of light per meter. Curve 1—sample 5, not filtered when collected, measured August 10, 1938, after shaking. Curve 2—sample 5, not filtered when collected, measured August 11, 1938, after Berkefeld filtering. Curve 3—double-distilled water, measured in ceresin-lined tube. (Curve displaced downward by 10 units to avoid interference.)

the second. Such differences as did occur between duplicate observations were confined to the short wave-length end of the spectrum and were particularly noticeable at 3650A. This situation can be accounted for in part by the fact that measurements are less precise in this region (because of the smaller amount of energy emitted by the source and the extremely high transparency of the water here) and in part by the fact that the absorption of water itself is so high at longer wave-lengths that the effect of other substances is masked. Insofar as any foreign matter present causes an increase in scattering (as distinct from true absorption), one would expect a greater effect toward the short wave-length end of the spectrum.

The absorption of those samples of water from Stations *C*, *B*, *A* and 3 which were not filtered at the time of collection was first measured immediately after moderate shaking (curve 1, in Figs. 1–4). Following this in each case the water was run out of the tube, passed through the Berkefeld filter, and then measured again (curve 2). These two measurements may be compared with doubled-distilled water† (curve 3) tested in the same tube under identical conditions. At Station *C* a second sample (sample 6) was collected in the same way as the first, but its absorption was found to be very much greater (Table II). Since the sample appeared perceptibly milky as it stood in the carboy, it was obvious that contamination of some sort had taken place. Although Berkefeld filtering reduced the absorption of this water to a minimum of 1.7 percent at 5040A, the value at 3650A is seen to be very much higher than that for the first Station *C* sample (sample 5). Much of the foreign matter present was therefore either in solution or in the form of very small particles.

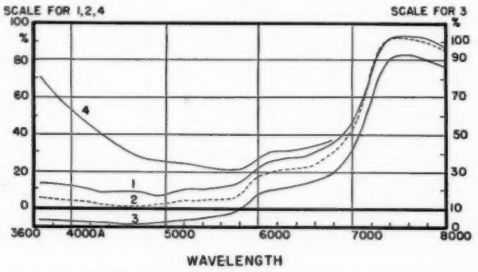

FIG. 2. Continental Slope water. Station *B*. Percentage absorption of light per meter. Curve 1—sample 7, not filtered when collected, measured August 12, 1938, after shaking. Curve 2—sample 7, not filtered when collected, measured August 12, 1938, after Berkefeld filtering. Curve 3—double-distilled water measured in ceresin-lined tube. Curve 4—sample 8, paper filtered when collected, measured August 10, 1938, after shaking.

The absorption measurements of those samples of sea water which were filtered at the time of collection (curve 4, Figs. 2–4), may be compared with the foregoing cases. Contrary to expectation, samples 8 and 10 (from Stations *B* and *A*), which were paper filtered, exhibited a greatly increased absorption in the short wave-length part of the spectrum. Since both samples behaved in the same way, one supposes that the water picked up a large amount of material from the filter paper. No further study of these samples seemed worthwhile.

The curve for the second sample at Station 3 (sample 12), which was Berkefeld filtered at the time of collection, is closely similar in shape to that for the first sample (sample 11), which was filtered in the Wisconsin laboratory, although the former lies somewhat above the latter at the shorter wave-lengths. After this initial measurement, sample 12 was Berkefeld filtered again, this time in the Wisconsin laboratory. Since the

† Distilled water redistilled in a tin still and run into Pyrex glass container. The absorption measurements were carried out on the same day. A second portion of the water prepared in this way agreed as well as could be expected with the first (cf. reference 1). The absorption curve of this sample was not appreciably changed by passing it through the same Berkefeld filter. Proof was thus furnished that the filtering process does not add "color" or otherwise affect the water itself.

absorption remained unchanged, we have proof that the Berkefeld filter used at Wisconsin did not affect appreciably the absorption characteristics of sea water. It is possible that the filter used in Woods Hole added "color" to the water since the absorption in the blue region of the spectrum was higher for sample 12 than for sample 11 after Berkefeld filtering. The difference is so slight, however, that it may well be caused by a difference in the two original samples. The fact that sample 11 has a lower absorption strongly indicates that no colored material dissolved out of the particles present in this sample during the period between collection off Woods Hole and filtering at Wisconsin (thirteen days). An average between curves 2 and 4 (Fig. 4) would therefore give a reliable picture of the absorption of Station 3 water with suspensoids removed.

The samples collected earlier (samples 1–4) from locations near shore (Station 3, 4 and 5) may be considered briefly (Figs. 5–7). Although the absorption of these samples was measured in

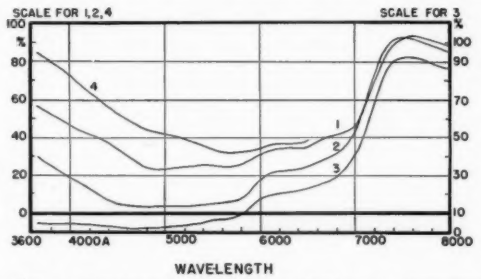

FIG. 3. Continental Shelf water.Station *A*. Percentage absorption of light per meter. Curve 1—sample 9, not filtered when collected, measured August 13, 1938, after shaking. Curve 2—sample 9, not filtered when collected, measured August 13, 1938, after Berkefeld filtering. Curve 3—double-distilled water measured in ceresin-lined tube. Curve 4—sample 10, paper filtered when collected, measured August 11, 1938, after shaking.

the paraffin-lined tube, some reliance can evidently be placed on these observations since the curve for sample 4, Station 3, for shaken water (curve 1, Fig. 5) agrees fairly well with the corresponding curve for sample 11 (curve 1, Fig. 4) taken five weeks later at the same station and run under more precise circumstances.

After settling for forty-eight hours, the transparency of the samples from all three stations was considerably increased. The greatest difference between shaken and settled water was found in the case of the sample from Vineyard Sound (Station 4). Since this is the most turbulent of the localities sampled, it may be that the particles present in this case were heavier and hence would settle out faster. The settling process resulted in reduction of absorption throughout the spectrum and the effect was generally uniform between wave-lengths 4000 and 7000A. Above 7000A the high absorption of water itself largely obscures the effect of other material; below 4000A the effect of filter-passing material appears, as will be discussed below. We conclude that the effect of particles large enough to settle out within forty-eight hours is nonselective within this central part of the spectrum.

C. Artificial sea water

An attempt to test the effect of the principal salts of sea water on absorption was made by preparing an artificial sea water and comparing it with distilled water. Four gallons of double-distilled water were prepared and divided into two parts. To one part the following salts were added in the proportions indicated (same formula as used by Hulburt[3]):

NaCl	26.40 g
KCl	.75
$MgCl_2$	3.15
$MgSO_4$	2.07
$CaSO_4$	1.33
	33.70
H_2O	966.30
	1000.00 g

All salts were of "reagent quality" with the exception of the $CaSO_4$ which was Mallinckrodt "pure precipitated." Due allowance was made for the water of crystallization. Since $MgCl_2$ is highly hygroscopic, some water was unavoidably included, with the result that the amount of this salt was probably slightly too small. The solution was thoroughly shaken and allowed to stand for two days. At the end of this time the water was not perfectly clear to the naked eye, but contained very fine particles—whether of undissolved salts or of impurities could not be determined. After Berkefeld filtering the solution was clear and its absorption was measured the following day. The second portion of double-distilled water was similarly passed through the

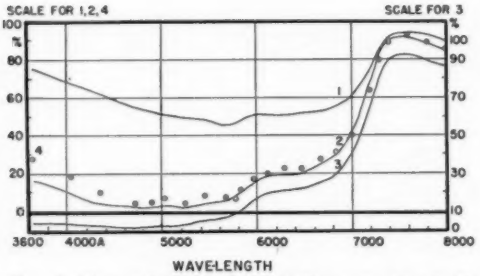

FIG. 4. Vineyard Sound Whistle Buoy. Station 3. Percentage absorption of light per meter. Curve 1—sample 11, not filtered when collected, measured August 11, 1938, after shaking. Curve 2—sample 11, not filtered when collected, measured August 11, 1938, after Berkefeld filtering. Curve 3—double-distilled water measured in ceresin-lined tube. Curve 4—sample 12, Berkefeld filtered when collected, measured August 9, 1938, after shaking.

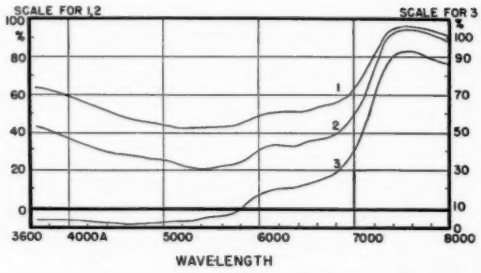

FIG. 5. Vineyard Sound Whistle Buoy. Station 3. Percentage absorption of light per meter. Curve 1—sample 4, not filtered when collected, measured July 6, 1938, after shaking. Curve 2—sample 4, not filtered when collected, measured July 6, 1938, after settling 48 hours. Curve 3—double-distilled water measured in ceresin-lined tube.

Berkefeld filter and a comparative measurement made (Fig. 8).

The absorption of the artificial sea water is seen to be practically identical with the double-distilled water from 8000A to 5460A. At shorter wave-lengths the artificial sea water exhibits a higher absorption, especially at 3650A. This effect is probably caused chiefly, if not entirely, by filter-passing impurities and not to the salts in solution, because our clearest samples taken from the ocean and Berkefeld filtered, which contain the same salts, exhibited an absorption only slightly greater than distilled water (cf. curves 2, Figs. 1 and 2). Hulburt[3] similarly concluded that the salts of sea water exerted no appreciable effect on absorption at wave-lengths longer than 3400A. Furthermore, we obtain no evidence from these measurements that the presence of these salts in sea water could reduce the absorption below that of distilled water. The significance of this conclusion will appear below in the discussion.

TABLE II. *Comparison of absorption per meter of samples 5 and 6 at five wave-lengths. Both samples were taken at Station C. Neither was filtered at the time of collection, but sample 6 had evidently become contaminated.*

Wave-Length	Water Freshly Shaken		Water Berkefeld Filtered	
	Sample 5	Sample 6	Sample 5	Sample 6
5790A	14.0%	48.8%	7.2%	8.4%
5460	13.6	47.3	4.3	6.2
4359	15.1	61.9	1.0	10.0
4047	17.8	69.1	2.8	16.7
3650	22.5	72.5	5.4	27.8

OBSERVATIONS AT SEA

The measurements at sea were made according to our usual procedure and in close conformity to the recommendations of the Committee of the International Council for the Exploration of the Sea.[8] Our submarine photometer and deck photometer contain Weston "Photronic" cells which possess a maximum spectral sensitivity at 5800A.[9] For the present measurements a Schott-Jena filter, type VG-2 (practically identical to the VG-9 recommended by the Committee) was placed between the plate glass window of the photometer case and the opal glass diffusing disk.* The transmission of this filter reaches a maximum at 5300A and drops off to 10 percent of the maximum at about 6200A and 4600A. The point of maximum sensitivity of the combination of cell plus filter can safely be taken as 5500A.

The observations at sea at Stations *C*, *B*, *A* and 3 are presented graphically in Fig. 9. Since the curves, plotted on a logarithmic scale, approach a straight line, we know that the water

[8] A. Angstrom, W. R. G. Atkins, G. L. Clarke, H. Pettersson, H. H. Poole and C. L. Utterback, 1938. "Measurements of Submarine Daylight," J. du Conseil Perm. Intern. pour l'Exp. de la Mer **13**, 37–57 (1938).

[9] Weston Electrical Instrument Corporation Technical Data Pamphlet.

* For high light intensities a diaphragm was placed over this disk to reduce the illumination. Both photometers were carefully calibrated against a photoelectric cell which was known to be linear in its response (Powell and Clarke, reference 10).

[10] W. M. Powell and G. L. Clarke, "The Reflection and Absorption of Daylight at the Surface of the Ocean," J. Opt. Soc. Am. **26**, 111–120 (1936).

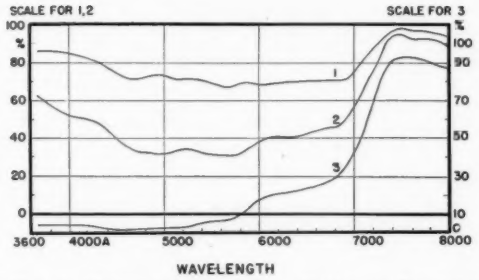

FIG. 6. Vineyard Sound water. Station 4. Percentage absorption of light per meter. Curve 1—sample 2, not filtered when collected, measured July 7, 1938, after shaking. Curve 2—sample 2, not filtered when collected, measured July 7, 1938, after settling 48 hours. Curve 3—double-distilled water measured in ceresin-lined tube.

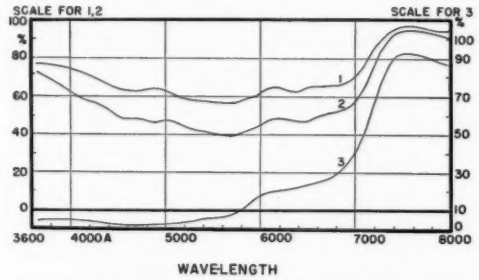

FIG. 7. Buzzards Bay water. Station 5. Percentage absorption of light per meter. Curve 1—sample 1, not filtered when collected, measured July 5, 1938, after shaking. Curve 2—sample 1, not filtered when collected, measured July 7, 1938, after settling 48 hours. Curve 3—double-distilled water measured in ceresin-lined tube.

was homogeneous optically.† The calculation of *average* values for the extinction coefficient‡ and for the percentage absorption for water is therefore appropriate (Table III). The values obtained are in close conformity to previous observations[11] in the several regions and demonstrate the presence of the clearest water in the Sargasso Sea (Station *C*). Water of progressively lower transparency was encountered in the Continental Slope area (Station *B*) and on the Continental Shelf (Station *A*). The extinction coefficient characterizing the water at the whistle buoy at the western entrance to Vineyard Sound (Station 3) was nearly the same as at Station *A* and falls within the narrow range of values previously obtained for Station 3 during the summer months.[6] Thus at all four stations the transparency of the sea at the time of collection of the water samples for laboratory measurements was shown to be entirely typical of the respective regions.

For field measurements at Stations 4 and 5 (Vineyard Sound and Buzzards Bay) we have the observations of Oster and Clarke[5] made on August 21 and August 28, 1934, respectively (Series 322 and 325), with instruments of almost identical spectral sensitivity and under similar conditions of tide (Table III). These measurements and others placed the transparency of Buzzards Bay somewhat below that found within Vineyard Sound and this in turn was considerably below that observed at the entrance to the Sound (Station 3).

Since the water samples for laboratory measurement were collected at the surface, one might suppose that their absorption values should be compared with field measurements made just beneath the surface. However, it is ordinarily impossible to carry out reliable field measurements at depths of less than one or two meters Furthermore, when the curves representing the measurements at greater depths (Fig. 9) are extended upwards from the shallowest point of observation to the surface, they do not strike the 0–m line at 100 percent, but at a lower value

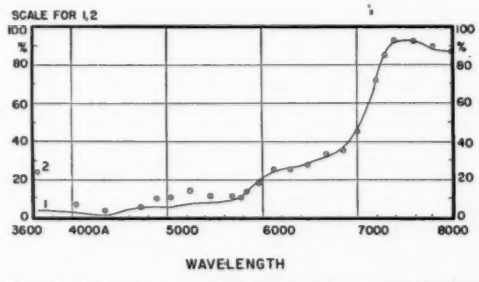

FIG. 8. Curve 1—percentage absorption per meter of one portion of double-distilled water after Berkefeld filtering. Curve 2—percentage absorption per meter of artificial sea water (see text) made from a second portion of the double-distilled water and passed through the Berkefeld filter.

† The decreased transparency indicated below 25 m at Station 3 (Series 480) is probably a result of mud stirred up from the bottom (depth 31 m).

‡ Extinction coefficient $= k$ in the equation $I/I_0 = e^{-kL}$ where L is the thickness of the water layer (in meters) in which the intensity is reduced from I_0 to I. The term "transmissive exponent" was formerly used for this quantity following Sawyer, reference 4, but has been changed to conform to the recommendations of the Committee (reference 8). "Absorption coefficient" has been used by certain other investigators in the same connection.

[11] G. L. Clarke, "Light Penetration in the Western North Atlantic and its Application to Biological Problems," Rapports et Procès-Verbaux. Con. Perm. Intern. Exp. Mer. **101**, Part 2, 3–14 (1936).

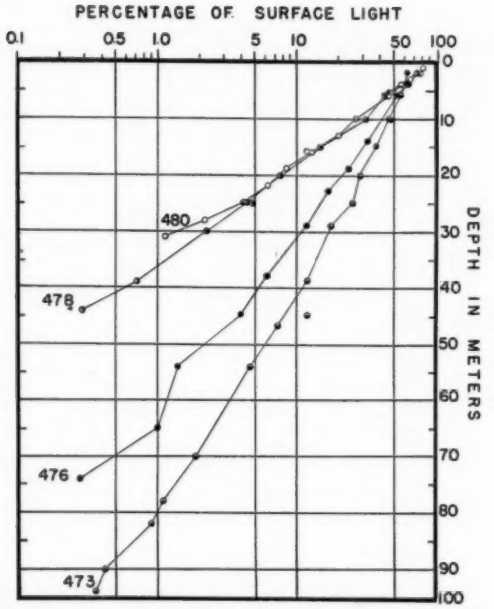

FIG. 9. Measurements of light absorption carried out at sea. Curves show relation between depth and illumination expressed as a percentage of the light just over the surface (logarithmic scale). Maximum sensitivity of photometer 5500A (photronic cell with VG-2 filter). Series number indicated at end of each curve (see Table I for additional data).

SERIES	LOCALITY	STATION	DATE	TIME (E.S.T.)	SKY	SEA	WIND
473	Sargasso Sea	C (3093)	July 10, 1938	11:37–12:13	*bc*	2	2
476	Continental Slope	B (3105)	July 14, 1938	12:47–13:30	*b*	5	5
478	Continental Shelf	A (3111)	July 17, 1938	11:46–12:10	fog	1	1
480	Vineyard Sound Whistle Buoy	3	July 29, 1938	11:50–12:30	*o*	2–3	2–3

ranging down to 70 percent in the present case. This effect, termed the "surface loss," has been shown to be caused in only a small degree by actual reflection at the surface. The greater part of the "loss" is accounted for by the greatly increased absorption of the water layer (about one meter thick) just beneath the surface (probably caused by bubbles) under all conditions except absolute calm.[10] Obviously this situation within the upper meter is a local and temporary effect yielding an extinction value not inherent in the water itself. Since the ocean water in the regions under consideration is thoroughly stirred down to at least 25 m, an average value for the absorption over this depth has been taken for comparison with the laboratory measurements (Table III).

DISCUSSION

A. Comparison of laboratory measurements with observations at sea

If the same picture of submarine illumination is obtained from the extrapolation of laboratory measurements of absorption as is derived from actual observations at sea, work on board ship would be greatly simplified and measurements could be carried out under ideal conditions on shore. A comparison of the curves for the shaken samples from all the stations (Fig. 10) shows that the transparencies of the samples follow the same general sequence as that based on measurements at sea. There are two exceptions: The sample from the Continental Slope (Station *B*) exhibited less absorption than that from the Sargasso Sea (Station *A*), and the sample from Buzzards Bay (Station 5) was less opaque than that from Vineyard Sound (Station 4).

For the comparison of absolute values we may take the absorption observed in the laboratory for wave-length 5500A since this is the region of maximum sensitivity of the photometer used at sea (see above). It is seen that the absorption per meter as measured in the laboratory is from 2 to 4 times greater than the absorption based on the field measurements (Table III). Higher absorption is likewise found even if the minimum value for each curve at any wave-length is taken. The water was evidently considerably changed by the time it reached the Wisconsin laboratory. This situation was anticipated because according to common experience any semi-transparent organic tissue present would be rendered opaque by the preservative. In addition, the water may have reacted with the glass of its containers. If the latter explanation was operative, its effect must have been small since we have one unfiltered sample (sample 7) in which the absorption was very little above distilled water and the action of the sea water would be expected to be the same in all cases. Furthermore, after Berkefeld filtration, the absorption of samples 5 and 7 was reduced practically to that of distilled water although the samples had stood in their containers for over a month. It seems more likely that the transparency of suspended particles had become radically altered. Such action of the preservative on *different types* of organic matter

would account for the differences in amount of change undergone by the various samples. For example, the transparency of the water at Station *A* was closely similar to that at Station 3 as measured at sea, but an absorption of twice the magnitude was obtained for the latter station from the laboratory samples. The conclusion is obvious that much though we may learn from laboratory studies of light absorption, they cannot give a reliable picture of the illumination actually to be found at various depths in the ocean. For this, observations at sea are essential.

B. Comparison of "pure" sea water with distilled water

The absorption of "pure" sea water, as represented by samples taken from the off-shore stations (Stations *B* and *C*) and passed through the Berkefeld filter, was found to be practically identical with the ordinary double-distilled water measured in the ceresin-lined tube within the variation of measurement (Table IV). The absorption values for the best samples of distilled water measured in a silver lined tube[1] are somewhat lower than for sea water. It is of interest to note that our values for the absorption of both of these samples of sea water at wave-lengths 4047A and 3650A are lower than those of Sawyer[4] for distilled water, the difference being about fourfold at 3650A (Table V). (They are also lower than the values reported by Hulburt[3] for distilled water and for sea water at 3660A and the value of Dawson and Hulburt[12] for distilled water at 3600A.) This fact adds strong support to the evidence from the distilled water measurements of James and Birge that Sawyer's values for distilled water in this part of the spectrum are too high. In addition field measurements made in the Sargasso Sea of absorption in the blue region[13] and in the violet region[5] agree closely with our present laboratory measurements and yield values lower than those of Sawyer for distilled water in the corresponding parts of the spectrum (Table V). At the time the discrepancies were assigned to inaccuracies unavoidable in work at sea, but now our laboratory measurements have confirmed the earlier field observations, and both are consistent with the values for distilled water obtained by James and Birge.

Darby, Johnson and Barnes[14] have reported a

[12] L. H. Dawson and E. O. Hulburt, "The Absorption of Ultraviolet and Visible Light by Water," J. Opt. Soc. Am. **24**, 175–177 (1934).

[13] G. L. Clarke, "Observations on the Penetration of Daylight into Mid-Atlantic and Coastal Waters," Biol. Bull. **65**, 2, 317–337 (1933).

[14] H. H. Darby, E. R. F. Johnson and G. W. Barnes, "Studies on the Absorption and Scattering of Solar Radiation by the Sea. Spectrographic and Photoelectric Measurements," Carnegie Inst. of Wash. Publication, No. 475, 191–205 (1937).

TABLE III. *Summary of the measurements of the penetration of the "green" component of daylight into the sea and comparison with laboratory measurements of absorption of unfiltered samples taken from the same stations.*

Station	Location	Series Number	Range of Measurements	Av. Extinction Coeffi-cient, k, over Range in Previous Col.	Average Absorption per Meter for Sea Measure-ment	Sample Number	Absorption per Meter at 5500A for Sample in Laboratory	Minimum Absorption per Meter for Lab. Sample	Wave-Length at Which Minimum Absorp. is Found
			Meters	k	%		%	%	*A*
C	Sargasso Sea	473	2–94 2–25	0.056 .040	3.9	5	13	10	4900
B	Continental Slope	476	4–74 4–23	.062 .061	5.7	7	10	7	4900
A	Continental Shelf	478	2–44 2–25	.13 .12	11.3	9	26	22	4900
3	V. S. Whistle Buoy	480	1–31 1–25	.14 .125	11.7	11 4	48 43	45 42	5790 and 5685 5250
4	Vineyard Sound	322	1–21	.20	18.1	2	69	67	5685
5	Buzzards Bay	325	1–15	.25	22.1	1	57	57	5685

BOSTON UNIVERSITY
COLLEGE OF LIBERAL ARTS
LIBRARY

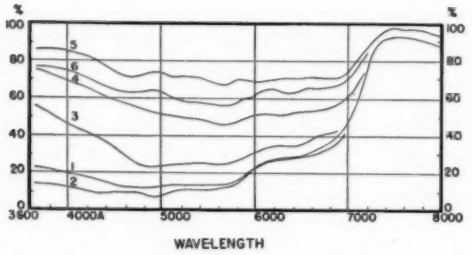

FIG. 10. Comparison of percentage absorption of light per meter for unfiltered samples of sea water from all stations measured after shaking.

CURVE	LOCALITY	STATION	SAMPLE
1	Sargasso Sea	*C*	5
2	Continental Slope	*B*	7
3	Continental Shelf	*A*	9
4	Vineyard Sound Whistle Buoy	3	11
5	Vineyard Sound	4	2
6	Buzzards Bay	5	1

very much lower rate of absorption for ultraviolet by sea water on the basis of field measurements near the Tortugas Laboratory (Gulf of Mexico) than found by Sawyer and by Hulburt. Since the work of Darby *et al.* yielded only relative values, comparisons with other measurements are difficult. Since field measurements by Clarke[15] in the visible part of the spectrum gave very low values for the extinction coefficient in the Gulf of Mexico, there is no doubt that the water in this region is extremely transparent. But whether the penetration of the far ultraviolet is as effective as suggested by Darby *et al.* remains to be confirmed. The determination of absolute values in this biologically important region of the spectrum is seriously needed. Certainly the low absorption values as far as 3650A obtained in the present investigation lend support to the view that ultraviolet is not reduced in intensity by sea water as rapidly as was previously supposed.

As regards the long wave-length end of the spectrum, our measurements show that the values for k of 0.567 and 0.480 for sea water at 7600A and at 7000A, respectively, reported by Atkins and Poole[16] are far too low. Atkins[17] believes the explanation to lie in erroneous ratings of the average wave-lengths transmitted by the combinations of filters used by him. The table of "accepted values" for the extinction coefficients of distilled water given by Cooper and Milne[18] is consequently seriously in error. Since there is no reason to suppose that the transparency of sea water can ever exceed that of distilled water, we must conclude that the measurements of James and Birge give a truer description of distilled water than those of earlier investigators. Furthermore, our present investigation shows that "pure" sea water approaches the transparency of distilled water *as reported by James and Birge* in all parts of the spectrum.

C. The effect of suspensoids and of filter-passing material on absorption

Since Berkefeld filtering sea water from Station 3 after a period of storage (sample 11) had es-

TABLE IV. *Comparison of "pure" sea water with distilled water. Percent absorption per meter.*

WAVE-LENGTH	BERKEFELD-FILTERED SEA WATER		DISTILLED WATER	
	STATION B SAMPLE 7†	STATION C SAMPLE 5†	CERESIN-LINED TUBE	SILVER-LINED TUBE*
8000	85.2	86.6	86.8	88.9
7800	89.0	89.7	89.5	90.2
7600	91.6	92.2	92.3	91.4
7400	91.5	91.2	89.5	88.5
7300	85.0	84.5	80.5	
7200	71.0	69.8	65.5	64.5
7000	42.7	42.2	39.3	45.0
6850	32.3	31.8	29.7	38.0
6680	28.7	28.3	28.6	33.0
6480	22.0	24.4	22.8	28.0
6300	20.6	22.3	21.0	25.0
6125	19.7	21.2	19.9	22.4
5970	16.6	15.2	16.2	17.8
5840	8.2	9.6	9.1	9.5
5790	7.6	7.2	8.9	
5685	5.0	7.4		4.6
5460	4.8	4.2	6.5	3.8
5250	4.1	6.2	3.9	1.8
5040	2.6	4.5	4.0	1.0
4900	1.7	2.8	2.2	
4730	1.0	3.6	1.7	0.49
4480				0.70
4359	2.8	1.0	2.3	0.78
4047	4.4	2.8	4.1	1.1
3650	6.6	5.4	4.5	3.6

* From James and Birge, 1938, Table I.
† Ceresin-lined tube.

[15] G. L. Clarke, "Light Penetration in the Caribbean Sea and in the Gulf of Mexico," J. of Marine Research **1**, 85–94 (1938).

[16] W. R. G. Atkins and H. H. Poole, "The Photo-electric Measurement of the Penetration of Light of Various Wave-Lengths into the Sea and the Physiological Bearing of the Results," Phil. Trans. Roy. Soc. London. **B222**, 129–164 (1933).

[17] Private communication.

[18] L. H. N. Cooper and A. Milne, 1938. "The Ecology of the Tamar Estuary. II. Under-Water Illumination," J. Mar. Biol. Ass. **22**, 509–528.

TABLE V. *Comparison of field measurements of light absorption in the blue and violet regions with laboratory measurements of sea water and of distilled water.*

FIELD MEASUREMENTS IN SARGASSO SEA						LABORATORY MEASUREMENTS				
	MAX. SENSITIVITY OF PHOTOMETER	AV. ABSORPTION FOR WHOLE SERIES		MIN. ABSORPTION FOR 10 m STRATUM		WAVE-LENGTH	FILTERED SEA WATER		DISTILLED WATER	
							STATION *B*	STATION *C*	SAWYER	JAMES AND BIRGE
SERIES	*A*	*k*	% per m	*k*	% per m	*A*	% per m	% per m	% per m	% per m
12*	4359	0.031	3.1	0.011	1.1	4359	2.8	1.0	2.6	0.78
						4047	4.4	2.8	6.0	1.3
310†	3650	0.048	4.8	0.022	2.2	3650	6.6	5.4	21.6	3.6

* Reported by Clarke (1933).
† Reported by Oster and Clarke (1935).

sentially the same effect on absorption as immediate filtration (sample 12), we may assume in the case of this and of all the other samples that no significant amount of absorbing material dissolved out of the particles occurring in the water during the period of storage. The filtration process naturally exerted a greater effect on absorption in the case of samples from coastal regions (Stations *A* and 3)* than on samples from off-shore (Stations *B* and *C*) since the former were more turbid initially. The significant fact is that for all four stations Berkefeld filtering reduced the absorption practically to distilled water values for wave-lengths between 8000A and 4730A. The agreement between all curves of filtrates and distilled water is remarkably close (curves 2 and 3, Figs. 1–4). Proof is thereby furnished that between 8000A and 4730A the greater absorption brought about by sea water than by distilled water is entirely caused by suspensoids, i.e., to particles large enough to be removed by the Berkefeld filter.

For the spectral region from 4730A to 3650A suspensoids similarly appear to account for all of the absorption *in the case of samples from the off-shore stations* with the possible exception of the shortest wave-lengths. It is doubtful whether the slightly higher position of the filtrate curves is more than would be accounted for by the variation in measurement. In the case of the inshore samples, however, although the absorption was greatly reduced by filtering in all parts of the spectrum, the curves remain far above distilled water at the short wave-lengths after the samples had been passed through the Berkefeld (curves 2 and 3, Figs. 3 and 4). This fact demonstrates the presence of significant quantities of filter-passing material which has a pronounced absorptive action on light. This material may consist of particles of extremely small size (practically all bacteria are stopped by the Berkefeld filter—cf. Clarke and Gellis[19]) or of substances in true solution.† We may well imagine that material of both kinds would result from the decomposition of plankton, which is much more abundant in coast regions than off-shore, and of littoral organisms. Soluble pigments derived from disintegrating plant cells might account for selective absorption (cf. Kalle[20]). In addition discrete particles as small as is indicated would have a highly selective effect on the scattering of light.

The absorption of settled lake waters has been assigned numerically to (1) water as water, (2) "suspensoids," (3) "color" by James and Birge

* The samples from the other coastal stations were not Berkefeld filtered.

[19] G. L. Clarke and S. S. Gellis, 1935. "The Nutrition of Copepods in Relation to the Food-Cycle of the Sea," Biol. Bull. **68**, 231–246 (1935).

† Our present method gave no possibility of distinguishing between these two elements; the matter presents a problem for future investigation. It has recently been found that the residual color of many lake waters can be removed entirely or in part by the use of a Cellophane filter (Juday, unpublished communication).

[20] K. Kalle, "Zum Problem des Meereswasserfarbe. Annalen der Hydrographie und Maritimen meteorologie," Heft. I, 1–13 (1938).

TABLE VI. *Percentage transmitted by filter-passing material = C ("color"), and by filter-retained material = S ("suspensoids"), in reducing the transmission of distilled water = W to that observed for the shaken sample = N (see text).*

Wave-Length	Double-Distilled Water	Vineyard Sound Whistle Buoy Station 3 Sample 11					Continental Slope Water Station B Sample 7				
	W	*N*	*Fi**	*F = N/W*	*C = Fi/W*	*S = F/C*	*N*	*Fi**	*F = N/W*	*C = Fi/W*	*S = F/C*
8000	13.2	9.8	14.7	74	111†	67	13.6	14.8	103	112†	92.0
7600	7.7	5.6	7.9	73	103	71	7.4	8.4	96.2	109	88.3
7200	34.5	24.8	31.0	72	90†	80	28.0	29.0	81.1	84.2†	96.3
7000	60.7	39.8	59.9	65	99	66	54.1	57.3	89.0	94.4	94.4
6680	71.4	46.3	73.0	65	102	64	67.6	71.3	94.7	100	94.7
6300	79.0	49.0	80.2	62	101	61	72.6	79.4	91.9	100	91.9
5970	83.8	49.9	85.6	60	102	59	79.2	83.4	94.6	100	94.6
5790	91.1	51.9	91.3	57	100	57	87.5	92.4	96.0	101	95.1
5460	93.0	51.1	95.5	54	101	53	89.8	95.1	96.6	102	94.6
5040	96.0	49.0	96.7	51	101	51	91.7	97.4	95.6	101	94.6
4730	98.3	44.8	97.1	46	98.8	47	90.6	99.0	92.2	101	91.6
4359	97.7	38.6	96.6	40	98.8	41	91.3	97.2	93.4	99.5	93.9
4047	95.9	32.6	90.0	34	93.9	36	88.0	95.6	91.8	99.7	92.1
3650	95.5	25.1	83.6	26	87.6	30	86.2	93.4	90.3	97.9	92.2

* *Fi* = transmission of filtered sample. All measurements made in ceresin-lined tube.
† Departure from 100 percent probably due to variation of measurement as indicated by other series of observations.

on the basis of a three-component analysis. The absorption of the water itself is based on the distilled water curve. A similar analysis (Table VI) has been carried out on the two samples of sea water which exhibited the greatest and the least effect resulting from Berkefeld filtering, but in the present case the analysis is based on the shaken water rather than on the settled water for reasons stated above. The factors involved are derived as follows:

N = percentage transmission of shaken sea water*
W = " " " distilled water
Fi = " " " Berkefeld-filtered sea water

$$\frac{N}{W} = F = \text{general factor}$$

$$\frac{Fi}{W} = C = \text{color factor}$$

$$\frac{F}{C} = S = \text{suspensoid factor}$$

$$\therefore CSW = N.$$

The foregoing method of analysis allows one to calculate the part played respectively by suspensoids and by "color" at any desired wave-length in reducing the transmission of pure water to that of the sample under investigation. For example, in the case of off-shore water (sample 7, Station *B*, Table VI) suspensoids reduced the transmission to about 93 percent of that of distilled water with very little difference in any part of the spectrum. Practically no "color" was present since the factor for the transmission allowed by this component does not depart significantly from 100 percent (if questionable values at the long wave-length are disregarded) with the possible exception of wave-length 3650A. In the case of coastal water (sample 11, Station 3) suspensoids account for the reduction of light to values varying from 30 percent at 3650A to 70 percent or 80 percent at the long wave-lengths. Here the effect of suspensoids is considerable throughout the spectrum, but greatest at the shorter wave-lengths. It must be remembered, however, that we have evidence that the transparency of the suspensoids has been seriously changed by the preservative: the factor for suspensoids for *fresh* sea water would be smaller.* The "color" factor for coastal water departs slightly from 100 percent at certain long wave-lengths, but other series of observations show that this is caused by variation of measurement. At the short wave-length end of the spectrum,

* The symbol "*T*" is used for the transmission of settled water by James and Birge.

* There is no evidence that the preservative affects appreciably the filter-passing material, but this point should be checked when opportunity arises.

however, the pronounced selective action of this factor is clearly indicated. Coastal sea water thus possesses some "color" not removable by a Berkefeld filter. We conclude, in sum, that a distinct optical difference exists between off-shore and coastal water: In the former the absorption, beyond that of the water itself, is caused chiefly by suspensoids and these are largely nonselective in their effect on light. In the latter the greater absorption is due to filter-passing material as well as to suspensoids and each of these elements exerts a highly selective action on light.

Summary

(1) The absorption of light by preserved samples of sea water collected at coastal and at off-shore stations in the North Atlantic was measured in the monochromater previously employed by James and Birge.[1] One sample from each station was left unfiltered at the time of collection and was measured (a) after moderate shaking, (b) after settling for forty-eight hours, and (c) after Berkefeld filtering. Other samples were passed through paper or Berkefeld filters at the time of collection.

(2) Artificial sea water exhibited an absorption practically identical with distilled water except at the shorter wave-lengths where the absorption was greater probably because of impurities.

(3) The absorption per meter of the shaken samples was much greater than the average value per meter for the absorption observed at sea. This fact, undoubtedly caused by the action of the preservative on organic particles, demonstrates the necessity of field observations for an accurate knowledge of submarine illumination.

(4) The absorption of "pure" sea water, as represented by Berkefeld-filtered off-shore samples, was found to be practically identical with distilled water measured in the same tube. Thus no support is furnished to previous reports by others of lower absorption and additional evidence is obtained that the values of Sawyer[4] for distilled water in the ultraviolet may be too high.

(5) The difference between the absorption of unfiltered samples of sea water and of distilled water is caused chiefly by suspensoids for wave-lengths 8000A to 4730A, and for 4730A to 3650A in the off-shore areas. In coastal areas both filter-passing material and suspensoids are effective and each exerts a highly selective action on light with greatest absorption at the shorter wave-lengths.

Transparent and Opaque Screens for the Near Infra-Red

A. H. PFUND
The Johns Hopkins University, Baltimore, Maryland
(Received November 28, 1938)

WHILE there is a wealth of information on the transmission of optical screens in the visible and ultraviolet regions of the spectrum, relatively little is known in the near infra-red. This region is becoming increasingly important because of the development of infra-red photography, infra-red photoelectric cells, physical photometry, etc. The information to be presented is of an incidental nature—having been collected over a period of years in connection with other work. In addition to the discussion of the remarkable transparency of vanadyl sulphate $(VO)(SO_4)$ and of the opacity of ferrous ammonium sulphate $Fe(NH_4)_2(SO_4)_2$ a number of additional screens are described.

For many years the favorite materials chosen to absorb the infra-red and transmit visible light have been salts of copper dissolved in water. The regions of absorption of these materials were supposed to overlap so thoroughly that no measurable amount of infra-red radiation would be transmitted. That this is not the case was noticed long ago by the writer[1] in his attempt to formulate a luminosity filter for objective (physical) photometry. Similar observations were made more recently by Gibson, Teele and Keegan.[2] An attempt to find a more efficient filter, i.e., one which eliminates the infra-red more effectively, while retaining a high degree of transparency to light, was made during the past year. For these studies a thermopile, galvanometer and a (Fuess) glass monochromator whose range extends from 0.4μ to 2.7μ were employed.

Since it is customary[2] to use water in layers five cm thick, the transmission curve for such a layer was determined (Fig. 1(A)) as was, likewise, the transmission curve for copper sulphate "alone." To obtain the latter curve (Fig. 1(B)) ten cc of an aqueous solution of $CuSO_4$, saturated at 22°C, were diluted with 120 cc of water and some of the mixture was poured into a glass cell one cm thick. A second cell of the same thickness was filled with water. By taking the ratio of the intensity of radiation transmitted by these two cells, it was possible to evaluate the transmission of the $CuSO_4$ alone. From curve A it is evident that water has a pronounced transmission band near 1.05μ in which region $CuSO_4$ is becoming increasingly transparent. This circumstance, coupled with the large amount of radiant energy from an incandescent lamp near 1μ, results in an annoying and persistent infra-red transmission. To increase greatly the concentration of the $CuSO_4$ solution would make the filter too blue to enable it to function as a portion of a luminosity filter. The writer has found recently that this difficulty may be minimized through the use of an aqueous solution of ferrous ammonium sulphate. Some C.P. salt is dissolved in distilled water which had been boiled previously and cooled down to room temperature. (Hot water changes the green ferrous salt into the yellow, ferric modification.) A solution of this ferrous salt, saturated at 22°C, is stored in a large glass tube supplied with a stopcock at its lower end. A layer of mineral oil covers the solution so as to prevent oxidation.* Some of this solution was

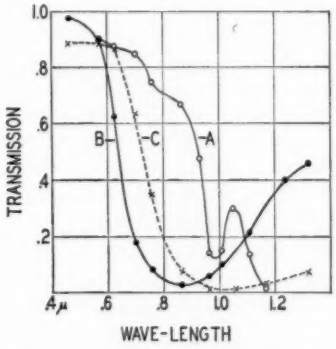

FIG. 1. Showing the transmission of: A—5-cm layer of water, B—$CuSO_4$ solution (to the exclusion of water), C—$Fe(NH_4)_2(SO_4)_2$ solution (to the exclusion of water).

[1] A. H. Pfund, see J. Guild, Trans. Opt. Soc. 27, 123 (1925–26).
[2] K. S. Gibson, R. P. Teele and H. J. Keegan, Program of Annual Meeting of the Optical Society of America, Oct. (1938), Paper no. 21.

* Under all conditions of use, the ferrous ammonium sulphate solution must be kept covered with a layer of

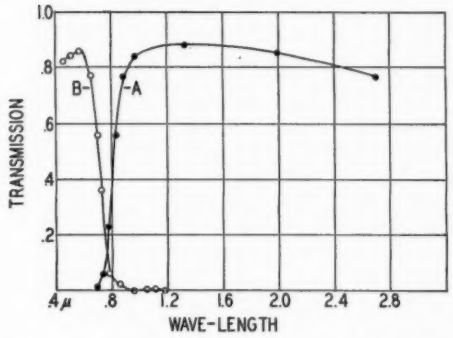

FIG. 2. Showing the transmission of: A—Iodine in CCl_4 (heat-filter), B—$Fe(NH_4)_2(SO_4)_2$ solution, 18 mm thick.

poured into the one-cm cell and the transmission of ferrous ammonium sulphate alone was determined (Fig. 1(C)). The small transmission near 1.05μ coupled with high transmission in the visible spectrum make this material unique. In thicknesses of five cm the solution is only a very pale green, hence such a layer, in consequence of the already great opacity of the one-cm cell, would render the infra-red quite innocuous.

In this connection it seemed of interest to study the ratio of "light to heat" transmission for this material. This subject has been discussed fully by Gage[3] in connection with the Corning heat-absorbing glass "Aklo." In the determination of the light to heat ratio, the simple procedure of Sir William Crookes[4] was essentially followed—the principal point of departure being the use of a reproducible "heat-filter." To measure the light-transmission, a cell, 18 mm thick, was filled with a saturated solution of ferrous ammonium sulphate and mounted between a 100-watt gas-filled Mazda lamp and a Macbeth illuminometer. To measure the heat, it was first necessary to devise a suitable and reproducible heat-filter. It has long been known[5] that iodine dissolved in CS_2 is highly transparent in the infra-red. Because of its lower volatility CCl_4 was chosen as the solvent in place of CS_2.*

A saturated solution of iodine in CCl_4 was poured into a cell (5 mm thick) with windows of polished rocksalt. The transmission curve for this cell is shown in Fig. 2(A), as is also the transmission curve of the 18-mm layer of $Fe(NH_4)_2(SO_4)_2$, Fig. 2(B). These two solutions in series, were placed in front of a windowless thermopile connected to a galvanometer. As before, the 100-watt Mazda lamp, at a distance of about a meter, served as the source. The results are given in Table I.

Without making the calculation for the ratio of light to heat transmission, it is shown that the 18-mm (ferrous ammonium) cell, while transmitting 0.89 as much visible light as the same cell filled with water, transmits only $\frac{1}{2}$ of 1 percent of the heat rays from a Mazda lamp filtered by the iodine-CCl_4 solution.

As for the materials which become transparent in the near infra-red, vanadyl sulphate $(VO)(SO_4)$ is among the most interesting. A saturated solution of this deep-blue salt was diluted with two parts of water. The compartments of the one-cm cell were filled, respectively, with vanadyl solution and with water so that the transmission of vanadyl sulphate alone might be determined. The results are shown in Fig. 3(A) from which the remarkably steep rise from 0.9μ on is evident. To examine the behavior of an actual cell, two glass plates were separated by 1.5 mm and the space between them was filled with saturated vanadyl solution. The resultant transmission curve Fig. 3(B) shows that while the water reduces greatly the transmission around 1.5μ, the transmission around 1.1μ remains high. The transparency in the blue and green is eliminated

TABLE I.

	LIGHT	LIGHT TRANSMISSION
I	18-mm cell filled with water	91%
II	18-mm cell filled with $Fe(NH_4)_2(SO_4)_2$ solution	81%
III	Ratio transmission II/transmission I	89%
	HEAT	**GALVANOMETER DEFLECTIONS**
IV	5-mm cell filled with CCl_4	237. mm
V	5-mm cell filled with iodine solution	215. mm
VI*	5-mm cell filled with iodine solution in series with 18-mm cell containing $Fe(NH_4)_2(SO_4)_2$ solution	1.1 mm

* Heat transmission of combination VI = $\frac{1}{2}$ of 1 percent.

mineral oil. The best filter for the elimination of heat yet made by the writer contains ferrous ammonium sulphate solution to which a little copper sulphate has been added.

[3] H. P. Gage, Trans. Ill. Eng. Soc. 30, 411 (1935).

[4] Sir William Crookes, Phil. Trans. 214, 1–25 (1914).

[5] H. Becquerel, Ann. Chem. Phys. 5, 30 (1883).

* The blue and violet transmission of the iodine-CCl_4 solution may be eliminated through the addition of a yellow "oil soluble" dye.

by the use of a Corning signal-red screen. This combination is so effective that it is impossible to see the faintest trace of the disk of the sun.

In a previous paper,[6] attention was directed to a series of screens whose transmission sets in at wave-lengths less than 1μ. Here, an additional series of screens whose regions of transparency lie at greater wave-lengths is presented. Fig. 4(A) applies to a layer of celluloid 0.58 mm thick containing Milori (iron) blue. This is really an excellent screen. The material used for curve B was copper butyl-phthalate (of unknown concentration) dissolved in CCl_4. While the transmission at the maximum does not rise very high, transmission does not set in until the wave-length 1μ is reached. Curve C applies to a fragment of bulb-green glass* having a thickness of 1.2 mm; and curve D applies to the pigment, basic carbonate of white lead which was mulled with water containing a little gum arabic and spread as a layer on a glass plate. After the water had evaporated, a dilute solution of nitrocellulose in amyl-acetate was flowed over the surface and was allowed to dry; finally, the entire system was immersed in water so that the pigmented film could be lifted off and mounted over a hole in a piece of cardboard.† Such powder-filters[7] have the advantage that, by choosing pigment particles of the proper size, the region of increasing transparency may be shifted to almost any desired portion of the infra-red spectrum. All of the screens in Fig. 4, with the possible exception of the one containing Milori blue, show a far less abrupt rise than do vanadyl sulphate and aniline dyes. The only excuse for discussing these additional screens is that their regions of transparency set in at wave-lengths greater than 1μ.

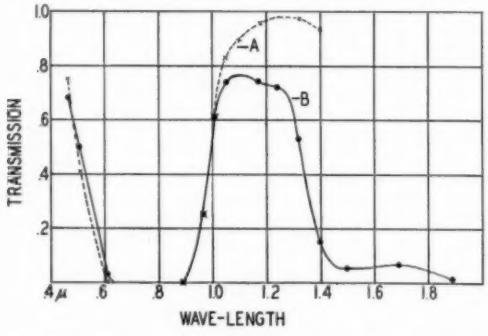

FIG. 3. Showing the transmission of: A—vanadyl sulphate solution (alone), B—vanadyl sulphate solution (total).

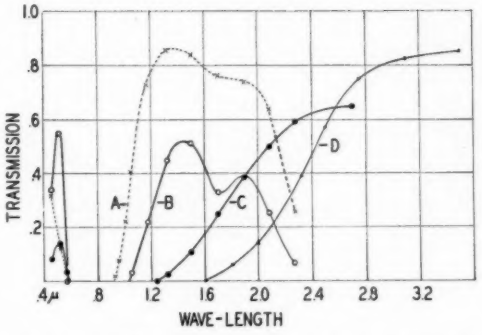

FIG. 4. Showing the transmission of: A—Milori blue, B—copper butyl-phthalate, C—bulb-green glass, D—film of white lead.

[6] A. H. Pfund, Zeits. f. Wiss. Phot. **12**, 341 (1913).

* According to a letter from Dr. H. P. Gage of the Corning Glass Works, bulb-green glass contains the largest amount of copper which had been incorporated in glass by the Corning Glass Works up to 1930.

† These measurements were obtained with a rocksalt spectrometer.

[7] A. H. Pfund, Phys. Rev. **36**, 71 (1930); J. Opt. Soc. Am. **23**, 375 (1933).

An Optical Investigation of Oxide Films on Metals

C. E. LEBERKNIGHT
Department of Physics, Carnegie Institute of Technology, Pittsburgh, Pennsylvania
AND
BENJAMIN LUSTMAN
Metals Research Laboratory Fellow, Carnegie Institute of Technology, Pittsburgh, Pennsylvania
(Received December 17, 1938)

Observations were made on the ellipticity resulting when plane-polarized light was reflected from iron and nickel surfaces covered with oxide films continuously increasing in thickness through the temper-color range. It was found that the results could be interpreted by the assumption of multiple reflections occurring within the film. The method permits a determination of the thickness and average optical properties of the film and may apparently be applied to the accurate measurement of the rate of formation of a film of any composition on a metal surface through the temper-color range. The index of refraction of the film on iron was found to be complex and to have the value 2.13–i.41. The optical constants of pure iron were also found to vary with temperature in such a manner that n in the expression $n(1-ix)$ increased with increasing temperature, while x decreased. It is further shown that the assumption of multiple reflections within the film gives the same results for thin films as the Drude transition layer theory.

PREVIOUS WORK ON DETERMINATION OF FILM THICKNESSES

VARIOUS methods have been employed for the determination of oxide film thicknesses on metals. H. A. Miley[1] has employed an electrometric method involving the measurement of the quantity of electricity required to reduce the film. A gravimetric method, in which the weight increments due to the oxidation of large metal surfaces were determined by the Conrady method of weighing, was used by W. H. J. Vernon.[2] The wave-lengths of maximum or minimum intensity of reflection from metal covered with oxide of temper-color thickness were measured spectrophotometrically by F. H. Constable;[3] knowing the index of refraction of the oxide, the film thickness may be determined. R. F. Mehl and E. L. McCandless[4] compared the temper color with a standard color gauge made of given thicknesses of a material with known optical properties. The optical behavior of oxide films on metals varying in thickness from 0 to 100A has been studied intensively by many investigators and recently especially by L. Tronstad;[5] the change in the state of polarization of light reflected from metal surfaces was observed, and the results were interpreted by application of the Drude transition layer theory.

Of the methods cited above, none is applicable to the continuous, accurate measurement of the growth of oxide films on small metal surfaces, except the last mentioned; and it appears improbable that the theory used by Tronstad can be extended to thicknesses of oxide films showing temper colors. It was therefore the purpose of this investigation to explore the possibility of applying the polarized light method to thick oxide films through the temper-color range of thicknesses; it is believed that the experimental method and theory outlined below furnish a reasonably accurate determination of the average optical constants and thickness of the film.

EXPERIMENTAL PROCEDURE AND RESULTS

In a preliminary series of experiments, plane-polarized light (polarized at 45° to the plane of incidence) was reflected from iron surfaces covered with various thicknesses of oxide and then analyzed by means of a quarter-wave plate and Nicol prism. This analysis yields two quantities, the phase difference between the components of light resolved parallel and perpendicular to the plane of incidence and the ratio of the components of amplitude parallel and perpendicular to the plane of incidence. The

[1] H. A. Miley, J. Iron and Steel Inst. **25**, 197 (1936).
[2] W. H. J. Vernon, Trans. Faraday Soc. **31**, 1674 (1935).
[3] F. H. Constable, Proc. Roy. Soc. **A117**, 376 (1928).
[4] R. F. Mehl and E. L. McCandless, Trans. A. I. M. E. **125**, 531 (1937).
[5] L. Tronstad, Det. Kgl. Norsk. Vidensk. Selsk. Skrift. No. 1 (1931).

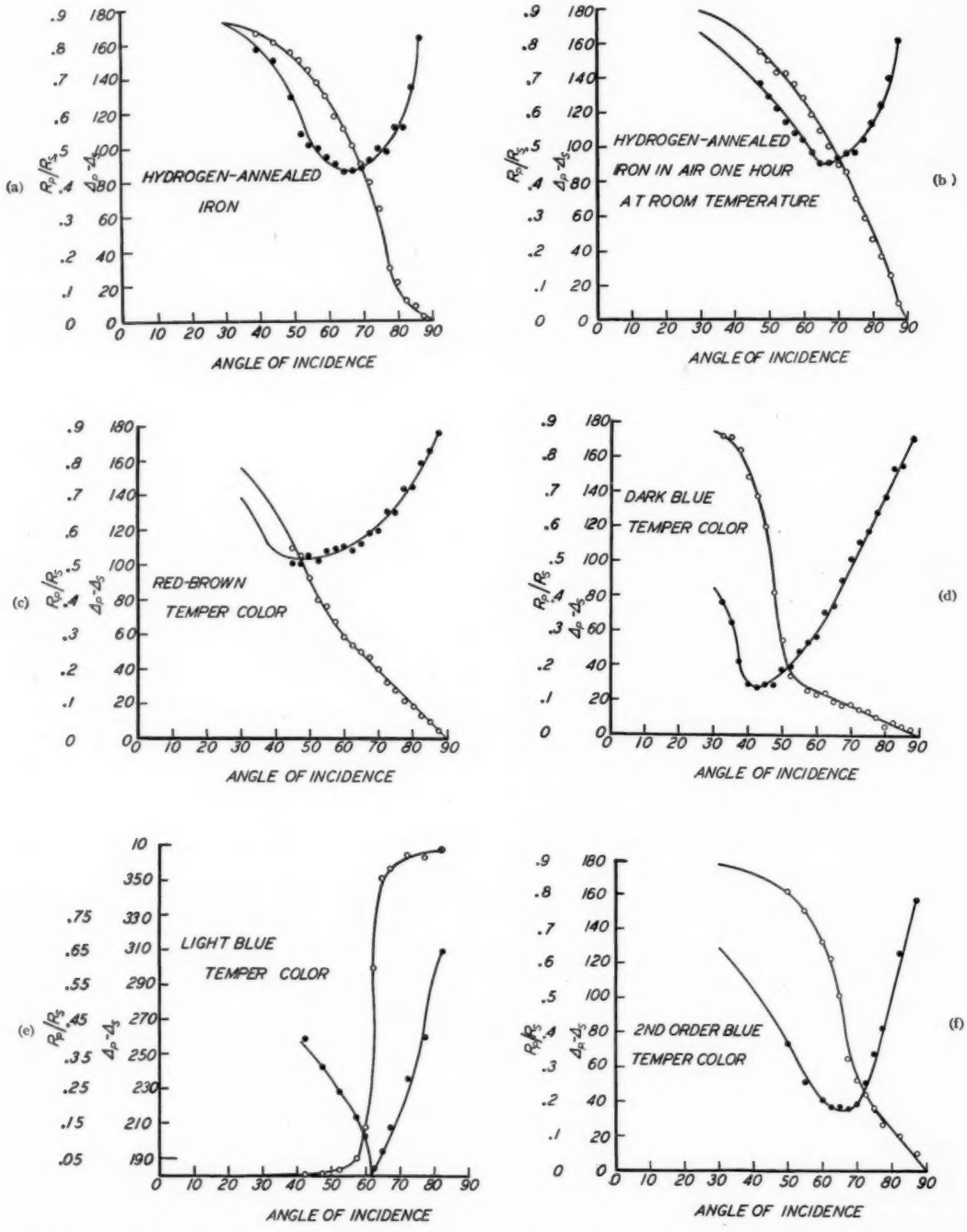

FIG. 1a–f. Variation with angle of incidence of phase difference and ratio of amplitudes for iron covered with various thicknesses of oxide films.

former quantity will be represented hereafter by the symbol $\Delta_p - \Delta_s$, the latter by R_p/R_s.

A group of experiments were carried out at various angles of incidence, and the results are plotted in Figs. 1a to 1f.* As the oxide thickness changes, it is evident that large changes occur in both phase difference and ratio of amplitudes. Similar experiments were performed on the natural bulk oxides hematite (Fe_2O_3) and magnetite (Fe_3O_4), and the results are shown in Figs. 2 and 3; these oxides are the ones formed on iron on heating in air below 570°C. Choosing the constant angle of incidence of 60°, it is evident that the phase difference decreases with increasing film thickness, and that the ratio of amplitudes curve goes through a minimum.

Having established the fact that large changes occur in the state of polarization of reflected plane-polarized light due to increasing thickness of oxide films even in the temper-color range, a more accurate apparatus, suitable for experimentation at constant angle of incidence, was constructed. The analysis was made considerably more accurate by the use of a half-shade analyzer described by Bruhat.[6] Provision was made for heating the specimen in purified hydrogen to remove the air-formed film prior to its oxidation; after this treatment the specimen was exposed to air and the course of its oxidation observed. The state of polarization of the reflected light could be observed during both oxidation and reduction. In Fig. 4 are plotted the results for the oxidation at 340°C of an iron single crystal previously deoxidized in hydrogen at 850°C. An angle of incidence of 60° was employed; a mercury arc light source together with a filter which transmitted only the green line of wave-length 5461A was used for these measurements. Experiments were also performed on a nickel polycrystalline specimen oxidized at 570°C, and the results are shown in Fig. 5.

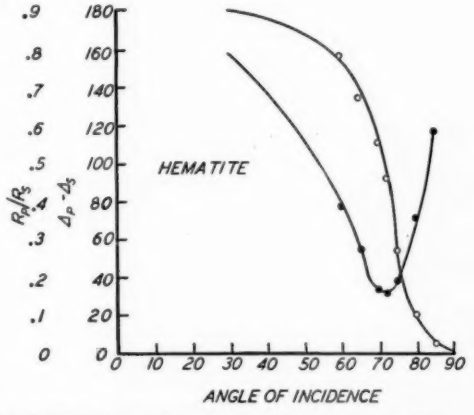

FIG. 2. Variation with angle of incidence of phase difference and ratio of amplitudes for hematite (Fe_2O_3).

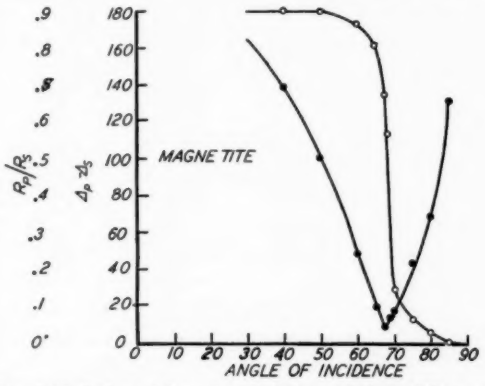

FIG. 3. Variation with angle of incidence of phase difference and ratio of amplitudes for magnetite (Fe_3O_4).

For a purely diffusional mechanism of oxide film growth, the square root of time plot used should make the abscissa directly proportional to thickness.[7] However, for the more complicated mechanism probably occurring in the formation of these thin films, this type of plot serves merely to emphasize the shape of the first part of the curves. In Fig. 4 the oxide film on iron has increased through one order of temper colors in the time shown; for nickel in Fig. 5, about two and one-half orders of temper colors have been formed. The types of curves obtainable at other constant angles of incidence may be derived from Figs. 1a to 1f.

THEORY

The state of polarization of light reflected from a film-covered metal may be calculated if it is assumed that reflection occurs at the top and

* In all the experimental curves, open circles refer to the phase difference, closed circles to the ratio of amplitudes.

[6] G. Bruhat, *Cours d'Optique* (Masson et Cie, 1935), p. 452.

[7] See *Review of Oxidation and Scaling of Heated Solid Metals* (H. M. Stationery Office, London, 1935), p. 1.

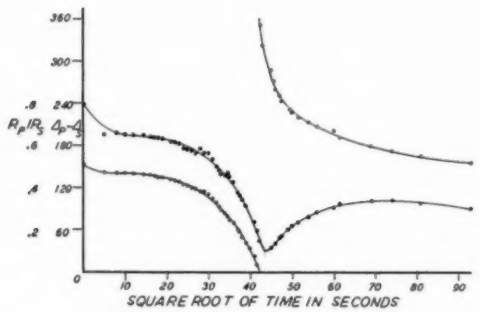

FIG. 4. Change in phase difference and ratio of amplitudes with time on heating iron at constant temperature in air as observed at an angle of incidence of 60°.

bottom surfaces of a homogeneous layer of finite thickness whose optical constants vary discontinuously from those of the underlying metal. Such an assumption is consistent with the mechanism of production of temper colors which is generally believed to be an interference process. G. Hauschild[8] indeed suggested this, but he showed no quantitative connection between observed and theoretical optical changes.

Assuming an infinite number of reflections within the film, Eq. (1) below may be derived.[9]

$$\bar{R}^* = (\bar{r} + \bar{r}_1 e^{-2i\bar{\delta}})/(1 + \bar{r}\bar{r}_1 e^{-2i\bar{\delta}}),$$

$$\bar{R}_p/\bar{R}_s\dagger = [R_p/R_s]e^{+i(\Delta_p - \Delta_s)}$$

$$= [(\bar{r}_p + \bar{r}_{1p}e^{-2i\bar{\delta}})(1 + \bar{r}_s\bar{r}_{1s}e^{-2i\bar{\delta}})]/$$

$$[(1 + \bar{r}_p\bar{r}_{1p}e^{-2i\bar{\delta}})(\bar{r}_s + \bar{r}_{1s}e^{-2i\bar{\delta}})], \quad (1)$$

where $\bar{r}$ = the Fresnel reflection formula for reflection at the air-layer surface and $\bar{r}_1$ = the Fresnel reflection formula for reflection at the layer-metal surface.

$$\bar{r}_p = (\bar{n}_2 \cos\phi_1 - \cos\bar{\phi}_2)/(\bar{n}_2 \cos\phi_1 + \cos\bar{\phi}_2),$$

$$\bar{r}_{1p} = (\bar{n}_3 \cos\bar{\phi}_2 - \bar{n}_2 \cos\bar{\phi}_3)/(\bar{n}_3 \cos\bar{\phi}_2 + \bar{n}_2 \cos\bar{\phi}_3),$$

$$\bar{r}_s = (\cos\phi_1 - \bar{n}_2 \cos\bar{\phi}_2)/(\cos\phi_1 + \bar{n}_2 \cos\bar{\phi}_2), \quad (2)$$

$$\bar{r}_{1s} = (\bar{n}_2 \cos\bar{\phi}_2 - n_3 \cos\bar{\phi}_3)/(\bar{n}_2 \cos\bar{\phi}_2 + \bar{n}_3 \cos\bar{\phi}_3),$$

$$\bar{\delta} = (2\pi l/\lambda_0)\bar{n}_2 \cos\bar{\phi}_2,$$

where ϕ_1 = the angle of incidence on the film
$\bar{\phi}_2$ = the angle of refraction into the film
$\bar{\phi}_3$ = the angle of refraction into the metal
$\bar{n}_2$ = the index of refraction of the film
$\bar{n}_3$ = the index of refraction of the metal
l = the thickness of the layer
and λ_0 = the wave-length of the light in air.

If, as an approximation, only the first reflection at the top surface of the film and the first at the bottom surface are considered, Eq. (1) becomes

$$[R_p/R_s]e^{+i(\Delta_p - \Delta_s)} = [\bar{r}_p + e^{-2i\bar{\delta}}(1 - \bar{r}_p^2)\bar{r}_{1p}]/$$

$$[\bar{r}_s + e^{-2i\bar{\delta}}(1 - \bar{r}_s^2)\bar{r}_{1s}]. \quad (3)$$

If the index of refraction of the film is complex, there is obtained from Eq. (3) the following equation, letting

$$2\bar{\delta} = (4\pi l/\lambda_0)(\bar{n}_2^2 - \sin^2\phi_1)^{\frac{1}{2}} = A - iB,$$

$$[R_p/R_s]e^{+i(\Delta_p - \Delta_s)} = \{\bar{r}_p + e^{-B}[e^{-iA}(1 - \bar{r}_p^2)\bar{r}_{1p}]\}/$$

$$\{\bar{r}_s + e^{-B}[e^{-iA}(1 - \bar{r}_s^2)\bar{r}_{1s}]\}. \quad (4)$$

Evidently with a complex film index a damped phase difference-thickness or ratio of amplitudes-thickness curve will be obtained, which as the thickness increases will tend to approach the form for reflection from the film-air surface alone.

$$[R_p/R_s]e^{i(\Delta_p - \Delta_s)} = \bar{r}_p/\bar{r}_s.$$

In Figs. 6, 7 and 8 some curves are plotted from Eq. (4) for various assumed values of the index of the film. The only approximations made in calculating these curves were the use of two reflections instead of an infinite number and the neglecting of $\sin^2\phi_1$ as compared to $\bar{n}_3^2$.

If the index of the film is assumed to be real, Eq. (3) may be solved directly for thickness. However, as will be shown below, such an assumption is invalid in this case.

DISCUSSION AND CONCLUSIONS

By comparison of the curves above with the experimentally derived curves (Figs. 4 and 5), it is evident that while the assumption of real indices will explain qualitatively the changes in phase difference, such a postulate will by no means explain the course of the ratio of amplitudes. The assumption of a complex index will, however, cause closer correspondence of theoretical and experimental curves. It will further be

[8] G. Hauschild, Ann. d. Physik **10** (15), 816 (1920).
[9] K. Försterling, *Lehrbuch der Optik* (Verlag von S. Hirzel, 1928), p. 124.
* Barred quantities are complex.
† The subscripts p and s refer, respectively, to the components parallel and perpendicular to the plane of incidence.

noted from Figs. 6, 7 and 8, that while the substitution of various absorption indices in Eq. (4) causes only a lateral shift in the phase difference curves, certain characteristic changes varying in amount with change in the real part of the optical constants occur in the ratio of amplitudes curves. Therefore, by comparison of the theoretical and experimental ratios of amplitudes at the same phase difference values, one may estimate an average value for the optical properties of the film. Thus for the oxide film on iron, an average index of 2.13–i.41 seems to be the most probable value.

For the films considered in this investigation, both refractive and absorptive indices as well as film thickness are unknown. It is therefore impossible from a single reading to determine all three quantities. However, by the use of a continuously increasing film thickness experimentally obtained by allowing the metal to oxidize uninterruptedly at constant temperature, curves may be obtained which depend characteristically on the optical constants of the film. Thus, although the abscissas of the experimentally derived curves 4 and 5 may bear no apparent relation to the thickness of the film, the course of the complete oxidation cycle allows the determination of an average index by the method outlined in the preceding paragraph; using this average index, the thickness of the film may be determined.

The experiment on nickel shown in Fig. 5 was made to confirm the validity of the theory. Nickel is known to go through more orders of temper colors on oxidation than does iron; this evidently means that the film on nickel is less absorbing than that on iron. It was found, in fact, that an index for the nickel oxide film of 2-i.2 (see Fig. 6) gives a theoretical curve corresponding closely to that actually observed. Curves 6, 7 and 8 are, of course, not strictly comparable to Fig. 5, since the former were calculated from the optical constants of iron; however, the constants of iron and nickel are sufficiently alike to make a qualitative comparison permissible.

It will be noted from Figs. 6, 7 and 8 that the phase difference and ratio of amplitudes curves for various film indices do not extrapolate to the same points on the zero thickness axis. This is because Eq. (4) is not rigorously correct for very small film thicknesses and does not reduce to the form for metallic reflection alone at zero film thickness as does the complete expression (1). However, the error in using Eq. (4) is comparatively small, and at film thicknesses exceeding some 50A the difference between the infinite reflections and the two-reflection expressions is negligible. Indeed for absorbing films the latter assumption would seem to be sufficiently correct.

That the oxide film on iron at least through the temper-color range is Fe_2O_3 is substantiated by considerable evidence. It is indicated, for example, by the chemical evidence of Miley[1] and by the electron diffraction results of Nelson.[10] The value of the index of refraction ordinarily given for bulk Fe_2O_3 is 3, which is the value obtainable from Fig. 2. Tronstad,[5] indeed, found for very thin films of oxide on iron an index of 3 by application of the Drude theory. It will be observed that this value differs considerably from that obtained in the present investigation. Constable[3] finds, on the other hand, an index for the oxide film on iron very close to the real part of the index experimentally determined in this investigation.

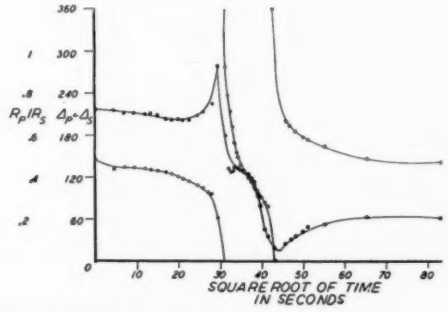

FIG. 5. Change in phase difference and ratio of amplitudes with time on heating nickel specimen in air at constant temperature as observed at an angle of incidence of 60°.

As may be seen from Eq. (5), it should be possible to obtain the index of the film (if it is absorbing) by observation of the constant values of R_p/R_s and $\Delta_p-\Delta_s$ toward which the curves tend. This value of index is found to be approximately 2-i.9, which as is evident from Fig. 4

[10] H. R. Nelson, J. Chem. Phys. 5, 252 (1932).

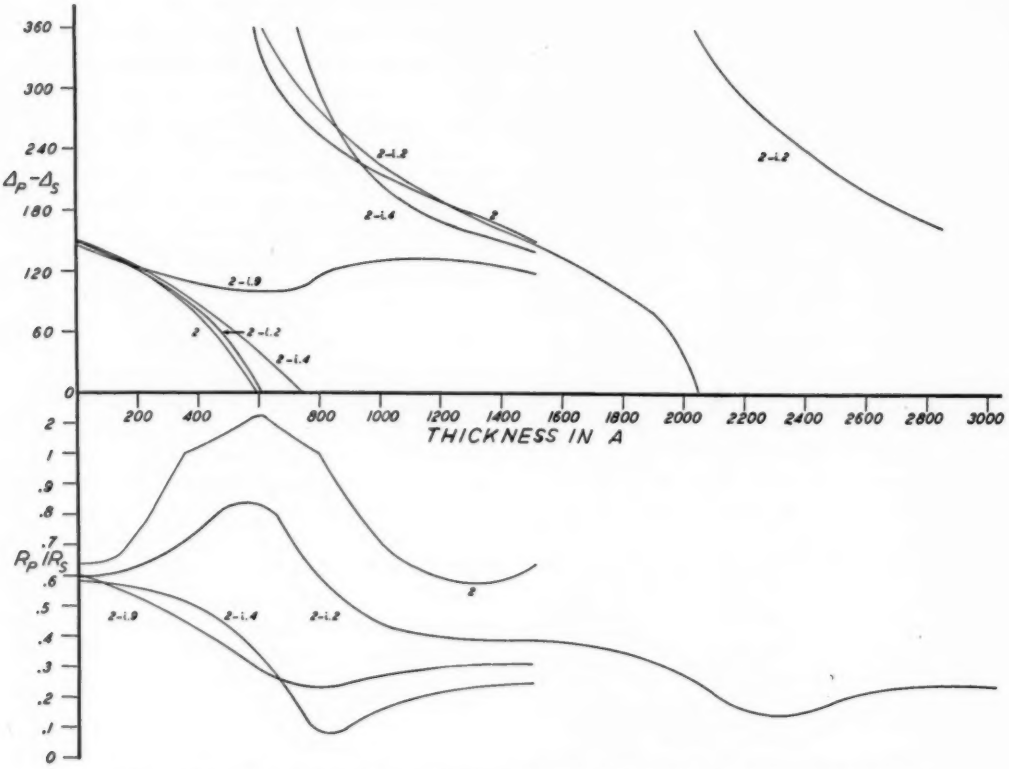

FIG. 6. Calculated variation of phase difference and ratio of amplitudes with increasing thickness of film of various assumed indices.

does not fit the experimental values. However, Evans[11] has found that an underlying layer of Fe_3O_4 tends to form below the Fe_2O_3 layer at film thicknesses near the end of the second order of temper colors which may account for the high absorption index.

The optical constants n and x (in the expression $\tilde{n}_3 = n(1-ix)$) of oxide film-free iron were found to vary with temperature as shown in Fig. 9. These curves were obtained in the following way. A polished specimen of iron was heated to 850°C for two hours in purified hydrogen and then cooled to room temperature. It was then heated slowly in hydrogen to the upper temperature shown in Fig. 9, being stopped at certain temperatures to allow determination of the optical constants. The specimen was then cooled in the same way, with readings taken at the same temperatures as on heating, and finally was reheated. Thus each of the points in Fig. 9 are averages of three readings, and the individual curves on each heating and cooling coincide to within the limits of accuracy of the method used. Thus the change in the constants could hardly be attributed to the formation and reduction of a film since the film would hardly form and disappear reversibly. Most of the previous work summarized by J. B. Nathanson[12] has shown very slight, if any, change in the optical constants of metals with temperature. If these results represent a real variation of the optical constants of pure iron, then another variable is introduced into the determination of oxide thicknesses at the temperature of oxidation; this in no way

[11] U. R. Evans, J. Chem. Soc. 1020 (1927); 428 (1930).

[12] J. B. Nathanson, J. Opt. Soc. Am. 28, 300 (1938).

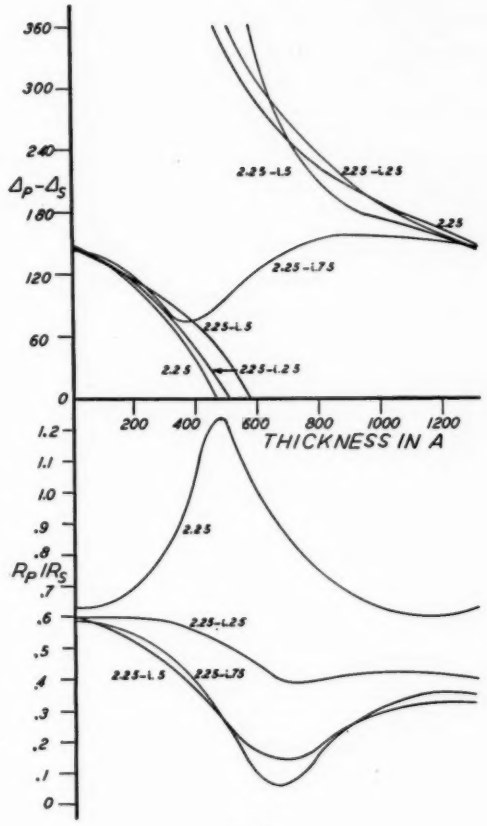

FIG. 7.

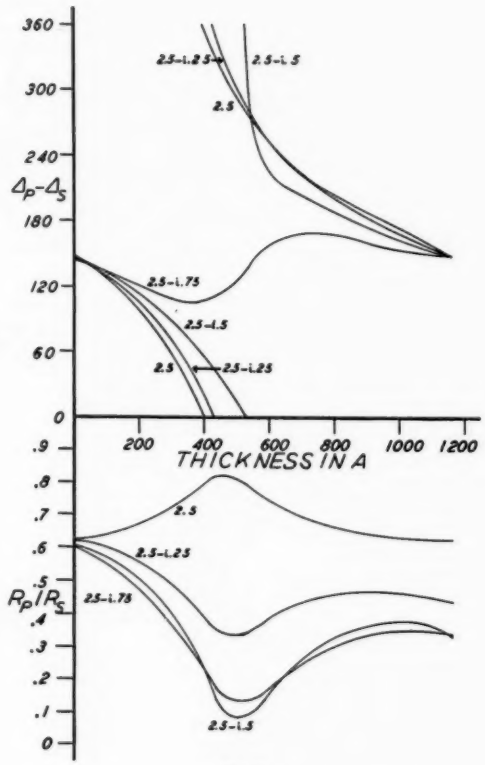

FIG. 8.

FIGS. 7, 8. Calculated variation of phase difference and ratio of amplitudes with increasing thickness of film of various assumed indices.

reduces the validity of the method, although the complexity of evaluation of experimental data is increased.

It will be noted that Eq. (4) explains the complete course of the oxidation cycle, and that recourse need not be had to the transition layer theory for small film thicknesses. Indeed it appears probable that the Drude theory is but an approximation for small thicknesses to the more rigorous form of Eq. (1). That this is so will be shown in the appendix.

APPENDIX

In order to show that the assumption of multiple reflections within a thin film separating two media gives essentially the same result as that obtained by Drude's assumption of a transition layer, first consider a plane electromagnetic wave striking the boundary between two media having refractive indices n_1 and n_2. Let the plane of incidence be the x-z plane (Fig. 10a); the z axis being positive downwards. Resolve the electric and magnetic vectors of the incident, reflected, and refracted waves into com-

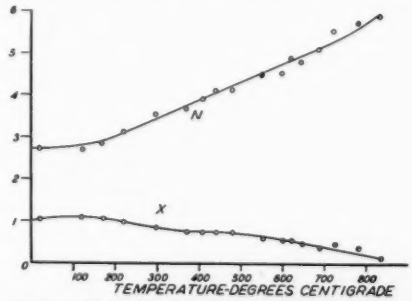

FIG. 9. Variation of optical constants of iron with temperature.

ponents parallel and perpendicular to the plane of incidence. The positive direction of the parallel components is shown in Fig. 10a, while the positive direction of the perpendicular components projects from the plane of the paper, i.e., along the y axis. The x, y, and z components of the electric and magnetic vectors of the waves then have the following values: (the subscripts p and s refer to the parallel and perpendicular components respectively)

$$\left.\begin{aligned} x_1&=E_p\cos\phi_1 e^{(ir2/\lambda_0)(ct-n_1 s_1)}\\ y_1&=E_s\qquad e^{(ir2/\lambda_0)(ct-n_1 s_1)}\\ z_1&=-E_p\sin\phi_1 e^{(ir2/\lambda_0)(ct-n_1 s_1)}\end{aligned}\right\}\ \text{incident electric vector}$$

$$\left.\begin{aligned} \alpha_1&=-n_1E_s\cos\phi_1 e^{(ir2/\lambda_0)(ct-n_1 s_1)}\\ \beta_1&=\ n_1E_p\qquad e^{(ir2/\lambda_0)(ct-n_1 s_1)}\\ \gamma_1&=\ n_1E_s\sin\phi_1 e^{(ir2/\lambda_0)(ct-n_1 s_1)}.\end{aligned}\right\}\ \text{incident magnetic vector}$$

There are similar expressions for the reflected and refracted waves. In the above expressions, c=velocity of light in vacuum, λ_0=wave-length in vacuum, and $s_1=x\sin\phi_1+z\cos\phi_1$.

Now consider the system of reflected waves shown in Fig. 10b to be replaced by the system shown in Fig. 10c, where R is a wave equivalent to all the reflected waves leaving the film, D is the equivalent of all waves entering medium (3), and A and B are the equivalent of all waves in the film. Applying the usual boundary conditions at the boundaries $z=0$ and $z=l$ the following equations are obtained.

At the surface $z=0$:

$$\begin{aligned}(E_p-R_p)\cos\phi_1&=(A_p-B_p)\cos\phi_2\\ (E_p+R_p)n_1&=(A_p+B_p)n_2,\end{aligned}\qquad(1)$$

$$\begin{aligned}E_s+R_s&=A_s+B_s\\ (E_s-R_s)n_1\cos\phi_1&=(A_s-B_s)n_2\cos\phi_2.\end{aligned}\qquad(2)$$

At the surface $z=l$:

$$\begin{aligned}(A_pe^{-i\tau_A}-B_pe^{-i\tau_B})\cos\phi_2&=D_pe^{-i\tau_D}\cos\phi_3\\ (A_pe^{-i\tau_A}+B_pe^{-i\tau_B})n_2&=D_pe^{-i\tau_D}n_3,\end{aligned}\qquad(3)$$

$$\begin{aligned}A_se^{-i\tau_A}+B_se^{-i\tau_B}&=D_se^{-i\tau_D}\\ (A_se^{-i\tau_A}-B_se^{-i\tau_B})n_2\cos\phi_2&=D_se^{-i\tau_D}n_3\cos\phi_3,\end{aligned}\qquad(4)$$

where
$$\begin{aligned}\tau_A&=2\pi/\lambda_0 n_2(x\sin\phi_2+l\cos\phi_2)\\ \tau_B&=2\pi/\lambda_0 n_2(x\sin\phi_2-l\cos\phi_2)\\ \tau_D&=2\pi/\lambda_0 n_3(x\sin\phi_3+l\cos\phi_3).\end{aligned}$$

By eliminating D_p and B_p/A_p from Eqs. (1) and (3), the following equation is obtained:

$$\frac{R_p}{E_p}=\left(\frac{n_3\cos\phi_1-n_1\cos\phi_2}{n_3\cos\phi_1+n_1\cos\phi_3}\right)\left(\frac{1+aP}{1+bP}\right),\qquad(5)$$

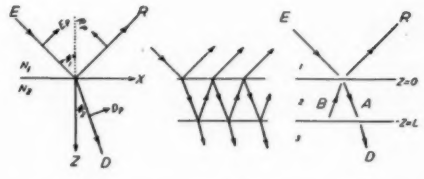

FIG. 10. a. Illustration of sign convention. b. Reflection system assumed to occur within the film. c. Reflection system assumed equivalent to system of 10b.

where
$$a=\frac{n_1\cos\phi_1}{n_3\cos\phi_1-n_1\cos\phi_3}\left(\frac{n_2\cos\phi_3}{n_1\cos\phi_2}-\frac{n_3\cos\phi_2}{n_2\cos\phi_1}\right)$$

$$b=\frac{n_1\cos\phi_1}{n_3\cos\phi_1+n_1\cos\phi_3}\left(\frac{n_2\cos\phi_3}{n_1\cos\phi_2}+\frac{n_3\cos\phi_2}{n_2\cos\phi_1}\right)$$

$$P=\frac{e^{i(\tau_A-\tau_B)}-1}{e^{i(\tau_A-\tau_B)}+1}=\frac{i\sin\delta}{1+\cos\delta},$$

where $\delta=\tau_A-\tau_B=(4\pi l/\lambda_0)n_2\cos\phi_2$.

In a similar manner, the following equation is obtained from Eqs. (2) and (4):

$$\frac{R_s}{E_s}=\left[\frac{n_1\cos\phi_1-n_3\cos\phi_3}{n_1\cos\phi_1+n_3\cos\phi_3}\right]\left[\frac{1+cP}{1+dP}\right],\qquad(6)$$

where

$$c=\frac{1}{n_1\cos\phi_1-n_3\cos\phi_3}\left(\frac{n_1n_3\cos\phi_1\cos\phi_3}{n_2\cos\phi_2}-n_2\cos\phi_2\right)$$

$$d=\frac{1}{n_1\cos\phi_1+n_3\cos\phi_3}\left(\frac{n_1n_3\cos\phi_1\cos\phi_3}{n_2\cos\phi_2}+n_2\cos\phi_2\right).$$

In Eqs. (5) and (6) the first brackets give the Fresnel reflection coefficients if there were no film present. Hence, for thin films for which P reduces to $i\delta/2$, the terms involving P can be regarded as small quantities, and then division of Eq. (5) by Eq. (6) gives as a result the following expression in which the dielectric constants have been substituted for the square of the refractive indices:

$$\frac{R_p}{R_s}=\frac{(r_{1,3})_p}{(r_{1,3})_s}\left\{1+\frac{4\pi lk_2\sqrt{k_1}\cos\phi_1\sin^2\phi_1}{\lambda_0(k_3-k_1)k_3\cos^2\phi_1-k_1\sin^2\phi_1}\times\left(k_2+\frac{k_1k_3}{k_2}-k_1-k_3\right)\right\}.$$

This expression is identical with the result obtained by the Drude transition layer theory.[13]

[13] M. Born, *Optik* (Julius Springer, 1933), p. 39.

The Effect of Gradual Light Absorption in Photographic Exposure*

LUDWIK SILBERSTEIN
Eastman Kodak Research Laboratories, Eastman Kodak Company, Rochester, New York
(Received October 21, 1938)

IN our previous treatment of the subject all the silver halide grains contained in the layer of emulsion were assumed to be exposed to one and the same light intensity. This is legitimate in the case of a very thin coating, the so-called single-layer coating, as applied in microphotographic experiments. Under usual circumstances, however, when the thickness of the emulsion layer is not negligible, the radiation is gradually absorbed in traversing the layer, so that the grains placed at a greater depth receive a lesser exposure than those spread at or near the upper surface of the layer. It has, therefore, seemed interesting to investigate to what extent our previous formulae are modified by this factor.

The effect of gradual light weakening by absorption has been treated by W. J. Albersheim.[1] His investigation, however, is limited to the ideal case of equal grains, and the resulting formula contains an integral which cannot be evaluated in a finite form and is thus not amenable to an easy quantitative discussion. The corresponding sensitometric curve, for single quantum hits, is in Mr. Albersheim's own opinion "unsatisfactory," though it is somewhat improved by the assumption of double quantum hits. It may be mentioned also that Albersheim's elementary exposure formula does not imply at all the size of the grains.

Now, it has occurred to me that if instead of equal grains a whole range of grain sizes is considered, especially of the exponential type of frequency distribution, the aforesaid integral can be readily evaluated in finite form, leading to a compact aggregate of rational algebraic and logarithmic terms. The reason for this reducibility is that an integration over all sizes simplifies (rationalizes) the expression which is then easily integrated over the whole thickness of the emulsion layer. This remark will become plain from the actual derivation which follows.

The total thickness of the emulsion layer being b, let, in our previous notation, $E=\epsilon n$ be the incident exposure (*viz.* at the upper surface $x=0$), κ the absorption coefficient of the emulsion and, therefore, if we assume Beer's simple law,

$$E_x=Ee^{-\kappa x} \tag{1}$$

the exposure at a depth x. Let $N_a=f(a)da$ be the number, per unit area of the base, of grains of size (area) ranging from a to $a+da$, supposed to be uniformly distributed throughout the thickness of the emulsion. Then the number of such grains contained within a layer of thickness dx placed at a depth x will be $N_a dx/b$, and the number of those affected by the exposure E_x, on the single-quantum assumption,

$$\frac{N_a dx}{b}(1-e^{-aE_x}).$$

Thus, the total number of grains of this class made developable within the whole layer,

$$k_a=(N_a/b)\int_0^b (1-e^{-E_x a})dx.$$

Instead of x introduce the integration variable $z=e^{-\kappa x}$. Then, by (1), $E_x=Ez$, $dx=-dz/\kappa z$, and

$$k_a=\frac{N_a}{b\kappa}\int_{e^{-\kappa b}}^1 (1-e^{-aEz})\frac{dz}{z}.$$

Here $e^{-\kappa b}=T$ is the *transparency* of the plate and $bk=-\log T$, so that

$$k_a=N_a+\frac{N_a}{\log T}\int_T^1 e^{-aEz}\frac{dz}{z}.$$

Thus, the density $D=M\Sigma a k_a$ due to grains of all sizes,**

$$D=M\int_0^\infty af(a)da + \frac{M}{\log T}\int_{a=0}^\infty af(a)\int_{z=T}^1 e^{-aEz}\frac{dz}{z}\cdot da,$$

* Communication No. 691 from the Eastman Kodak Research Laboratories.

[1] W. J. Albersheim, J. Soc. Mot. Pict. Eng., p. 417, October (1937).

** We assume, of course, that the opaque emulsion with the unaffected grains is removed in the process of fixing and thus does not contribute to the density D.

where $M=\text{Log } e=0.4343$, or, since

$$M\int_0^\infty af(a)da=M\cdot N\bar{a}=D_m$$

is the limiting density,

$$D=D_m+\frac{M}{\log T}\int_0^\infty af(a)\left[\int_T^1 e^{-aEz}\frac{dz}{z}\right]da.$$

Now, as mentioned above, the bracketed integral, relating to equal grains, is not reducible to elementary functions.† But we can invert the order of integrations with respect to z and a, writing

$$D-D_m=\frac{M}{\log T}\int_T^1\frac{dz}{z}\int_0^\infty af(a)e^{-aEz}da, \quad (2)$$

and then, for certain forms of the frequency function $f(a)$, the second integral becomes a simple algebraic function of z and the complete integral can at once be evaluated.

Such is the case especially for an exponential size-frequency distribution. In fact, if

$$f(a)=(N/\bar{a})e^{-a/\bar{a}},$$

where N is the total number of grains over unit area of the plate and $\bar{a}$ the average grain size, then

$$\int_0^\infty af(a)e^{-aEz}da=\frac{N}{\bar{a}}\int_0^\infty ae^{-a(Ez+1/\bar{a})}da=\frac{N\bar{a}}{(1+\bar{a}Ez)^2}.$$

Thus, by (2), and recalling that $MN\bar{a}=D_m$,

$$\frac{D}{D_m}=1+\frac{1}{\log T}\int_T^1\frac{dz}{z(1+\bar{a}Ez)^2}=1+\frac{1}{\log T}\int_{\bar{a}ET}^{\bar{a}E}\frac{du}{u(1+u)^2}.$$

Now, $$\int\frac{du}{u(1+u)^2}=\log\frac{u}{1+u}+\frac{1}{1+u}.$$

Thus, with the abbreviation $y=\bar{a}E$, the photographic density formula ultimately becomes

$$\frac{D}{D_m}=\frac{1}{\log T}\left\{\log\frac{1+Ty}{1+y}+\frac{1}{1+y}-\frac{1}{1+Ty}\right\}. \quad (3)$$

Here T is the transparency of the unexposed material, a proper fraction which is, generally, about $\frac{1}{3}$ and sometimes even as low as $\frac{1}{10}$. Thus the effect of the gradual light absorption will be considerable.

If we let $T=1-\alpha$ tend to unity (perfect transparency), then

$$\log\frac{1+Ty}{1+y}=-\frac{dy}{1+y}, \quad \frac{1}{1+Ty}-\frac{1}{1+y}=\frac{dy}{(1+y)^2},$$

and since $\log T=-\alpha$, (3) reduces to

$$\frac{D}{D_m}=\frac{y(2+y)}{(1+y)^2}, \quad (3.1)$$

identical with our previous formula based on the assumption of a unique exposure, equal for all grains.

To see the effect of gradual absorption take the case of $T=0.1$. Then $\log T=-1/M$ and Eq. (3) becomes

$$\frac{D}{D_m}=\text{Log}\frac{1+y}{1+0.1y}+M\left(\frac{1}{1+0.1y}-\frac{1}{1+y}\right).$$

This gives the following set of relative densities.

y	$\frac{1}{32}$	$\frac{1}{16}$	$\frac{1}{8}$	$\frac{1}{4}$	$\frac{1}{2}$	1
D/D_m	0.024	0.047	0.089	0.163	0.279	0.437
y	∞	1.466	2	4	8	16	32
D/D_m		0.536	0.615	0.776	0.892	0.957	0.986.

The corresponding curve, with

$$\text{Log } y=\text{Log } (\bar{a}E)$$

as abscissa and D/D_m as ordinate, is drawn in Fig. 1, together with the curve (3.1) corresponding, *caeteris paribus*, to $T=1$. The two curves show a marked difference.

Returning to formula (3), for any T, let us write it briefly

$$D=\frac{D_m}{\log T}F(y)=\frac{MN\bar{a}}{\log T}F(y).$$

† $\int_\infty^{-z}(e^{-z}/z)dz$ is the so-called exponential integral, usually denoted by $Ei(z)$.

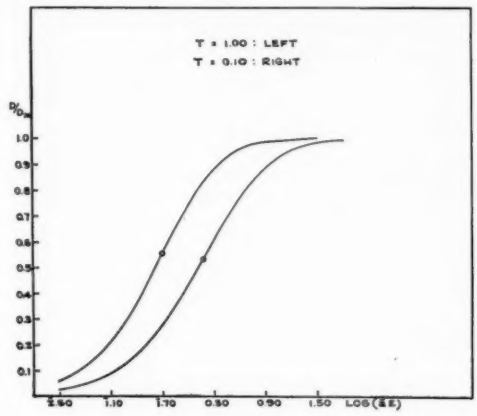

FIG. 1.

The gradient at any point of the D, Log y curve is

$$g=\frac{N\bar{a}}{\log T}yF'(y).$$

The inflection point of the curve is determined by $(dg/dy)=0$, i.e., by the equation

$$F'(y)+yF''(y)=0.$$

Now, by (3),

$$F'(y)=\frac{T(2+Ty)}{(1+Ty)^2}-\frac{2+y}{(1+y)^2},$$

whence F'', and the last equation becomes, after simple reductions, $(1+Ty)^3=T(1+y)^3$, or

$$\frac{1+T\bar{y}}{1+\bar{y}}=T^{\frac{1}{3}}, \tag{4}$$

a linear equation for $\bar{y}=\bar{a}\bar{E}$, belonging to the inflection point. The corresponding density is, by (3),

$$\frac{\bar{D}}{D_m}=\frac{1}{3}-\frac{1-T^{\frac{1}{3}}}{(1+T\bar{y})\log T}. \tag{4.1}$$

Finally, substituting $\bar{y}$ in the general expression of the gradient g, we have gamma or the "contrast,"

$$\gamma=\frac{N\bar{a}}{\log T}\bar{y}F'(\bar{y}), \tag{5}$$

where $F'(y)$ is as above.

Thus, e.g., for $T=\frac{1}{10}$,

$$\left.\begin{aligned}\bar{y}=\bar{a}\bar{E}=1.466,\quad \bar{D}/D_m=0.536,\\ \gamma=0.259N\bar{a}.\end{aligned}\right\}(T=0.1)$$

For $T=1$ we have, by formula (3.1),

$$\bar{y}=\tfrac{1}{2},\quad \gamma=(8/27)N\bar{a}=0.296N\bar{a},\quad (T=1)$$

so that γ is somewhat lowered by the gradual absorption of light, while the inflection point is shifted from $\bar{a}\bar{E}=\frac{1}{2}$ to 1.47, i.e., to an almost threefold exposure, as shown in the diagram of the two curves.

We have, so far, adhered to the assumption of single-quantum hits. The case of two or more light quanta, as the minimum required for the developability of a grain, can be treated with equal ease, leading again (for exponential frequency distribution) to rational algebraic integrals. It may suffice to develop here in detail the case of two quanta. At the same time, however, the general formula (2) can be written, for any distribution, in a more convenient form.

The exposure at a depth x being $E_x=E\cdot e^{-\kappa x}$, as before, let

$$\bar{D}_x(dx/b)$$

be the photographic density contributed by the layer dx under this exposure. Since the distribution of grains throughout the depth is supposed to be uniform, $\bar{D}_x$ itself stands for the density which would be given by the whole coating if it had received throughout a unique exposure E_x, i.e., in absence of absorption. Now, the total actual density D is the sum or integral of the densities contributed by the infinitesimal layers. Thus, if we write again $e^{-\kappa x}=z$,

$$D=\frac{1}{b}\int_0^b \bar{D}_x dx=-\frac{1}{b\kappa}\int_1^T \bar{D}_z\frac{dz}{z}$$

or, ultimately,

$$D=\frac{1}{\log T}\int_1^T \bar{D}(Ez)\frac{dz}{z}, \tag{6}$$

where $\bar{D}(Ez)$ is the density which would be obtained by giving to *the whole emulsion a unique exposure* Ez, in other words, as if the plate were perfectly transparent. This equation holds, of course, for any emulsion and independently of

any theory of exposure, being based only on the additivity of densities.

Thus, if $\bar{D}$ is known as a function of exposure, the density D, modified by the gradual absorption, follows from it by the indicated integration, whether the $\bar{D}$, E curve has been arrived at theoretically or is just an empirical curve.

Before applying the Eq. (6) to a particular form of $\bar{D}$, we may derive from it some general conclusions.

Write for the moment $Ez=u$. Then, since $d\bar{D}/dE=z\bar{D}'(u)$, we have from (6)

$$\frac{dD}{dE}=\frac{1}{E\log T}\int_E^{TE}\bar{D}'(u)du=\frac{\bar{D}(TE)-\bar{D}(E)}{E\log T}.$$

Now, the gradient at any point of the D, Log E curve is $g=(E/M)(dD/dE)$. Thus,

$$g=\frac{\bar{D}(TE)-\bar{D}(E)}{\text{Log } T}. \tag{6.1}$$

If the $\bar{D}$, E curve is given, say graphically, the gradient of the resultant D, Log E curve can be read off directly by taking the difference of pairs of ordinates $\bar{D}$, at E and at TE. If, for example, $T=0.1$, Log $T=-1$, and

$$g=\bar{D}(E)-\bar{D}(\tfrac{1}{10}E).$$

Thus, if but a single point of the D, Log E curve is known, the whole curve can be traced.

The inflection point of the D, Log E curve is determined by $dg/dE=0$, and thus by the equation

$$T\bar{D}'(T\bar{E})=\bar{D}'(\bar{E}), \tag{6.2}$$

and if the value of $\bar{E}$ derived therefrom is substituted in (6.1), we have

$$\gamma=\frac{1}{\text{Log } T}[\bar{D}(T\bar{E})-\bar{D}(\bar{E})], \tag{6.3}$$

without ever evaluating the integral in (6).

Let us now apply these general formulae to the case of an exponential distribution $f(a)$, as before, but under the assumption that, instead of one, *two quanta* are required for the developability of a grain. When the gradual absorption of radiation is disregarded, we have in this case[2]

$$\bar{D}=D_m\frac{y^2(3+y)}{(1+y)^3}, \tag{7}$$

where $y=\bar{a}E$, as before. Thus we have to substitute in (6)

$$\bar{D}(Ez)=D_m\frac{y^2z^2(3+yz)}{(1+yz)^3}. \tag{7.1}$$

This gives

$$\log T\cdot\frac{D}{D_m}=y^2\int^T\frac{z(3+yz)}{(1+yz)^3}dz=y^2\{3I_1+yI_2\},$$

where

$$I_1=\int_1^T\frac{zdz}{(1+yz)^3}=\frac{1}{y^2}\left|\frac{1}{2(1+u)^2}-\frac{1}{1+u}\right|_y^{Ty}$$

and $$I_2=\int_1^T\frac{z^2dz}{(1+yz)^3}=\frac{1}{y^3}\log\frac{1+Ty}{1+y}+\frac{1}{2y^3}\left[\frac{1}{(1+Ty)^2}-\frac{1}{(1+y)^2}\right]-\frac{2}{y}I_1.$$

Whence, after simple reductions, the required density formula corresponding to the assumption of *two quanta*,

$$\frac{D}{D_m}=\frac{1}{\log T}\left\{\log\frac{1+Ty}{1+y}+\frac{y}{(1+y)^2}-\frac{Ty}{(1+Ty)^2}\right\}. \tag{8}$$

The first bracketed term is as in (3), for single-quantum hits, but the last two terms are modified. This makes an essential difference. For, whereas, for a single quantum D is initially proportional to the first power of the exposure, we now have, from (8), the power series

$$\log T\cdot\frac{D}{D_m}=y^2\left\{\frac{3}{2}(T^2-1)-\frac{8}{3}(T^3-1)y+\cdots\right\}, \tag{8.1}$$

which starts with *the square of the exposure*, $y^2=\bar{a}^2E^2$. Notice that $\log T<0$, so that the terms of the series for D are intermittently positive and negative. Such, in fact, is also the

[2] Cf. L. Silberstein and A. Trivelli, J. Opt. Soc. Am. **28**, 441 (1938).

series in absence of absorption, but the coefficients of the terms are now numerically modified.

From (7) follows

$$\bar{D}' = 6D_m y/(1+y)^4,$$

so that the Eq. (6.2) for *the inflection point* of the D, Log E curve becomes

$$T^2\bar{y}/(1+T\bar{y})^4 = \bar{y}/(1+\bar{y})^4,$$

whence the simple formula

$$\bar{y} = \bar{a}\bar{E} = 1/\sqrt{T}. \qquad (8.2)$$

For $T=1$, $\bar{y}=1$, in agreement with our previous result. With decreasing transparency the inflection point is, of course, shifted forward, the inflection-exposure being proportional to the square root of the opacity. This value of $\bar{y}$ gives at once, by (6.3) and (7), the formula for the corresponding *gamma*,

$$\frac{\gamma}{D_m} = \frac{(3+\sqrt{T})T-(1+3\sqrt{T})}{\text{Log } T\cdot(1+\sqrt{T})^3} = \frac{F(T)}{\text{Log } T}, \text{ say.} \qquad (8.3)$$

The ratio of γ and the limiting density is thus a function of the transparency T alone. For $T=1$ its value is $3/8M$,* and for $T=\frac{1}{10}$ somewhat smaller, namely, $0.308/M$.

The formulae (8) to (8.3) hold under the *two-quanta* assumption. We might treat, with equal ease, the case of three or more quanta, which would give densities initially proportional to the cube or higher powers of the exposure. But since none of the emulsions so far investigated shows an increase of density more rapid than that of E^2, the two cases treated above will suffice.

The relative photographic density D/D_m is expressed by (8) as a function of the variable y alone with the transparency T of the emulsion layer or, practically, of the whole film,† as parameter, without any adjustable constants. The variable y has been defined by $y=\bar{a}E$, $E=\epsilon n$, so that

$$y = \bar{a}\epsilon n,$$

where ϵ is a purely numerical fraction, to be evaluated experimentally, and n the total number of light quanta, per unit area, penetrating the layer of emulsion just at its uppermost surface. The number n is thus proportional to the *total exposure* given to the film, say expressed in ergs/cm^2. Let us henceforth denote this exposure by E, dropping the previous meaning of this symbol. If the exposure is monochromatic, of wave-length λ, each light-quantum carries the energy $h\nu = ch/\lambda$, where, in c.g.s. units, $c=3.10^{10}$, $h=6.55\cdot10^{-27}$ (light velocity and Planck's constant). Hence, $E=chn/\lambda$ and

$$y = (\epsilon\bar{a}\lambda/ch)E. \qquad (9)$$

With $\lambda=4358$A, as in the experiments to be considered presently, $\lambda/ch = 2.22\cdot10^{11}$. The average grain size $\bar{a}$ is a moderate fraction of a squared micron or 10^{-8} cm^2. Thus, if $\bar{a}$ stands henceforth for the average grain size expressed in μ^2, we may conveniently write

$$y = 2220\epsilon\bar{a}E. \qquad (9.1)$$

Of course, if we plot the theoretical densities against Log y and the observed ones against Log E, the passage from y to E amounts only to *a rigid shift* along the axis of *abscissae*, so that for a comparison of theory with experiment a preliminary knowledge of the numerical value of the coefficient in (9.1) is not needed. When, however, the theoretical and the observed sensitometric curves have been brought by such a shift into the best possible fit, formula (9.1) will enable us to evaluate the fraction ϵ representing the "intrinsic sensitivity" of the grains of known size $\bar{a}$.

Manifestly, before applying such rigid shifts, the scale of ordinates of the two curves, D or D/D_m, must be properly adjusted. Now, the observed limiting density D_m, even if available in some cases, is not at all reliable for the purpose of such comparisons, owing to certain complications** with regard to the covering power of the blackened grains at high densities D which, so far, do not seem amenable to a mathematical treatment. Under these circumstances it is imperative to limit the comparison to low and moderate densities, not exceeding $D=1$, or so. Thus the factor D_m has to be eliminated altogether, and this is best done by substituting for

* Which is about 9/7 times the value corresponding to the single-quantum assumption.

† If the opacity of the base is negligible.

** Especially for long developments.

γ in (8.3) the observed gamma. Formula (8) will then give D itself as function of y alone. This amounts to giving to the theoretical curve the (maximum) *gradient* of the observed one, and it remains then to be seen whether the "toes" and some part at least of the so-called "straight line" portion of the two curves can be brought into close coincidence by a *mere shift* along the Log E axis. The "toe," moreover, and the steepness of ascent (gamma) are the most important characteristics of an emulsion or its sensitometric curve.

To test the theoretical formulae developed above, two pairs of films, No. 1340, 1341 and No. 1342, 1343, were used. Each two were coated with the same emulsion, but at different concentrations or with different numbers N of grains, per square micron of the film, namely, in μ^2,

No.	$\bar{a}$	σ	N
1340.	0.44	0.31	21 $\pm$4.3
1341.	0.44	0.31	10.5$\pm$2.2
1342.	0.72	0.53	8.5$\pm$1
1343.	0.72	0.53	4.2$\pm$0.5

where σ is the standard deviation of grain sizes. Our formulae, corresponding to an exponential size distribution, contain of course only $\bar{a}$, but the values of σ are relevant, since they will enable us to find whether the size-frequency characteristics of these emulsions are at all approximated by the assumed exponential distribution function.

All these films were exposed to light of wave-length 4358A, the exposure values being determined in ergs/cm^2. From the carefully measured reflectance and transmission followed the T-values of these films (not blackened of course) for the same wave-length,

No.	1340.	1341.	1342.	1343.
T	0.20	0.371	0.232	0.457.

The diffuse densities obtained on these films for a set of exposures and after various times of development, in a DK-50 developer at 65°F, were measured in the usual way.

Before passing to compare them with our formulae let us ascertain whether the size frequency characteristics of these emulsions do not clash prohibitively with our assumed exponential distribution, $f(a)=Ne^{-a/\bar{a}}:\bar{a}$. This is easily accomplished. In fact, with this distribution function we have

$$(a^2)_{Av}=\frac{1}{\bar{a}}\int_0^\infty a^2 r^{-a/\bar{a}}da=\bar{a}^2\int_0^\infty x^2e^{-x}dx,$$

i.e., $(a^2)_{Av}=2\bar{a}^2$. Now, $\sigma^2=(a^2)_{Av}-\bar{a}^2$. Thus,

$$\sigma=\bar{a}, \tag{10}$$

a remarkably simple result. For an exponential distribution, standard deviation equal to average size. Neither pair of our films deviates from this relation very much, their ratios $\sigma/\bar{a}$ being about $\frac{3}{4}$ and 5/7. The sensitometric properties, moreover, are mainly influenced by $\bar{a}$ (apart from N), and only in a secondary way by σ. Thus, if the foundations of the theory are correct, our formulae ought to cover approximately the facts.

Let us now turn to consider in detail the case of the film No. 1340. (For the remaining films it will then suffice to state concisely the results.) The set of densities measured on this film, with a six-minute development and after the subtraction of the slight fog 0.04, starts as follows:

Log $E'=$	$\bar{2}.59$	$\bar{2}.89$	$\bar{1}.19$	$\bar{1}.49$	$\bar{1}.79$
$D=$	0.05	0.19	0.47	0.89	1.40

and then increases proportionally to the increments of Log E'. Here E' stands for the *incident* exposure in ergs per cm^2. Since the reflectance of this film is 35.5 percent, our last-defined E is, in this case,

$$E=0.645E'.$$

(This conversion will be required only later, for the evaluation of ϵ.) The exposure ratio in successive steps is 2, as usual. The "straight-line" portion of this experimental sensitometric curve is practically reached at $D=0.80$, so that, in accordance with the preceding remarks, we may be content with representing these five densities.

From the first two measurements we see that when the exposure is doubled, the density is very nearly quadrupled, so that, initially, $D\propto E^2$. Now, we have seen that on the single-quantum hypothesis the power series for D starts with an E term and on the two-quanta assumption with an E^2 term. Generally, as shown in a previous

paper,[2] if at least r quanta are required for the developability of each grain, the series starts with an E^r term. In the present case, then, the single-quantum assumption is ruled out and we are driven to use the *two-quanta* formulae (8) to (8.3). It will be kept in mind, however, that $D \propto E^2$ (initially) indicates only the absence of grains made developable by a single quantum hit and the presence of a considerable percentage of grains requiring only two quanta, while others may require three or more quanta. For in that case, also, will the series start with an E^2 term, being a superposition of series starting with E^2, with E^3, and so on. Thus we might consider a superposition of D formulae based on $r=2$, $r=3$, etc. But before resorting to such complications we shall first ascertain whether and to what extent the observed densities can be covered by the pure *two-quantic* formulae.

Now, in order to eliminate D_m, as explained above, divide Eq. (8) by (8.3). This gives

$$D/\gamma = M/F(T)\{\text{as in (8)}\},$$

where $F(T)$ is as in (8.3) and, for this film, $T=0.20$. Thus $F(T)=-0.545$, and since $M=0.4343$, we have

$$\frac{D}{\gamma}=0.797\left\{\log\frac{1+y}{1+Ty}+\frac{Ty}{(1+Ty)^2}-\frac{y}{(1+y)^2}\right\}.$$

Let us now substitute for γ its observed value which is 1.44, as derived from a considerable stretch (segment) of the "straight-line" portion of the experimental curve. In doing so, it must be kept in mind that, while our D stands for the specular density, the observed densities, and thus also gamma derived from them, are all *diffuse* densities which are, of course, smaller than the specular ones. Generally, the relation between the specular and the diffuse densities, D and D', is expressed by the theoretical and extensively tested formula[3]

$$10^{-D}=\zeta\cdot 10^{-D'}+(1-\zeta)\cdot 10^{-\beta D'},$$

where β and ζ are constants, the latter being the fraction of the total scattered light flux contained in the normally emerging beam. By the definition and the manner of derivation of our D the coefficient ζ is nil, so that the formula is reduced to $D=\beta D'$. Thus also $\gamma=\beta\gamma'$ and

$$D'/\gamma'=D/\gamma.$$

If, therefore, the observed gamma is simply substituted for our γ, the last formula will give the *diffuse* density, which will thus be directly comparable with the observed densities.

Thus, substituting $\gamma=1.44$, which amounts only to giving to our theoretical curve the (maximum) *slope* of the observed sensitometric curve, we have ultimately, for the diffuse density as function of $y \propto E$,

$$D=1.148\left\{\log\frac{1+y}{1+Ty}+\frac{Ty}{(1+Ty)^2}-\frac{y}{(1+y)^2}\right\},$$

$$T=\tfrac{1}{5}, \quad \text{(No. 1340)}$$

a formula containing no adjustable parameters. This gives, to three decimals, the following pairs of corresponding values:

$y=$	$\frac{1}{8}$	$\frac{1}{4}$	$\frac{1}{2}$	1	$\sqrt{2}$	2	4	8
$D=$	0.017	0.068	0.196	0.459	0.646	0.855	1.275	1.59.

The density corresponding to $y=1$ is practically identical with the observed density 0.47 for Log $E'=\bar{1}.19$, i.e., $E'=0.155$ ergs/cm^2. Thus, if we place the unit of our y scale at this (the incident) exposure, the correlation between the theoretical and the observed values is as follows:

$D_{calc}=$	0.07	0.20	0.46	0.86	1.28
$D_{obs}=$	0.05	0.19	0.47	0.89	1.40.

The first four points are practically coincident, so that the "toe" with a good part of the "straight" portion is represented very closely, as shown also in the diagram (Fig. 2). The agreement is close enough even up to $D=1.30$. Beyond that the observed densities exceed the theoretical ones considerably. These might be represented, perhaps, by amplifying and thus complicating our formula, but for the present—and in view of the previous remarks—this simple rendering of the lower and most characteristic part of the observed curve for film No. 1340 may suffice.

Since E' stands for the incident exposure and since, for this film, $E=0.645E'$, to $y=1$ corresponds $E=0.645$. 0.155, so that, by (9.1) and

[3] L. Silberstein and C. Tuttle, "The Relation between the Specular and the Diffuse Photographic Densities," J. Opt. Soc. Am. **14**, 365–373 (1927).

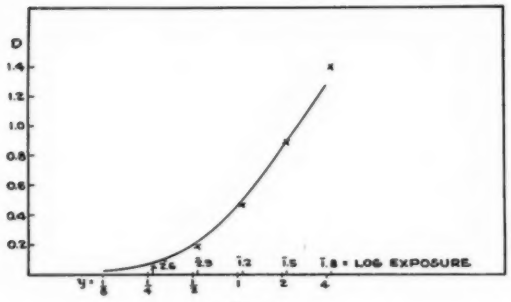

FIG. 2.

with the average grain size $\bar{a}=0.44$,

$$1=97.7\epsilon,$$

whence

$$\epsilon=0.010_2. \qquad \text{(No. 1340)}$$

This is slightly greater than the highest "intrinsic sensitivity" hitherto determined, which was $\epsilon=0.0077$, for the experimental emulsion No. 73.[2]

Let us now consider the film No. 1341. The six lowest densities observed on this film after an 8′ development are (with the same notation as above)

Log $E'=\bar{2}.59$	$\bar{2}.89$	$\bar{1}.19$	$\bar{1}.49$	$\bar{1}.79$	0.09
$D=0.04$	0.16	0.42	0.76	1.14	1.52.

Here again D is initially proportional to E^2, so that the *two-quanta* formulae are to be used. Since, for this film, $T=0.371$, one finds $F(T)=-0.357$, and the observed gamma being 1.27, we derive from (8) and (8.3), in much the same way as in the preceding case,

$$D=1.543\left\{\log\frac{1+y}{1+Ty}+\frac{Ty}{(1+Ty)^2}-\frac{y}{(1+y)^2}\right\},$$

$$T=0.371. \qquad \text{(No. 1341)}$$

This gives, for $y=0.50,\ 0.75,\ 1$,

$$D=0.223,\ 0.368,\ 0.502,$$

respectively. Whence, by graphical interpolation, $D=0.42$ for $y=0.85$, which would, then, correspond to Log $E'=\bar{1}.19$. With this correlation of the exposure scales, y and E', the results are as follows:

$y=0.21_3$	0.425	*0.85*	1.70	3.40	6.80
$D_{calc}=0.04_8$	0.18	0.42	0.78	1.14_4	1.37
$D_{obs}=0.04$	0.16	0.42	0.76	1.14	1.52.

The agreement up to, and a stretch beyond, $D=1.14$ is very close indeed, as shown also in Fig. 3. Beyond 1.40 the observed densities are in excess, as before. Turning to the evaluation of the intrinsic sensitivity ϵ, we have for this film, at the stated wave-length, the reflectance 34 percent, so that $E=0.66E'$, and since $y=0.85$ corresponds to $E'=0.155$, and $\bar{a}=0.44$, formula (9.1) gives

$0.85=99.9\epsilon$, whence

$$\epsilon=0.0085. \qquad \text{(No. 1341)}$$

This is, to all purposes, the same as for the film No. 1340, the difference scarcely exceeding the limits of error implied in the measurements of their transmission and reflectance and the uncertainty of the exposure values and of the adjustment of the two scales. Practically, the calculated values are $\epsilon=0.010$ and 0.09. Now, these two films were coated with batches of the same emulsion, only at different concentrations. The satisfactory coincidence of their ϵ-values or "intrinsic sensitivities" thus arrived at seems, therefore, to be one more confirmation of the soundness of the foundations of the proposed theory.

Let us now pass to the second pair of films which were coated with a different emulsion (consisting of larger grains, etc.), again the same for both films, but at different concentrations, and hence different T values. The lowest densities measured on the film No. 1342, with an eight-minute development, are, after the subtraction of a slight fog (0.06), as in the preceding cases:

Log $E'=\bar{2}.59$	$\bar{2}.89$	$\bar{1}.19$
$D=0.03_5$	0.15	0.37.

The density D is, initially, again very nearly proportional to the square of the exposure, thus calling for an application of the *two-quanta* formulae. For this film, $T=0.232$, and therefore, $F(T)=-0.503$. The observed gamma is 1.12. Thus, proceeding exactly as in the first two cases, we have the density formula, converted in this way (as before) into one for the diffuse densities,

$$D=0.969\left\{\log\frac{1+y}{1+Ty}+\frac{Ty}{(1+Ty)^2}-\frac{y}{(1+y)^2}\right\},$$

$$T=0.232. \qquad \text{(No. 1342)}$$

This happens to give for $y=1$, $D=0.375$, practically identical with the observed density for Log $E'=\bar{1}.19$. This, then, fixes the adjustment of the y and E' scales, and the final results are:

$y=$	$\frac{1}{4}$	$\frac{1}{2}$	1	2	4	8
$D_{calc}=$	0.057	0.16	0.375	0.69	1.01	1.24
$D_{obs}=$	0.03_5	0.15	0.37	0.69	1.06	1.39.

The congruence of the first five pairs of "points" is as close as before, and the curves (Fig. 4) continue to coincide up to about $D=1.15$, beyond which the calculated densities are in defect, as before. In fine, the toe only with a good segment of the "straight" portion of the observed sensitometric curve are very closely represented by the simple *two-quantic* formula. The reflectance of this film being 0.31, we have $E=0.69E'$. The average grain size is $\bar{a}=0.72$, and since $y=1$ corresponds to Log $E'=\bar{1}.19$ or $E'=0.155$, formula (9.1) gives, for this film, $1=171\epsilon$, whence

$$\epsilon=0.0059. \qquad \text{(No. 1342)}$$

Lastly, the six lowest densities measured on the film No. 1343, with a five-min. development are, after the subtraction of 0.03 as fog,

Log $E'=$	$\bar{2}.59$	$\bar{2}.89$	$\bar{1}.19$	$\bar{1}.49$	$\bar{1}.79$	0.09
$D=$	0.03	0.12	0.28	0.51	0.73	0.96.

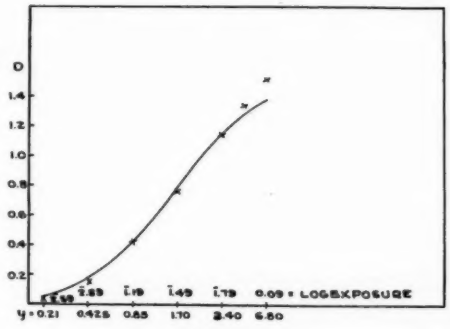

FIG. 3.

Here we have again, initially, $D \propto E^2$, calling for the two-quantic formulae. Since, in the present case, $T=0.457$, one finds $F(T)=-0.286$. The observed gamma is 0.73. Thus our two-quantic formula becomes

$$D=1.108\left\{\log\frac{1+y}{1+Ty}+\frac{Ty}{(1+Ty)^2}-\frac{y}{(1+y)^2}\right\},$$

$$T=0.457. \qquad \text{(No. 1343)}$$

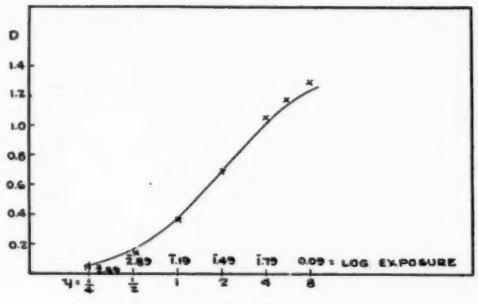

FIG. 4.

This gives the following set of "steps":

$y=$	$\frac{1}{4}$	$\frac{1}{2}$	1	2	4	8
$D_{calc}=$	0.05	0.14	0.31	0.53	0.71	0.81.

Thus the first five observed densities are well represented by correlating Log $E'=1.\bar{1}9$ or $E'=0.155$ with little less than $y=1$, in round figures,

$$E'=0.16 \text{ with } y=1.$$

The curves fit then closely enough up to about $D=0.9$ (cf. Fig. 5), beyond which the observed densities (which seem to tend to a limiting density 1.6) are in excess, very much as for the first three films. The reflectance of this film is 0.30, so that $y=1$ corresponds to $E=0.16\cdot0.7=0.112$ erg/cm^2. Since the average grain size is again $\bar{a}=0.72$, formula (9.1) gives $1=2200\cdot0.72\cdot0.112\epsilon=178\epsilon$,

$$\epsilon=0.0056. \qquad \text{(No. 1343)}$$

This is practically identical with the ϵ value found for the preceding film, No. 1342, which was coated with the same emulsion, but twice as diluted. The coincidence of these numbers obtained from two very different observed sensitometric curves confirms again *the intrinsic meaning* of the coefficient ϵ (which otherwise might be considered as a mere adjustable parameter of the theoretical formula) as expressing the actual photoefficiency or "sensitivity" of a silver halide grain, in much the same sense of the word as when one speaks of the efficiency of a photoelectric cell. Moreover, as was pointed out in previous papers, the photographic and the photoelectric coefficients are of much the same order.

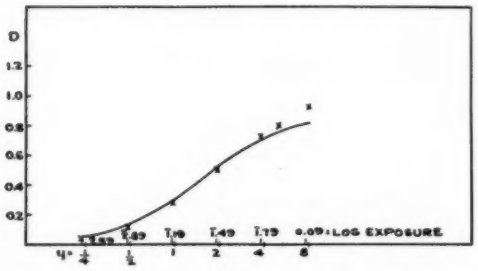

FIG. 5.

We now have, for the two pairs of films:

No.	ϵ	
1340	0.010	same emulsion,
1341	0.009	
1342	0.0059	same emulsion.
1343	0.0056	

The net result of the investigation is, so far, that the pure *two-quantic** formula (8), with the gradual absorption of light taken into account ($T<1$), gives a close representation of the toe and the lower straight portion of the observed sensitometric curves of these films and the correlation of the exposure scales, y and E, yields for films coated with the same emulsion the same value of the "intrinsic sensitivity" ϵ. The total probable or average number of light quanta per grain corresponding to an average number of efficient quanta $y=2$ is $n\bar{a}=2/\epsilon$, and thus about 200 and 330 in the case of the first and the second pair of films, respectively, which is in good agreement with Messrs. Eggert and Noddack's older findings.

The preparation of further material and data for testing the said formula and, in particular, the claimed intrinsic nature of the coefficient ϵ, is now in progress in the Kodak Research Laboratories. These data will enable us also to study that coefficient as a function of the wave-length.

My thanks are due to the Emulsion Research Laboratory and to Dr. Webb and Mr. Loveland of these laboratories for furnishing the experimental data utilized in this paper.

* That is to say, without the superposition of terms corresponding to three and more quanta as possible minimum required for the developability of some grains.

An Improved Calculator for Obtaining Tristimulus Values from Spectrophotometric Curves

FRANCIS W. SEARS
George Eastman Research Laboratory of Physics, Massachusetts Institute of Technology, Cambridge, Massachusetts
(Received October 26, 1938)

SWANK and Mellon[1] have described a calculator for obtaining tristimulus values from spectrophotometric data. The instrument herein described operates on essentially the same principle, but affords some advantages in simplicity of construction and operation.

Two instruments have been built, one manually operated and the other motor driven. The first is shown schematically in Fig. 1. A shaft *C*, one end of which engages the "free-wheeling" clutch *B*, carries a cylindrical drum *D* and a hand wheel *F*. The shaft is supported by hangars which are not shown. The spectrophotometric curve to be evaluated is mounted on the drum *D*. Against the surface of this drum rests the triangular scale *E*, on three concurrent edges of which are engraved the selected ordinates for Illuminant C. The same scale may be employed for another illuminant by removing it from its mountings, turning it end for end, and utilizing the edges which then face the drum for the selected ordinates of the second illuminant.

The construction of the clutch is shown at *G*. If carefully made with hardened steel rolls and bearing surfaces, the backlash may be reduced to a negligible amount.

In operation the drum is first rotated counterclockwise until it brings up against a stop, not shown. The paper carrying the spectrophotometric curve is now mounted on the drum with the axis of wave-lengths coincident with the edge of the scale. The drum is now rotated clockwise until the curve coincides with the first selected ordinate, then counterclockwise back to the zero stop, and so on. Rotation of the drum in the clockwise direction is transmitted by the clutch to the revolution counter *A*. In the opposite direction of rotation, the clutch releases, and rotation of the shaft between clutch and counter is prevented by a friction drag, not shown. There are thus imparted to the counter a series of angular displacements proportional to the values of reflectance or transmittance at the selected ordinates. The surface of the driven side of the clutch is graduated with 100 divisions, and both counter and clutch may be reset to zero. The instrument is calibrated by noting the reading of counter and clutch scale for ten or more "oscillations" from zero to 100 percent.

A reading glass, which slides on ways along the front of the instrument, is helpful in making settings, particularly for the *Z* function where the spacing of the selected ordinates is small.

The motor-driven instrument, shown in Fig. 2, is somewhat more rapid in operation, and has the advantage of not requiring the operator to return the drum to zero between successive settings. In this instrument the drum and hand wheel are mounted on a hollow shaft *H*, Fig. 2. Concentric with this shaft, but independently supported, is shaft *C*, which carries a disk *J* and which engages the clutch *B*. This shaft is driven through a worm and wheel *M* by an electric motor. The arm *K*, projecting from disk *J*, makes electrical contact with stop *L* on drum *D*, and may also make contact with a fixed stop, not shown, as the disk rotates counterclockwise. Shaft *C* is normally at rest with *K* in contact with this fixed stop.

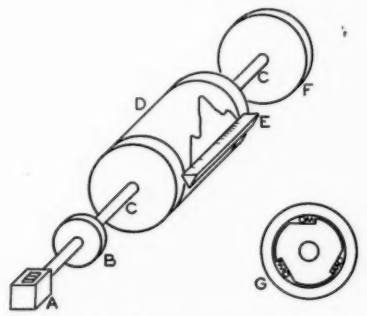

FIG. 1. *A*, revolution counter; *B*, clutch; *C*, shaft; *D*, cylindrical drum carrying spectrophotometric curve; *E*, triangular scale engraved with selected ordinates; *F*, hand wheel; *G*, detail of clutch.

[1] H. W. Swank and M. G. Mellon, J. Opt. Soc. Am. **27**, 414 (1937).

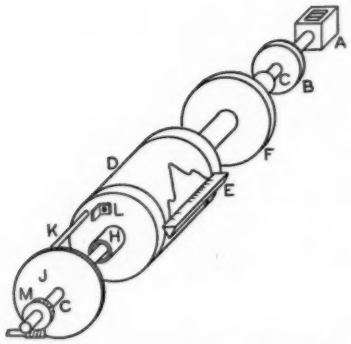

FIG. 2. *A*, revolution counter; *B*, clutch; *C*, shaft; *D*, cylindrical drum carrying spectrophotometric curve; *E*, triangular scale engraved with selected ordinates; *F*, hand wheel; *H*, hollow shaft; *J*, disk on shaft *C*; *K*, *L*, reversing contact; *M*, worm and wheel to motor drive.

To use the instrument, the drum is rotated in a counterclockwise direction until *L* and *K* are in contact. The spectrophotometric curve is then placed on the drum as before. The drum is then rotated clockwise until the curve coincides with the first selected ordinate. A foot switch is then depressed, which starts the motor and rotates shaft *C*, clutch *B*, and counter *A*, until *K* and *L* make contact. This contact, through a relay system, reverses the motor and returns *K* to contact with the fixed stop, a friction drag meanwhile preventing rotation of the counter. Thus the angular displacement imparted to the counter is equal to the angular displacement of the drum. The second setting may then be made and the process repeated. If the reflectance of the sample is of the order of 30 percent or more, the time interval of a few seconds required for the oscillation of shaft *C* is sufficiently long so that the foot switch may be left permanently closed, and the drum moved from one setting to the next while the shaft goes back to zero and returns. Under these conditions the time required for the addition of 30 ordinates is from one to two minutes.

The manually operated instrument was completed in June, 1938, and was put into immediate operation. Up to the present time, tristimulus values from more than 3000 spectrophotometric curves have been obtained with its aid, making a total of about 10,000 sums of 30 ordinates each.

The author wishes to thank Mr. Walter Kallenbach of the Physics Shop, and Mr. Harry E. Anderson, who constructed both instruments and suggested many details of their design.

A Simplified Derivation of the General Properties of an Electron-Optical Image*

E. G. RAMBERG
RCA Manufacturing Company, Camden, New Jersey
(Received November 15, 1938)

THE image-forming properties of axially symmetric electric and magnetic fields, together with the third-order (Seidel) aberrations of electron images, have been derived repeatedly, giving either explicit formulas for the aberrations[1] in terms of field parameters or merely the general form of the aberration figures.[2] The aim of the present discussion is to derive the latter, together with the properties of the Gaussian image, making use of elementary concepts only. Insofar as the laws governing light rays in isotropic media and electron paths in purely electric fields are identical, the refractive index in the one case and the electron velocity (or the square root of the electric potential) in the other playing the same role, the derivation also applies to ordinary optical systems and images.

Let us consider an axially symmetric array of electrodes at various potentials, as well as of magnets, with the z axis as their axis of symmetry. Normal to this axis let there be an object plane O with the coordinate system x_o, y_o and, beyond the focusing fields, an image plane I (whose position is yet to be fixed) with the coordinates x_i, y_i, the respective origins lying on the z axis (Fig. 1). We assume the space between O and I to be free from matter in the vicinity of the axis, so that Laplace's equation holds for both the electric and the magnetic field, and, furthermore, that the space surrounding the plane I is field-free. We now introduce between O and I, also normal to the z axis, an "aperture plane" A with coordinates x_a, y_a—close enough to I that the entire space between A and I may be regarded as field-free.[3] We give the same orientation to the several coordinate systems, so that, e.g., the x_o, x_a and x_i axes are coplanar.

Suppose now that electrons leave various points of the object plane, throughout with the same absolute velocity, though generally in different directions. If we fix our attention on one such electron, leaving the point x_o, y_o in the object plane and aimed so that it passes through the point x_a, y_a of the aperture plane, its path will, in view of the fixed field conditions, be uniquely determined and accordingly also its intersection x_i, y_i with the image plane. Hence we may regard the coordinates x_i and y_i as functions of the coordinates of the ray in the object and aperture planes, x_o, y_o, x_a and y_a, and, in view of the continuity of the force fields to which the electrons are subjected, express them in terms of a power

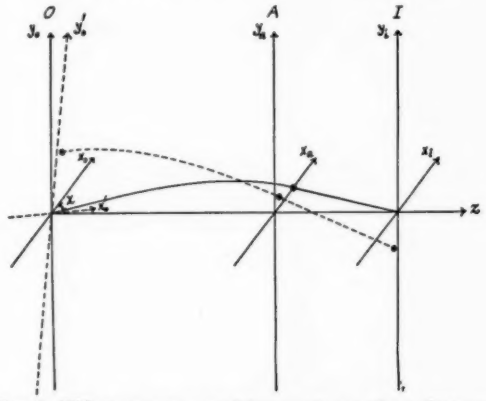

FIG. 1. Object, aperture and image planes of an electron-optical system.

series of these latter four coordinates, such as

$$x_i = a_o + a_1 x_o + a_2 y_o + a_3 x_a + a_4 y_a + a_5 x_o^2 + a_6 x_o y_o + a_7 y_o^2 + a_8 x_o x_a + \cdots. \quad (1)$$

There is a similar expression, with different coefficients, for y_i. We will see that we can simplify these expressions very considerably by making use of the symmetry conditions of the problem.

* Read before the Optical Society of America at its meeting at Niagara Falls, Ontario, October 28, 1938.

[1] See articles by W. Glaser and O. Scherzer in Busch and Brüche, *Beiträge zur Elektronenoptik* (J. A. Barth, Leipzig, 1937).

[2] W. Rogowski, Arch. f. Elektrotechnik **31**, 555 (1937).

[3] We define the aperture plane in the above manner for the sake of simplicity in representation. For all applications it is more appropriate to choose it as the plane in which the principal rays continued backwards from the image plane as straight lines intersect the axis. In this case it becomes, in general, a virtual plane—the plane of the "exit pupil" of the optical system—and the space between it and the image plane is field-free by definition. The derivation given is equally valid with the latter choice of the aperture plane.

We must here satisfy the obvious requirement, that, if we rotate the radius vectors to the ray intersections in planes O and A through any given angle φ, the corresponding intersection in plane I is found by rotating the radius vector to x_i, y_i through the same angle φ. Thus (1) must remain satisfied if we carry out the simultaneous substitution:

$$\begin{aligned} x_i &\rightarrow x_i\cos\varphi - y_i\sin\varphi;\\ x_o &\rightarrow x_o\cos\varphi - y_o\sin\varphi;\\ x_a &\rightarrow x_a\cos\varphi - y_a\sin\varphi;\\ y_o &\rightarrow x_o\sin\varphi + y_o\cos\varphi;\\ y_a &\rightarrow x_a\sin\varphi + y_a\cos\varphi. \end{aligned} \quad (2)$$

Putting $\varphi = 180°$ simply changes the sign of all the coordinates and we obtain

$$\begin{aligned} -x_i = a_o - a_1x_o - a_2y_o - a_3x_a - a_4y_a + a_5x_o^2\\ + a_6x_oy_o + a_7y_o^2 + a_8x_ox_a + \cdots; \end{aligned}$$

adding (1), we find that the sum of all the terms of even order in the coordinates must vanish:

$$O = 2a_o + 2a_5x_o^2 + 2a_6x_oy_o + 2a_7y_o^2 + 2a_8x_ox_a + \cdots.$$

As this must be true for all values in a continuous range of x_o, y_o, x_a, y_a, all the coefficients of the terms of even order a_o, a_5, a_6, a_7, $a_8\cdots$must vanish individually and we are left with terms in the first, third, fifth . . . order in the coordinates. If we confine our attention to regions of the object very close to the axis and electron rays leaving these which, also, strike the aperture plane very close to the axis (i.e., imaging pencils of very small aperture), we gain sufficient information regarding the pattern in the image plane if we consider the terms of the first order only. Let us make, then, the substitution (2) in (1) with φ left arbitrary. As the resulting equation must be valid for all φ, it must be fulfilled by the coefficients on the two sides of the equation of cos φ and sin φ individually. Hence we obtain

$$\begin{aligned} x_i^{(1)} &= a_1x_o + a_2y_o + a_3x_a + a_4y_a,\\ y_i^{(1)} &= -a_2x_o + a_1y_o - a_4x_a + a_3y_a, \end{aligned} \quad (3)$$

the superscript $^{(1)}$ indicating that the expressions constitute an approximation taking account of the first-order terms only.

Consider now a ray leaving the point $x_o=0$, $y_o=0$ and passing through $x_a=c$, $y_a=0$. For it we have

$$x_i^{(1)} = a_3c, \qquad y_i^{(1)} = -a_4c. \quad (4)$$

Now the only tangential forces which the electron undergoes arise from the action of the magnetic field. According to Larmor's theorem its angular velocity about the axis is, however, equal to $eH_z/(2m)$, where H_z is the longitudinal component of the magnetic field at the point of observation.[4] As, however, $H_z=0$ in the aperture plane and beyond, the angular velocity of the electron must here be zero throughout. The path of the electron between the aperture and image planes is thus a straight line proceeding in a meridional plane—in our example in the zx plane. Hence, in (4), $y_i^{(1)}=0$ and, as $c\neq 0$, $a_4=0$.

We now take one more step: the ray in the zx plane which we are considering will in general be inclined to the axis of symmetry. Let us, hence, follow it to its point of intersection with the axis and fix the image plane I as the plane normal to the axis passing through this point.[5] With this choice of I we have $x_i=0$ and hence also $a_3=0$. Thus we obtain finally:

$$\begin{aligned} x_i^{(1)} &= a_1x_o + a_2y_o = \beta x_o';\\ y_i^{(1)} &= -a_2x_o + a_1y_o = \beta y_o', \end{aligned} \quad (5)$$

where

$$\begin{aligned} x_o' &= x_o\cos\chi - y_o\sin\chi;\\ y_o' &= x_o\sin\chi + y_o\cos\chi; \end{aligned} \quad (6)$$

$$\chi = \arctan(-a_2/a_1); \quad \beta = (a_1^2+a_2^2)^{\frac{1}{2}}.$$

x_o', y_o' are the coordinates of the object point referred to a coordinate system rotated with respect to the original one (and the systems in planes A and I) through the angle χ. We thus have the final result that, to a first approximation in the coordinates of the object and aperture planes, all the rays leaving any point in the object plane O are reunited in a point in the

[4] Introducing the polar coordinates r, φ, the exact integration of Newton's equation for the φ-direction

$$d/dt(mr^2\dot{\varphi}) = r\cdot e(\dot{r}H_z - \dot{z}H_r),$$

taking account of Laplace's equation

$$\frac{\partial H_z}{\partial z} + \frac{1}{r}\frac{\partial}{\partial r}(rH_r) = 0,$$

yields

$$r^2\dot{\varphi} = (r^2\dot{\varphi})_{z=0} + \frac{e}{m}\left[\frac{1}{2}(H_z)_{r=0}r^2 - \frac{1}{16}\left(\frac{\partial^2 H_z}{\partial z^2}\right)_{r=0}r^4 + \frac{1}{384}\left(\frac{\partial^4 H_z}{\partial z^4}\right)_{r=0}r^6\cdots\right]_0^r.$$

This vanishes, if $r=0$ at $z=0$, in any plane in which $H_z=0$.

[5] Our original assumptions regarding the image plane I are equivalent to postulating that this point falls into the field-free space beyond the focusing fields.

image plane I. Furthermore, to any array of object points there corresponds a geometrically similar array of image points with separations magnified, or reduced, by the factor β and rotated, one relative to the other, through the angle χ. In short, to a first approximation our axially symmetrical field combination gives a sharp and faithful, "Gaussian," image of the object.

For purely electric fields (as for an ordinary optical lens system) the angle χ vanishes, as rays starting in a given meridional plane do not leave this plane—owing to the fact that in this case all of the forces acting on the electron are radial or axial the relation (1) must remain true if we reflect all of the coordinates at any meridional plane, e.g., change the signs of the x coordinates and leave those of the y coordinates unchanged (reflection at the yz plane). This requirement leads to $a_2=0$, and hence $\chi=0$.

If we drop the assumption of an image field of infinitesimal extent and imaging pencils of infinitesimal aperture, we must take into consideration the terms of higher order in the expressions for x_i and y_i. They inform us of the deviations of the real image from the Gaussian, sharp and geometrically faithful, image (the aberrations). For many purposes, i.e., if the image field and apertures are not too large, it is sufficient to restrict our attention to the terms of the third order, obtaining then the so-called third-order (Seidel) aberrations. Thus we may write, giving a new meaning to the coefficients a_1, a_2, a_3, a_4:

$$\begin{aligned}\Delta x_i = {} & a_1 x_a^3 + a_2 x_a^2 y_a + a_3 x_a y_a^2 + a_4 y_a^3 \\ & \text{Aperture Defect (Spherical Aberration)} \\ & + b_1 x_o' x_a^2 + b_2 x_o' x_a y_a + b_3 x_o' y_a^2 + b_4 y_o' x_a^2 \\ & \quad + b_5 y_o' x_a y_a + b_6 y_o' y_a^2 \qquad \text{Coma} \\ & + c_1 x_o'^2 x_a + c_2 x_o'^2 y_a + c_3 x_o' y_o' x_a + c_4 x_o' y_o' y_a \\ & \quad + c_5 y_o'^2 x_a + c_6 y_o'^2 y_a \qquad \text{Curvature of Field and Astigmatism} \\ & + d_1 x_o'^3 + d_2 x_o'^2 y_o' + d_3 x_o' y_o'^2 + d_4 y_o'^3 \\ & \qquad \text{Distortion} \qquad (7)\end{aligned}$$

and a similar expression for Δy_i, Δx_i and Δy_i being the third-order deviation of the ray intersection with the image plane from the corresponding first-order, Gaussian, intersection or image point:

$$x_i^{(3)} = x_i^{(1)} + \Delta x_i; \qquad y_i^{(3)} = y_i^{(1)} + \Delta y_i.$$

For convenience we now refer our object plane coordinates to the rotated (primed) coordinate system. To the right of every group of terms involving the same powers of the coordinates of the object plane and of the coordinates of the image plane we have written down the customary designation of the corresponding aberration.

An application of our symmetry condition will show that the twenty coefficients in (7) and the further twenty coefficients in the corresponding expression for Δy_i are by no means independent. Let us, then, make the substitution (2) in (7) and satisfy the resulting equation individually for the coefficients of $\sin\varphi$, $\cos\varphi$, $\sin^3\varphi$ and $\cos^3\varphi$. Expressing the coefficients in terms of each other as far as the resulting relations permit, we find:

$$\begin{aligned}\Delta x_i = {} & a_1 x_a (x_a^2 + y_a^2) + a_2 y_a (x_a^2 + y_a^2) \\ & + b_1 x_o' (x_a^2 + y_a^2) + b_5 y_a (y_o' x_a - x_o' y_a) \\ & + b_2 y_a (x_o' x_a + y_o' y_a) + b_4 y_o' (x_a^2 + y_a^2) \\ & + c_1 x_o' (x_o' x_a + y_o' y_a) + c_5 y_o' (y_o' x_a - x_o' y_a) \\ & + c_3 y_o' (x_o' x_a + y_o' y_a) + c_2 y_a (x_o'^2 + y_o'^2) \\ & + d_1 x_o' (x_o'^2 + y_o'^2) + d_2 y_o' (x_o'^2 + y_o'^2), \\ \Delta y_i = {} & -a_2 x_a (x_a^2 + y_a^2) + a_1 y_a (x_a^2 + y_a^2) \\ & - b_4 x_o' (x_a^2 + y_a^2) - b_5 x_a (y_o' x_a - x_o' y_a) \\ & - b_2 x_a (x_o' x_a + y_o' y_a) + b_1 y_o' (x_a^2 + y_a^2) \\ & + c_1 y_o' (x_o' x_a + y_o' y_a) - c_5 x_o' (y_o' x_a - x_o' y_a) \\ & - c_3 x_o' (x_o' x_a + y_o' y_a) - c_2 x_a (x_o'^2 + y_o'^2) \\ & - d_2 x_o' (x_o'^2 + y_o'^2) + d_1 y_o' (x_o'^2 + y_o'^2).\end{aligned} \qquad (8)$$

If we again consider a ray leaving the point on the axis in the object plane ($x_o'=y_o'=0$) and passing through the point ($x_a=c$, $y_a=0$) an extension of Larmor's theorem[4] tells us that the ray must proceed in the zx plane between A and I and that thus $\Delta y_i=0$ and hence $a_2=0$. We have thus reduced the number of independent third-order coefficients to 11. For purely electric fields, in which case, as we have mentioned, the relations must hold if we reflect the coordinates at any meridional plane, we have in addition $b_2=b_4=c_3=c_2=d_2=0$, so that the number of independent coefficients reduces to six. To reduce them to their true number, i.e., eight for mixed and five for purely electric fields, we must introduce a new factor into our considerations.

It is of interest, however, to note the extent of the uncertainty in the aberration figures remaining at this point. For purely electric fields

(or ordinary optical systems) the only residual removable uncertainty is in the angle θ of the coma figure (Fig. 2), which is here arbitrary, rather than 30° (for $b_5=2b_1/3$).

In the presence of a magnetic field, the uncertainty affects both coma and astigmatism. The coma figure is now given by

$$(\Delta x_i-(b_2/2+b_4)r_o r_a^2)^2 +(\Delta y_i-(b_1-b_5/2)r_o r_a^2)^2 =((b_5/2)^2+(b_2/2)^2)r_o^2 r_a^4 \quad (9a)$$

instead of by

$$(\Delta x_i-(2b_4/3)r_o r_a^2)^2+(\Delta y_i-(2b_1/3)r_o r_a^2)^2 =((b_1/3)^2+(b_4/3)^2)r_o^2 r_a^4 \quad (9b)$$

for an object point lying on the y_o' axis, with

$$r_o=y_o' \qquad \text{and} \qquad r_a^2=x_a^2+y_a^2,$$

which indicates that the arbitrariness of θ applies to all orientations of the coma figure, i.e., even for cases where $b_1=b_5=0$.

In the case of astigmatism the sole effect of the remaining uncertainty is the circumstance that the aberration figure in the presence of the magnetic field appears to be in general an ellipse of undetermined eccentricity rather than a circle (for $c_3=-2c_2$) even when the ordinary curvature of field vanishes ($c_1=-c_5$).

The remaining indefiniteness may be removed, as it is in the derivations based on the ray function or Hamiltonian characteristic function (e.g., reference 2) by making use of the existence of wave surfaces whose orthogonal trajectories constitute (in the case of purely electric fields) the electron rays. As in ordinary optics we write for one of the wave surfaces corresponding to a pencil diverging from a given object point P_0:

$$S(P)=\int_{P_0}^{P} n\,ds=\text{const.},$$

where n is the effective index of refraction[6] and s is the distance from the object point measured along an electron trajectory.

[6] The refractive index of the field may be written $n=v/c-e/(mc)\cdot A\cos\chi$, where the electron velocity $v=(2e\varphi/m)^{\frac{1}{2}}$; φ is the electric potential and A the magnetic vector potential of the field, χ being the angle between A and the electron trajectory s.

For field-free space n is constant; the direction cosines of the normal to the surface at one of its points x, y, z are given by $(1/n)\partial S/\partial x$, $(1/n)\partial S/\partial y$, $(1/n)\partial S/\partial z$. Consider now a point in the aperture plane, x_a, y_a. The normal to the surface $S=$ const. passing through this point must coincide with the ray of the pencil from $P_0(x_o', y_o')$ passing through x_a, y_a, whose intersection with the image

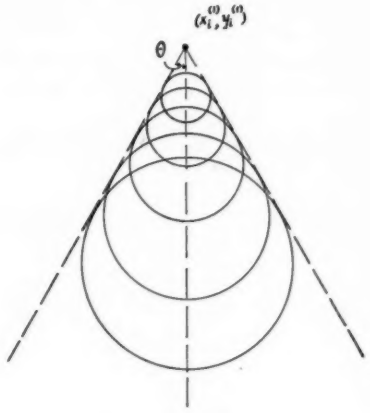

FIG. 2. Coma figure.

plane will be $x_i y_i$. Hence we must have

$$\begin{aligned}(1/n)\partial S/\partial x_a&=(x_i-x_a)/((x_i-x_a)^2 +(y_i-y_a)^2+(z_i-z_a)^2)^{\frac{1}{2}}\approx(x_i-x_a)/Z,\\ (1/n)\partial S/\partial y_a&=(y_i-y_a)/((x_i-x_a)^2 +(y_i-y_a)^2+(z_i-z_a)^2)^{\frac{1}{2}}\approx(y_i-y_a)/Z,\end{aligned} \quad (10)$$

where $z_i-z_a=Z$, the separation of the aperture and image planes, which we assume to be large compared to the lateral coordinate differences. Now, if the function S exists, we must have the relation

$$\partial^2 S/(\partial x_a\partial y_a)=\partial^2 S/(\partial y_a\partial x_a)$$

or, from (10),

$$\partial x_i/\partial y_a=\partial y_i/\partial x_a. \quad (11)$$

Owing to the approximation introduced in (10) this applies only to the terms of the third order in x_a and x_o in the expressions for x_i and y_i. The application of the relation (11) to (8) leads to $b_5=2b_1/3$, $b_2=-2b_4/3$, $c_3=-2c_2$ and

$$\begin{aligned}\Delta x_i=&a_1x_a(x_a^2+y_a^2)+(b_1/3)(x_o'(x_a^2+y_a^2)\\&+2x_a(x_o'x_a+y_o'y_a))+(b_4/3)(y_o'(x_a^2+y_a^2)\\&-2x_a(x_o'y_a-y_o'x_a))+((c_1+c_5)/2)x_a\\&\times(x_o'^2+y_o'^2)+((c_1-c_5)/2)(x_a(x_o'^2-y_o'^2)\\&+2x_o'y_o'y_a)+c_2(y_a(x_o'^2-y_o'^2)-2x_o'y_o'x_a)\\&+d_1x_o'(x_o'^2+y_o'^2)+d_2y_o'(x_o'^2+y_o'^2),\\\Delta y_i=&a_1y_a(x_a^2+y_a^2)+(b_1/3)(y_o'(x_a^2+y_a^2)\\&+2y_a(x_o'x_a+y_o'y_a))-(b_4/3)(x_o'(x_a^2+y_a^2)\\&+2y_a(x_o'y_a-y_o'x_a))+((c_1+c_5)/2)y_a\\&\times(x_o'^2+y_o'^2)-((c_1-c_5)/2)(y_a(x_o'^2-y_o'^2)\\&-2x_o'y_o'x_a)+c_2(x_a(x_o'^2-y_o'^2)+2x_o'y_o'y_a)\\&+d_1y_o'(x_o'^2+y_o'^2)-d_2x_o'(x_o'^2+y_o'^2).\end{aligned}\tag{12}$$

These are the familiar expressions for the third-order aberration of an electron-optical system, whose form has been discussed repeatedly.[1, 2]

We thus see that it is possible to derive the imaging properties including the complete form of the aberrations of the third order,

(1) in the case of axially symmetric electric fields, or ordinary optical systems, with the exception of the coma angle, by symmetry considerations only;

(2) in the case of axially symmetric magnetic and electric fields, with the exception of the coma angle and the eccentricity of the ellipse of magnetic astigmatism, by symmetry considerations and an extension of Larmor's theorem. To fix the coma angle and the eccentricity of the ellipse of magnetic astigmatism at their proper values the introduction of the wave surface becomes necessary.

While the image has been treated throughout as real the applicability of the derivation to the case of a virtual image is obvious. It is hoped that the elementary approach here given may prove of value in simplifying an understanding of the aberrations.

An Automatic Recording Spectroradiometer for Cathodoluminescent Materials*

V. K. Zworykin
RCA Manufacturing Company, Camden, New Jersey
(Received November 26, 1938)

An automatic recording spectrophotometer for the visible, especially adapted for the study of cathodoluminescent materials, is described. It consists of a demountable light source and an interrupter, a glass monochromator with compensation for the variation of the dispersion with wave-length, a photoelectric electron multiplier, a signal amplifier stabilized by negative feedback, and a motor drive amplifier controlling the deflection of the recording head. The wave-length scale is made linear by the introduction of a spiral cam of appropriate form. The system is distinguished by high sensitivity (usable for sources emitting one millilumen/cm^2), high speed (1¼ minutes for a record), linear wave-length scale, high stability and easy adjustment.

EXTENSIVE measurements in our laboratory on the spectral distribution of the radiation from luminescent substances used in cathode-ray tubes made it desirable to devise means of obtaining accurate distribution curves with a maximum of speed and a minimum of attention to the recording apparatus. An added desideratum was a linear wave-length scale, making possible a quick determination of the total energy in a band, this being given directly by the area under the curve. These demands led to the construction of the apparatus described below.

1. General Plan of the Apparatus

A view of the complete installation is given in Fig. 1. Fig. 2 is a diagram showing the relationship of the principal components of the device. The surface S of a sample excited by an electron beam is imaged on the collimator slit S_1 of a Gaertner glass monochromator and this slit, after passage of the light through the constant deviation prism, is then focused on the exit slit S_2 of the monochromator. Before entering the monochromator the light is "chopped" 150 times per second by a synchronously driven five-bladed sector disk, *Se*. The exit slit is imaged on the window of a magnetic electron multiplier with a horizontal slot, *Sl*, moving in unison with the prism table, being interposed in order to compensate the variation in the dispersion of the spectrograph and the photosensitivity of the multiplier. The 150-cycle component of the output current of the multiplier, which is about 400,000 times as great as the photocurrent, is further amplified by a 150-cycle a.c. signal

* Read before the Optical Society of America at its meeting at Niagara Falls, Ontario, October 27–29, 1938.

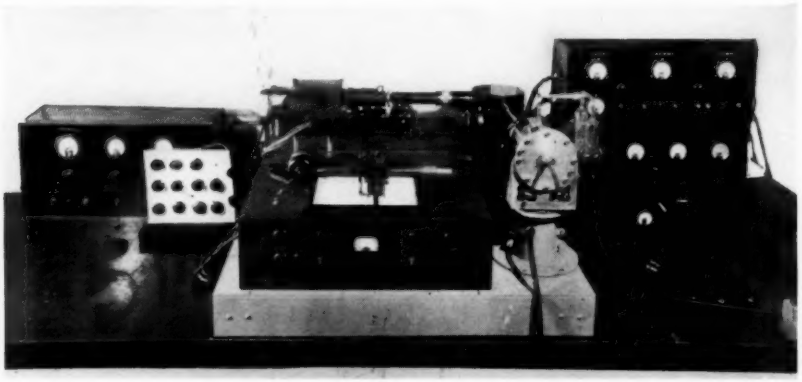

Fig. 1. General view of spectroradiometer installation.

amplifier—using the a.c. component eliminates disturbing effects caused by multiplier dark currents and d.c. amplifier drift. The amplified 150-cycle signal is rectified and the difference between it and the signal corresponding to the position of the recorder head *P* bearing the pen on the recorder potentiometer incorporated in the arm *A* is amplified in the d.c. motor drive amplifier and applied to the armature of the motor, *M*, controlling the ordinate position of the recording pen. The abscissa is controlled by a second motor which rotates the prism table; with the aid of a suitably shaped spiral helical cam, *Cm*, the abscissa motion is made such as to make equal distances correspond to equal wavelength intervals over the entire scale (from 4000 to 7300A).

2. The Light Source

The light source (Fig. 3) consists of a demountable vacuum tube containing a $3\frac{1}{2}''$ diameter Pyrex disk, *D*, and an electron gun, *G*, with its axis inclined 50° with respect to the normal

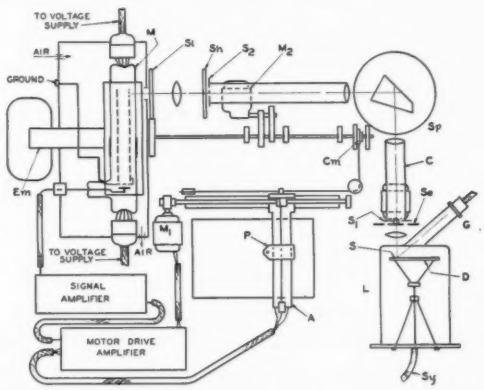

FIG. 2. Plan of spectroradiometer.

to the disk. On the disk may be deposited eight patches of different fluorescent materials, which may in turn be brought under the electron beam from the gun by rotating the disk with the aid of a sylphon joint, *Sy*. The electron gun, of standard type, may, like the disk, be removed from the tube and the cathode be replaced when necessary. So as to minimize the frequency of this operation, it proved advisable to employ a tungsten helix in place of the usual, indirectly

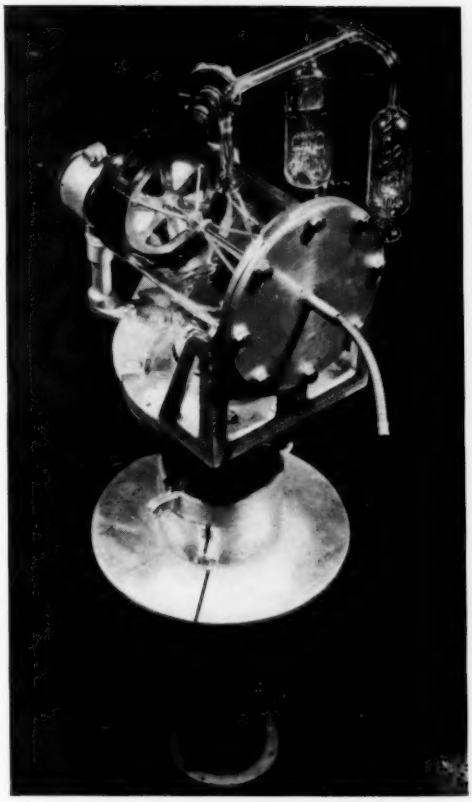

FIG. 3. The light source.

heated, oxide-coated element as cathode. The metal gun press is bolted to a Fernico collar sealed to the side tube, the joint being made vacuum-tight by the insertion between them of a tin ring. In the case of the junction between the round metal plate supporting the disk and the tube walls, a rubber gasket placed between the former and a metal flange sealed to the tube wall with Picein proved adequate. The tube is evacuated with the aid of a three-stage oil diffusion pump[1] backed by a Cenco Hyvac pump and the vacuum measured with the aid of a thermocouple gauge and an ionization gauge. The time required for evacuation is about $\frac{1}{2}$ hour, the operating vacuum about 3.10^{-5} mm Hg.

In the tube here discussed the luminescent material is deposited on the disk in a layer

[1] Designed by Dr. L. Malter. See L. Malter and N. Marcuvitz, Rev. Sci. Inst. **9**, 92 (1938).

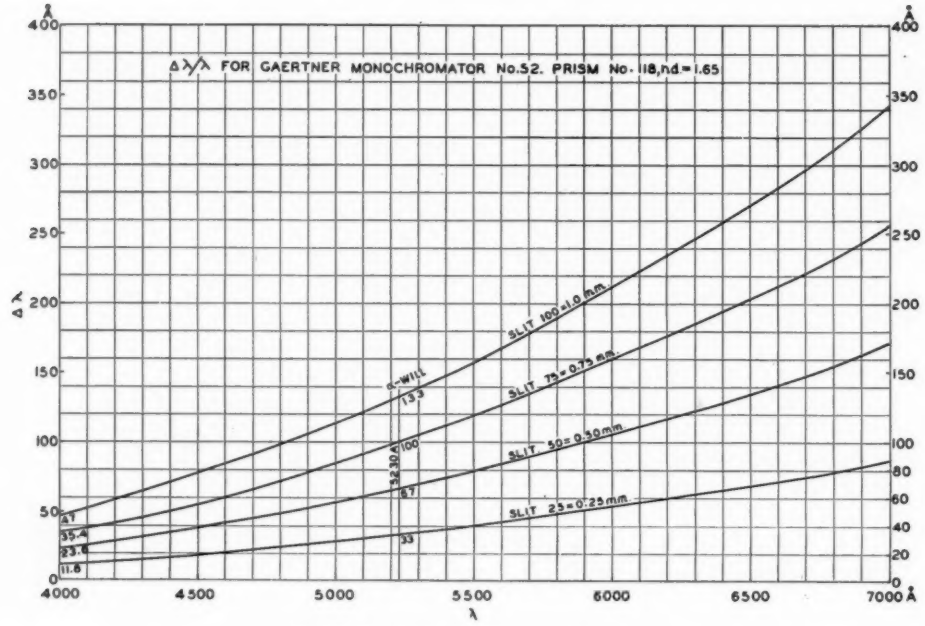

FIG. 4. Resolution of the monochromator.

sufficiently heavy to be opaque and the front surface is imaged on the slit of the monochromator; its distance from the front wall of the tube is less than an inch, making a good utilization of the light output possible. The standard bombarding velocity employed is 6000 volts. With 500 volts on the first anode of the gun we obtain under these circumstances a spot about one cm² in area. The normal operating current is between five and ten μA. The voltages for operating the tube are furnished by power packs operated from the line, the d.c. voltages for the first and second anode being filtered to reduce ripple. Placing 1000-cycle pulses on the control grid of the gun to make the bombardment intermittent proved of value in preventing "burning" of the sample.

3. The Monochromator and Compensating Slot

The monochromator is a calibrated Gaertner constant deviation glass monochromator with a direct-reading spiral wave-length scale. The calibration is checked periodically with the line spectrum of a mercury arc. Curves for the least resolvable wave-length separation $\Delta\lambda$ are shown for four different slit-widths in Fig. 4. Parallelism of the exit to the entrance slit is secured by rotating the former until a minimum response is obtained when the prism is set just off one of the mercury lines. A shutter, geared to the axis rotating the prism table, moves in front of the exit slit and covers it when the table moves beyond the 7300 and 4000A settings. Just beyond these points it acts, in addition, as a switch shutting off the motor driving the recorder arm and prism table. The arrangement of the wiring is such that the switch reversing the direction of the motor also closes once more the automatic shut-off switch. The exit slit, furthermore, is imaged into the plane of the disk provided with the compensating slot, immediately in front of the window of the multiplier. The width of the slot is made such that, for all positions of the prism, the photocurrent leaving the photosensitive cathode of the multiplier is directly proportional to the amount of energy radiated per unit range of wave-length by the source. This method of compensation is made possible by the fact that with the types of sources under considera-

tion the illumination along the exit slit of the monochromator is substantially uniform. The shape of the slot was determined by comparing the uncompensated output of the instrument, a standard tungsten ribbon lamp being used as source, with curves for the energy distribution for a radiator of the same color temperature published by the National Bureau of Standards.[2] A later check of the recorded curve for the standard lamp with the compensating slot in place with the above-mentioned published curve showed excellent agreement.

4. The Photoelectric Multiplier

The light passed by the compensating slot reaches the photocathode of the multiplier. The latter is of the magnetic type[3] and has ten stages of secondary emission multiplication. The sensitive surfaces are of oxidized silver sensitized with rubidium. The total gain is about 400,000, the over-all applied voltage 1600 volts. Regulated supplies are used for both the magnetic field—provided by a soft-iron yoke magnetized by a coil—and the voltages applied to the individual multiplier plates through a bleeder. Their circuits are shown in Figs. 5a and 5b, respectively. To eliminate all disturbing effects caused by humidity and stray light, the outside of the multiplier is painted with a grounded coat of Aquadag, covering the tube with the exception of the window and the regions near the terminals.

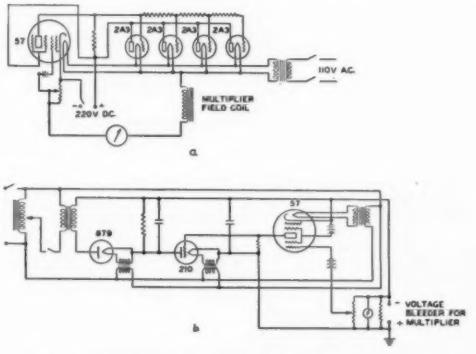

Fig. 5. Regulated current and voltage supplies for the multiplier.

[2] Miscellaneous Publications of the National Bureau of Standards No. 86.

[3] V. K. Zworykin, G. A. Morton and L. Malter, Proc. Inst. Rad. Eng. 24, 351 (1936).

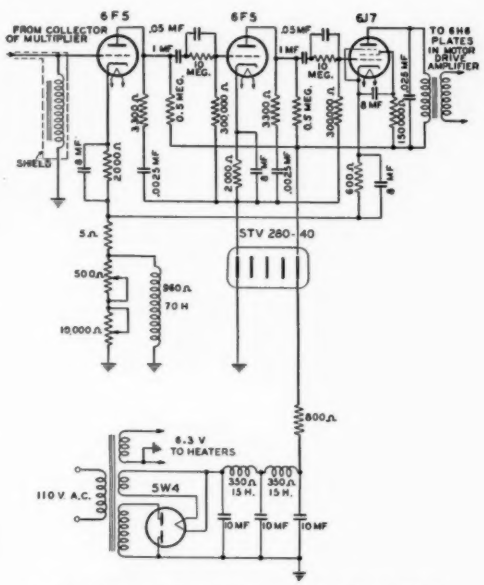

Fig. 6. Circuit diagram for the signal amplifier.

In addition, it is enclosed in a black Bakelite box through which dry air may be circulated. The great advantage of the multiplier in this case rests, as is brought out in reference 3, on the more favorable signal-to-noise ratio obtainable with it as compared with a photo-cell, coupling resistor and amplifier. It alone makes possible the obtention of satisfactory records with photocurrents of 10^{-14} ampere or less.

5. The Signal Amplifier

The output current of the multiplier flows to ground through a large reactor of several thousand henries, self-tuned to 150 cycles, and the a.c. voltage developed across the same is applied to the grid of the input tube of a three-stage degenerative current feed-back amplifier, whose circuit is sketched in Fig. 6. To eliminate microphonic noise the whole unit is suspended on springs. The gain is varied by changing the feed-back admittance with the aid of two potentiometer gain controls. Between the resistance-coupled stages condenser-resistor circuits are inserted to suppress oscillations. The output circuit of the last stage is tuned for 150 cycles and contains a 2 : 1 step-down transformer which provides the input for the recorder drive ampli-

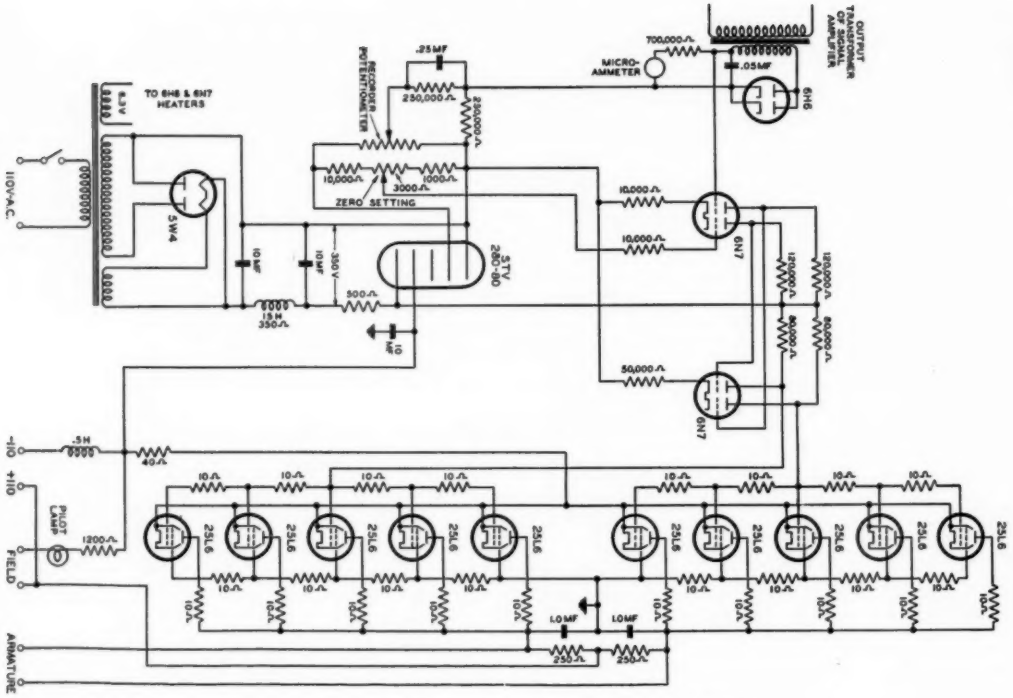

FIG. 7. Circuit diagram for the motor drive amplifier.

fier. The 280-volt plate supply is filtered as shown and shunted by a Stabilovolt glow tube to reduce fluctuations. In practice the gain is adjusted to give close to 35 volts transformer output on the peaks of the curves, as this corresponds to a full ordinate height on the record.

6. The Recorder Drive Amplifier

The output of the step-down transformer is rectified by a 6H6 double diode and applied to the input of the motor drive amplifier (Fig. 7) in the following manner: The d.c. signal generated over a 700,000-ohm resistor[4] is subtracted from half the voltage (divided by two $\frac{1}{4}$-megohm resistors) corresponding to the position of the pen on the recorder potentiometer (across which there is a drop of 70 volts derived from a Stabilovolt potential divider) and applied to one input grid of a three-stage class *A* d.c. push-pull resistance-coupled amplifier; the other input grid is adjusted permanently at a fixed voltage with respect to the negative end of the recorder potentiometer by the zero setting as shown. The last stage consists of five 25L6 screen grid tubes in parallel in each branch, whose filaments are connected in series and fed directly by the 110-volt a.c. line. Their output, shunted by two 250-ohm resistors, is fed directly to the armature of the motor driving the recorder head carrying the pen. The plate voltage as well as the motor field is supplied by the 220-volt d.c. line, whose negative terminal is joined to the cathodes and whose grounded midpoint is connected to the screen grids. A conveniently placed pilot light indicates whether the d.c. line is properly connected. The individual grids of the tubes are connected by resistors to suppress oscillations.

In this fashion a signal proportional to the difference in the input signal and that corresponding to the position of the point on the recorder rheostat is at all times fed to the armature of the motor; without further precaution this would cause the recorder head to overshoot

[4] A microammeter in series with this resistor is set in the front panel of the instrument, making it possible to read directly the rectified output signal of the signal amplifier.

its mark owing to inertia. Actually, by placing the $\frac{1}{4}$-megohm resistor shunted by a suitably dimensioned (0.25 μf) condenser in series with the potentiometer contact on the recorder head it is possible to advance the change in signal in the armature in such fashion that the motor comes to a dead stop at the proper position of the recorder head.

7. The Recording Mechanism

We thus, finally, arrive at the recording mechanism proper, which is sketched schematically in Fig. 8. The central portion consists of a frame, F, and bed-plate, B, for the graph paper (8×11 in.) on which the curves are to be traced. Over it moves the recorder arm, A, incorporating the recorder potentiometer on its lower side. The arm is anchored at one end, where it rolls on six rollers on the sides of two vertical V-shaped grooves. The carriage, P, bearing the recording pen and potentiometer contact moves in the same manner along the arm. The free end of the arm rolls on a single roller on a flat plate. The motion of the recorder arm, i.e., the motion along the wave-length scale, is controlled by a stranded phosphor-bronze cable, clamped to the arm by means of a thumb screw, T, facilitating zero adjustments, which is wound up over a pulley, P_1, on the spiral cam at the end of the shaft driving the prism table. The other end is kept taut by being wound up on a pulley, P_2, provided with a stiff inner spring.

The carriage is moved along the arm, on the other hand, by a phosphor-bronze cable whose two ends are fixed to a threaded pulley, P_3, at the anchored end of the arm and which passes over a plain pulley, P_4, at the free end of the same. The threaded pulley is rotated by a steel shaft of square cross section, along which it slides, forming a unit with the recorder arm. The shaft, in turn, is coupled by a worm gear to the amplifier-controlled motor, M_1. The speed of the latter is such that a full-scale deflection takes approximately one second.

The shape of the spiral cam, C_m (Fig. 9a), was first calculated, with the aid of the calibration curves for the monochromator, so as to give

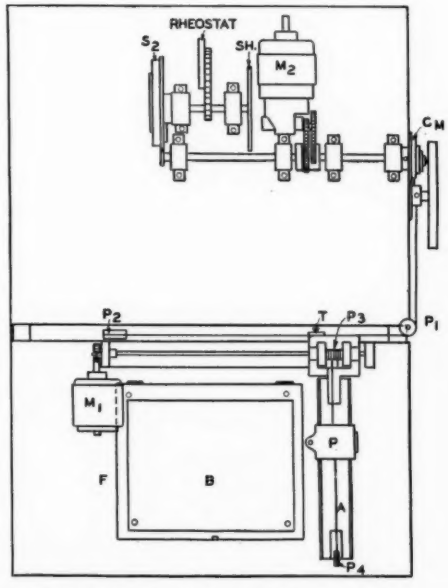

Fig. 8. Diagram of the recording mechanism.

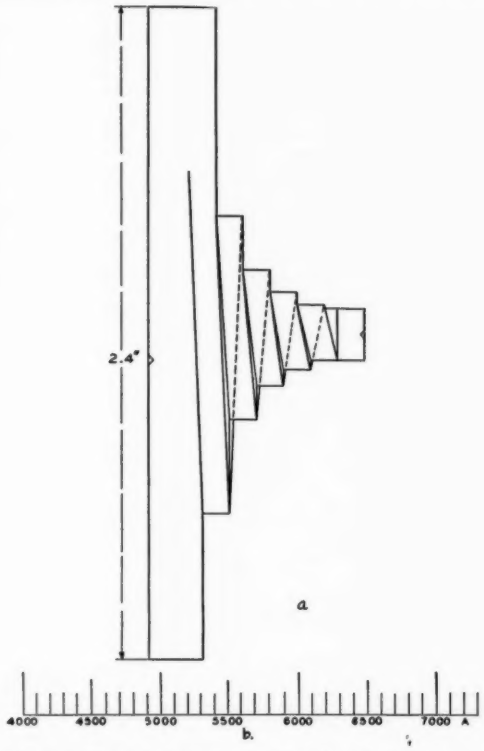

Fig. 9. The spiral cam and calibration of the wave-length axis.

equal distances of travel for equal wave-length intervals and then turned out of brass with the radius vector augmented by about $\frac{1}{8}''$ throughout. The grooves were filed by hand, checking the accuracy of the filing on the instrument continuously. A subsequent recording of equal wave-length intervals gave the result shown in Fig. 9b, which shows satisfactory, though not perfect, constancy throughout the scale.

The shaft geared to the prism table is coupled

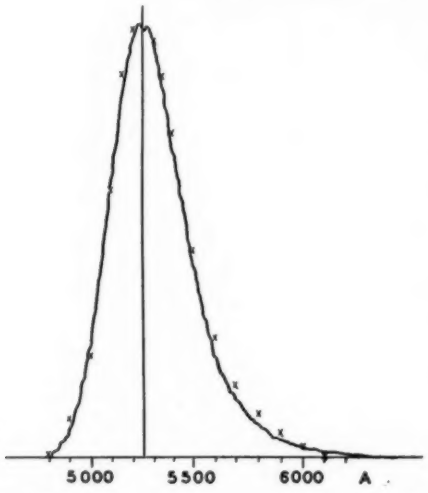

FIG. 10. Spectral response curve for green willemite.

by two chain drives, making possible a fast ($1\frac{1}{4}$ minutes for a complete record) and a slow (5 minutes for a record) movement, to the motor, M_2. The speed of the latter, in turn, is controlled by a rheostat in series with its armature current supply, the rheostat itself being coupled indirectly to the shaft. It is so dimensioned and arranged that the speed of motion of the recorder remains constant throughout the wave-length range, i.e., the speed is reduced in the region of low dispersion.

8. Performance of the Apparatus

As examples of the performance we show first, in Fig. 10, the spectral response of green willemite as obtained by point-by-point densitometer measurements on a plate taken with a Hilger quartz spectrograph (points indicated by crosses) and compare it with the record obtained with the present device. The agreement is seen to be satisfactory. The amplitudes were set equal at the peak of the curve. Another example, more characteristic of the normal employment of the apparatus, is given by Fig. 11, which shows the curves obtained for zinc beryllium silicate with one, two and four percent Mn added as activator, the heat treatment being the same throughout. These curves are obtained as follows: To begin with, the response of every one of the materials is measured in immediate succession at one or two wave-lengths, to establish the correct relative scales of the ordinates; thereafter, the curves for the several materials on the disk may be taken at leisure. Finally, they are replotted to the scale established by the original measurements on the same piece of graph paper, smoothing out eventual small oscillations, such as those shown on the record in Fig. 10.

If the curves obtained in this fashion are converted from units of energy to units of visual brightness by multiplication with the visibility curve, the areas under the resultant curves give a good measure of the relative visual brightness of the different samples; in fact, the values found in this manner agree normally with those obtained when the spectroradiometer is replaced by a Weston illuminometer within five percent.

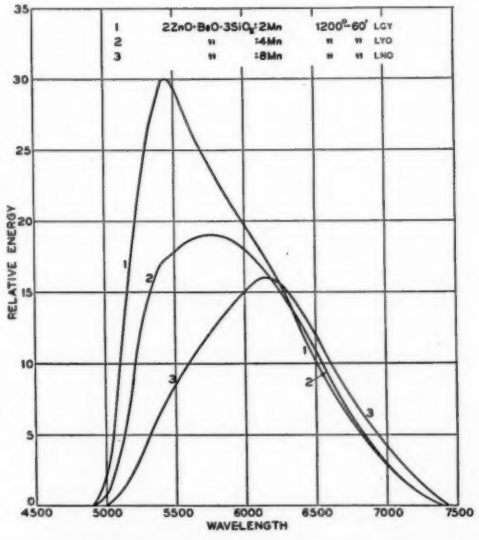

FIG. 11. Spectral response curves for zinc beryllium silicate with different percentages of manganese activator.

Thus, if a standard material, such as green willemite, whose absolute light yield is known, is included among the materials on the disk it becomes a relatively simple matter to convert the ordinates obtained into absolute units.

For the slit widths considered in Fig. 4 the resolution of the instrument is scarcely diminished by the recording mechanism, as the time required by the recording head to move the full distance of the ordinate scale corresponds to a motion along the wave-lengths scale of only 50A in the case of the high speed coupling of the wave-length axis and to 12A in the case of the low speed coupling.

As compared with any point-by-point or semi-automatic method of spectrum photometry, e.g., the taking of plates with a spectrograph and their measurement with a densitometer, the enormous gain in time obtained with the present instrument is obvious. As an automatic instrument it possesses, apart from high speed, the following advantages:

(a) Great sensitivity; satisfactory records may be made with a maximum input to the photocathode of only about 10^{-7} lumen[5] owing to the increase in the signal-to-noise ratio with the multiplier as compared with a photo-cell and thermionic amplifier. This is particularly important with cathodoluminescent materials as it reduces the likelihood of damaging them, or altering their response, by overloading.

(b) High amplifier stability owing to the use of negative feedback.

(c) Linear wave-length scale facilitating estimates of energy output.

(d) Uniform speed of recording for entire wave-length scale.

(e) Easy adjustment of all zeros and rigid connection between recording pen and potentiometer contact.

These, as well as other minor advantages which are evident from the text, should make the instrument a valuable aid in extending our knowledge of luminescence phenomena as well as in other fields requiring light measurements of a similar nature.

The instrument is a product of the cooperative efforts practically of the whole staff of the Electronics Research Laboratory. In particular, the author would like to acknowledge the assistance of Mr. A. W. Vance, who designed the amplifying system, and Mr. H. W. Leverenz, who adapted the instrument for luminescence research. Also, mention should be made of the work of Mr. I. E. Grosdoff, for the mechanical design; Dr. J. Van den Bouwhuysen, for the optical parts; and Mr. L. E. Flory, for the demountable vacuum part of the system, and Dr. E. G. Ramberg, for assistance in the preparation of this paper.

[5] With a wide slit (1.00 mm) this corresponds to a light emission of the sample of about 10^{-3} lumen/cm^2.

Laws and Corollaries of the Black Body

FRANK BENFORD
Research Laboratory, General Electric Company, Schenectady, New York
(Received July 21, 1938)

THE physicist and the engineer are apt to view the same phenomena from different angles and to formulate their working equations in different manners. This divergence extends even to such a fundamental of science as the black body or Planckian radiator. The physicist usually disregards the efficiency with which radiation is generated, while to the engineer the matter of efficiency may be of the greatest importance. For many radiation problems, while they are still in the hands of the physicist, the interest is only in the relative amounts of energy in various parts of the spectrum. The same problem, when it reaches the stage where it is turned over to the engineer, must be reconsidered from the standpoint of both input and output. Black body literature has been almost completely monopolized by the physicist, and in this paper some equations familiar to the physicist are combined to give expressions that perhaps may be better adapted for some physical research and for engineering applications. Accordingly, the characteristics of the black body are in this paper first presented in terms of one square centimeter of radiating surface, as is customary in physics, and then in terms of efficiency of generation, which is more in the way of thinking of the engineer.

The values of the physical constants C_1 and C_2 here employed are from Birge,[1] and the indirect values are used in preference to the experimental values. The erg sec.$^{-1}$ of Birge has been converted into microwatts, as this unit, it seems to the writer, is more directly applicable in the problems of both the physicist and the engineer.

The micron, $\mu(=10^{-6}$ meter), is used as the unit of wave-length, λ, and the temperature, T, is, of course, in degrees Kelvin. Where zones of the spectrum are used in the equations the width of zone is 0.01μ. This zone width divides the visible spectrum into thirty parts, and this spacing is close enough for most analytic purposes.

(1) Planck's radiation equation can be written in the specific form

$$J_\lambda=\frac{3.697\cdot 10^8}{\lambda^5[\exp(14317/\lambda T)-1]}$$ microwatts per cm^2 per 0.01μ zone of spectrum. (1)

This equation is for a surface that is a perfect radiator, that is, one that radiates the theoretical maximum and that gives a cosine distribution in space about an element of surface. Its optical analog is the lumen, which is power evaluated according to its ability to cause the sensation of light.

(2) The intensity of radiation, in a normal direction, from one square centimeter of plane surface is

$$\frac{J_\lambda}{d\omega}=\frac{1.176\cdot 10^8}{\lambda^5[\exp(14317/\lambda T)-1]}$$ microwatts per cm^2 per steradian per 0.01μ zone of spectrum. (2)

To obtain the intensity of radiation in a direction making an angle θ with the normal, the right-hand member of Eq. (2) is to be multiplied by $\cos\theta$. The optical analog of this unit is the candle, and the rules for computing irradiation are identical with those used for computing illumination.

(3) If a complete enclosure has a uniform temperature T, on the inner or radiating surface, then each cubic centimeter of space within the enclosure contains

$$\psi=\frac{4.933\cdot 10^{-2}}{\lambda^5[\exp(14317/\lambda T)-1]}$$ microwatts per cm^3 per 0.01μ zone of spectrum. (3)

If the enclosure is incomplete, the power in a cubic centimeter of space is proportional to the solid angle subtended by the enclosing walls, measured from the center of the space in question.

[1] Raymond T. Birge, Phys. Rev. Supp. 1, 1 (1929).

(4) The first differential with respect to wave-length λ of any of the above equations yields a maximum power at some wave-length λ_m.

$$\frac{d}{d\lambda}\frac{1}{\lambda^5[\exp(14317/\lambda T)-1]}=0.$$

This operation gives Wien's displacement law

$$\lambda_m T = 2883.6 \text{ micron-degrees}, \quad (4)$$

but the numerical value depends not upon Wien's radiation equation, but upon its successor, Planck's radiation law.

(5) The wave-length λ_m of maximum spectral power varies inversely as the temperature

$$\lambda_m = 2883.6/T \text{ microns}. \quad (5)$$

(6) The wave-length λ_m of maximum power is of particular interest as it makes a convenient point of reference on the wave-length scale.

$$J_{\lambda_m} = 1.303 \cdot 10^{-11} T^5 \text{ microwatts per cm}^2 \text{ per } 0.01\mu \text{ zone of spectrum.} \quad (6)$$

(7) All black body radiation curves have the same form, and by a proper choice of scales of ordinates and abscissae any two curves for different temperatures can be brought into exact coincidence throughout. One curve can therefore represent all temperatures.

In Fig. 1 the scale of wave-lengths is so chosen that λ_m falls at one on the scale of abscissae. The ordinate marked three, for example, can be used to find the relative power at $3\lambda_m$ for any temperature. To reduce the ordinates to absolute scale for any temperature, they are to be multiplied by a factor found by using Eq. (6).

(8) The total radiation from a black body varies as the fourth power of the temperature.

$$\int_0^\infty J_\lambda d\lambda = 5.7139 \cdot 10^{-6} T^4 \text{ microwatts per cm}^2. \quad (7)$$

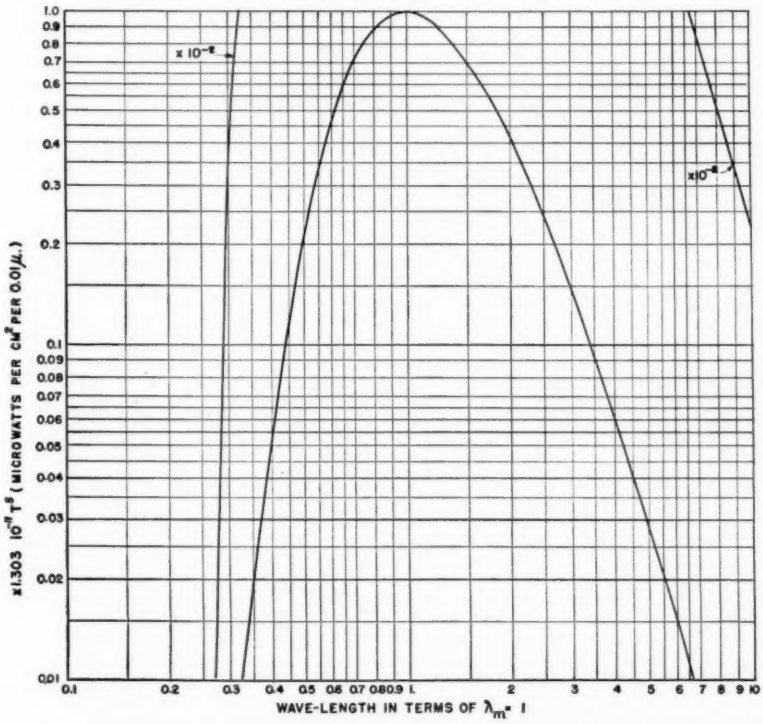

FIG. 1. The black body distribution of energy plotted to a wave-length scale making λ_m equal to 1, and J_λ equal to 1 at the maximum. The curve can be reduced to absolute scale for any temperature by using Eqs. (5) and (6).

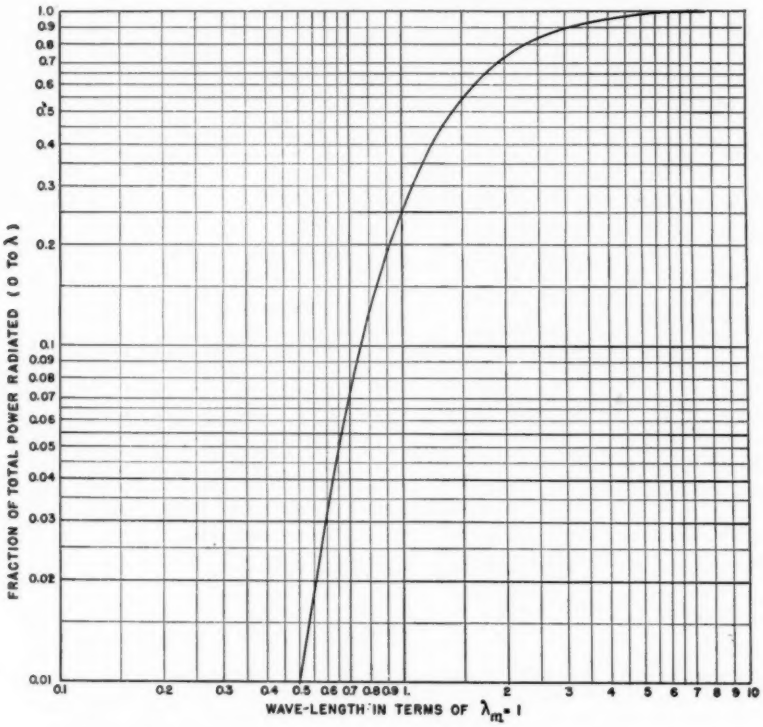

FIG. 2. The black body summation curve giving the energy from $\lambda=0$ up to any wave-length, given in terms of $\lambda_m=1$.

This is usually expressed as

$$J=\sigma T^4 \tag{8}$$

where σ is the Stefan-Boltzmann constant.

(9) All power-summation curves (integration under a distribution curve) of the black body from $\lambda=0$ to $\lambda=\infty$ have the same form and may be represented by the same curve. In Fig. 2 the scale of abscissae is chosen so that λ_m is at one, and the other wave-lengths are therefore given in terms of λ_m. The curve can be reduced to absolute scale by using Eq. (5) to find λ_m for any temperature T, and the scale of ordinates is determined by the use of Eq. (6) for J_{λ_m}.

(10) It has been found by carrying out the integration that the radiation from $\lambda=0$ to $\lambda=\lambda_m$ is numerically one-quarter of the total radiation.

$$\int_0^{\lambda_m} J_\lambda d\lambda = \tfrac{1}{4}\int_0^{\infty} J_\lambda d\lambda. \tag{9}$$

This simple relation of one-quarter* of the total radiation at wave-lengths less than λ_m to three-quarters at wave-lengths greater than λ_m gives a quick way of mentally estimating the distribution of power at any given temperature.

(11) The efficiency of production of radiation of any selected wave-length λ can be found by combining Eq. (1) and Eq. (8)

$$\frac{J_\lambda}{J}=\frac{6.471\cdot 10^{13}}{\lambda^5[\exp(14317/\lambda T)-1]T^4}\ \text{numeric.} \tag{10}$$

It is seen that the efficiency does not bear a simple relation to the temperature, as T appears as both a factor and an exponent in the denominator of Eq. (10).

(12) Another type of maximum is found by setting the derivative of Eq. (10) with respect to

* A computation of the integral shows the factor to lie between 0.250000 and 0.250056.

T equal to zero.

$$\frac{d}{dT}\frac{1}{\lambda^5[\exp(14317/\lambda T)-1]T^4}=0.$$

The solution of the equation is

$$\lambda_e T_e = 3652 \text{ micron-degrees.} \qquad (11)$$

This solution shows that at any selected wave-length λ_e there is an optimum temperature T_e that gives a maximum efficiency in producing radiation of wave-length λ_e.

In Fig. 3 is shown a group of constant-energy curves for temperatures from 2000°K to 3400°K. The area under all curves, when they are extended sufficiently far into the infra-red, is constant, as must be the case because the power is constant for all temperatures. The 2000°K-curve has a maximum near 1.4μ, but the 2600°K-curve has a higher ordinate at the same wave-length. The latter temperature therefore gives a higher generating efficiency for 1.4μ.

In Fig. 3 a locus is drawn through the maxima of the various individual curves. An enveloping curve is also drawn tangent to the group of radiation curves and this envelope is some 11.6 percent higher than the locus of maxima for the individual curves at all ordinates. The maximum point of an individual radiation curve is the maximum as the physicist ordinarily considers the curve, but when the radiation is judged by the ratio of zonal output to total input the best efficiency is found to be at a point on the curve at a wave-length longer than λ_m of Eq. (4).

As an illustration of the use of Eq. (11) in place of Eq. (4), consider the problem of therapeutics where maximum penetration of energy into the body is desired, but the heat toleration of the skin limits the power that can be used. The maximum penetration is at about 1.1μ. The temperature giving a maximum at 1.1μ is 2620°K according to Wien's displacement law. But, by using Eq. (11), a temperature of 3330°K will be found to supply 11.6 percent more energy effective in the deep tissues for equal amounts of energy incident upon the skin.

(13) The optimum temperature T_e for maximum efficiency at wave-length λ_e varies inversely as the wave-length.

$$T_e = 3652/\lambda_e \text{ degrees.} \qquad (12)$$

(14) The temperature to give an engineering maximum at any wave-length is 27.6 percent higher than the temperature for a physical maximum.

$$T_e = 1.276T \text{ degrees} \qquad (13)$$

where T has been determined by the displacement law. The same ratio holds between λ_e and λ_m for a fixed temperature.

(15) The power in a 0.01μ zone of the spectrum at wave-length λ_e and optimum temperature T_e, is, for a total output of one watt

$$J\lambda_e = 2.020T_e \text{ microwatts.} \qquad (14)$$

The efficiency, therefore, varies directly as the optimum temperature.

Equation (14) is an approximation that is good so long as the tangent of the 0.01μ zone does not depart too widely from the radiation curve. We may take 10,000°K as the upper limit of temperatures encountered in practice. Here λ_m is 0.2883μ and λ_e is 0.3652μ, and a change of 0.005μ at either point does not represent more than a two percent change in wave-length. From either Fig. 1 or Fig. 3 it is evident that a departure of $\pm$ two percent in wave-length at 1.276λ_m does not give a large difference between the areas

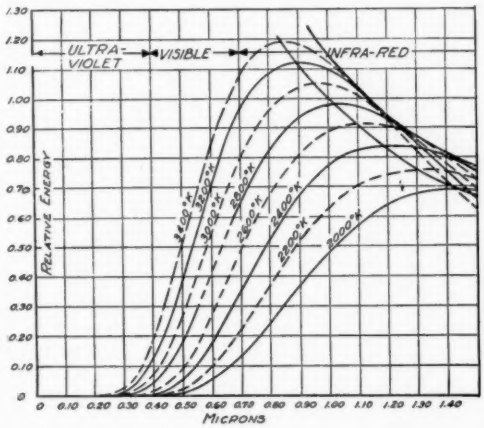

FIG. 3. The distribution curves are for equal energies radiated at temperatures between 2000°K and 3400°K. The equilateral hyperbola passing through the maxima of the curves gives Wien's displacement relation, while the parallel hyperbola tangent to the family of curves gives the conditions for maximum efficiency at any wave-length.

under the curve and under the tangent, and the error in Eq. (14) is therefore small. At lower, and more usual, temperatures the error becomes vanishingly small. However, if stellar temperatures of say 1,000,000°K are dealt with the use of Eq. (14) would indicate a two-watt output from a one-watt input—an obvious absurdity.

The same limitations apply to the other equations involving the 0.01μ spectral zone.

(16) The radiation from $\lambda=0$ to $\lambda=\lambda_e$ is 41.8 percent of the total radiation

$$\int_0^{\lambda_e} J_\lambda d\lambda = 0.418 \int_0^{\infty} J_\lambda d\lambda. \qquad (15)$$

A comparison of Eq. (15) with Eq. (9) shows that approximately one-sixth of the total power at any temperature lies between the λ_m of the physicist and the λ_e of the engineer.

Radiation Laws Describing the Emission of Photons by Black Bodies

A. G. WORTHING
Physical Laboratory, University of Pittsburgh, Pittsburgh, Pennsylvania
(Received November 7, 1938)

Photon Laws for Black Body Radiation: Starting with a relation showing the temperature volume changes for black body radiation which is undergoing an adiabatic change, it is shown how photon laws which correspond one by one with known radiant energy laws may be derived. In all instances, excepting two, namely $\lambda_m'T=$const and $\nu_m'T=$const, the photon relations differ from the corresponding radiant energy relations chiefly by having a power of T decreased by one, a power of λ increased by one, or a power of ν decreased by one. The entropy of black body radiation is strictly proportional to the number of photons involved. *Table of Black Body Radiation Constants:* A table includes values in common units for the collective groups of constants entering the various photon and radiant energy equations mentioned in the paper.

HAAS and Guth[1] recently showed that the rate of emission of photons by a black body varies as the third power of its temperature. The procedure is direct and simple, yet strangely, with all the attention which has been given to the quantum, no one, to the author's knowledge, had published the fact previously. Although we usually are concerned with the energy content of radiation, there are many occasions when the photon content may be of value, even of greater value. Illustrations occur in connection with photoelectric and photochemical processes where, because of a more nearly constant efficiency of production of effects, activities are sometimes viewed as depending quantitatively on the number of photons rather than on the amount of radiant energy involved. It seems pertinent, therefore, to consider the laws of black body radiation from this somewhat new standpoint.

The procedure of Haas and Guth seems to have been that of adopting Planck's universally accepted spectral distribution law, expressing the relation in terms of photons by means of the basic quantum equation

$$\epsilon=h\nu=hc/\lambda, \tag{1}$$

and integrating the expression to obtain the total rates of emission in terms of photons per unit of time. This method might be easily extended to yield the other common radiation laws.

On the other hand, it is interesting to see what may be deduced regarding photon laws following generally the procedure which occurred historically in the development of radiant energy laws. Such is the procedure of this paper.

Radiant Energy Laws

For comparison with the photon laws, a convenient collection of black body radiation formulae and constants, are given in Table II (see Table I for terminology) as Eqs. (2) to (12) inclusive.

Relations involving $\mathfrak{B}$ steradiancy (analogous to brightness) and spectral steradiancies $\mathfrak{B}_\lambda$ and $\mathfrak{B}_\nu$ may be obtained from equations involving $\mathfrak{R}$, $\mathfrak{R}_\lambda$ and $\mathfrak{R}_\nu$ by dividing both sides of their respective equations by the common factor "π steradians." Similar relations may also be derived for photons, but they will not be considered in this paper.

Total Photon Radiation Laws

We start with an evacuated, spherical enclosure with perfectly reflecting walls, which is filled with black body radiation. We imagine a uniform adiabatic expansion or contraction to take place and obtain the well-known relations,[2]

$$\frac{u_\lambda d\lambda}{u_{\lambda 0}d\lambda_0}=\frac{u_\nu d\nu}{u_{\nu 0}d\nu_0}=\left(\frac{r_0}{r}\right)^4=\left(\frac{T}{T_0}\right)^4 \tag{13}$$

where r represents the radius of the enclosure and the subscript $(_0)$ an initial or standard state.* The

[1] A. E. Haas and E. Guth, Phys. Rev. **53**, 324(A) (1938); also A. E. Haas, J. Opt. Soc. Am. **28**, 167 (1938).

[2] F. K. Richtmyer, *Introduction to Modern Physics* (McGraw-Hill), pp. 206–10.

* For the symbols and terminology in this equation and elsewhere throughout the paper, see Tables I and II.

TABLE I. *Symbols, quantities and units.*

SYMBOL	QUANTITY	COMMON UNIT	SYMBOL	QUANTITY	COMMON UNIT
λ	Wave-length	μ	$\mathfrak{R}_\nu$	Radiancy per unit frequency interval	erg/(cm² sec. vib./ sec.)
ν	Frequency	vibration/sec.	N	Photon emission rate per unit area	photon/(cm² sec.)
T	Temperature	$K°$	N_λ	Photon emission rate per unit area and unit wave-length interval	photon/(cm² sec. μ)
h	Planck's constant	erg sec.	N_ν	Photon emission rate per unit area and unit frequency interval	photon/(cm² sec. vib./sec.)
k	Boltzmann gas constant for a single molecule	erg/K°	c_2	Second radiation constant	μ K°
u	Radiant energy density	erg/cm³	λ_m	Wave-length at which, for a given T, $\mathfrak{R}_\lambda$ is a maximum	μ
u_λ	Radiant energy density per unit wave-length interval	erg/(cm³ μ)	λ_m'	Wave-length at which, for a given T, N_λ is a maximum	μ
u_ν	Radiant energy density per unit frequency interval	erg/(cm³ vib./sec.)	ν_m	Frequency at which, for a given T, $\mathfrak{R}_\nu$ is a maximum	vib./sec.
C	Photon concentration	photon/cm³	ν_m'	Frequency at which, for a given T, N_ν is a maximum	vib./sec.
C_λ	Photon concentration per unit wave-length interval	photon/(cm³ μ)	T_m	Temperature for the maximum spectral efficiency of production of radiant energy at wave-length λ	K°
C_ν	Photon concentration per unit frequency interval	photon/(cm³ vib./sec.)	T_m'	Temperature for the maximum spectral efficiency of photons production at wave-length λ	K°
s	Entropy density	erg/(cm³ K°)	λ_e	Effective wave-length for the total radiation	μ
σ	Stefan-Boltzmann constant for radiant energy	erg/(cm² sec. K°⁴)	ν_e	Effective frequency for the total radiation	vib./sec.
σ'	Stefan-Boltzmann constant for photons	photon/(cm² sec. K°³)			
a	Constant of the fourth power law relating to radiant energy density	erg/(cm³ K°⁴)			
a'	Constant of the third power law relating to photon concentration	photon/(cm³ K°³)			
$\mathfrak{R}$	Radiancy	erg/(cm² sec.)			
$\mathfrak{R}_\lambda$	Radiancy per unit wave-length interval	erg/(cm² sec. μ)			

fact that is particularly significant is that T varies inversely with r.

On the assumption that, in the adiabatic process, the photons or wave trains, whichever view one adopts, are neither created nor destroyed but changed to photons or wave trains of different frequencies or wave-lengths, we must conclude that the photon concentration in the enclosure varies inversely as r^3 and, therefore, directly as T^3. We therefore write

$$C = a'T^3, \tag{2'}$$

$$N = \sigma'T^3. \tag{3'}$$

The values of a' and σ' are obtained by integration from the distribution equations which are considered later. In addition to the one less power for T in (2') and (3') than occurs in (2) and (3), it is interesting to note that at all temperatures the photon concentration is directly proportional to the entropy density (see Eq. (4)). As it were, each photon carries its own entropy in enclosures where the radiation is in equilibrium.

PHOTON DISPLACEMENT LAWS

Returning to the evacuated, spherical enclosure and the relations of (13), we obtain at once with the aid of (1), the following photon-concentration relations,

$$\frac{C_\lambda d\lambda/\lambda}{C_{\lambda 0} d\lambda_0/\lambda_0} = \frac{C_\nu d\nu}{C_{\nu 0}\nu_0 d\nu_0} = \left(\frac{r_0}{r}\right)^4 = \left(\frac{T}{T_0}\right)^4. \tag{14}$$

Following the procedure commonly used in deriving Wien's laws we obtain in succession the general relations

$$C_\lambda = T^4 f_1'(\lambda T), \tag{5'}$$

$$C_\nu = T^2 f_2'(\nu/T), \tag{6'}$$

and the special relations,

$$\lambda_m' T = \text{const.}, \tag{7'}$$

$$\nu_m'/T = \text{const.} \tag{8'}$$

In (5') and (6') the powers of T are one less than in the corresponding equations (5) and (6). Corresponding to (7) and (8), we have identical forms in (7') and (8'), though the values of the constants differ. In consequence the wave-length for the maximum of the radiant energy curve is about 0.8 that of the corresponding photon curve (Fig. 1), while the frequency for the maximum of the radiant energy curve is about 1.8 times that of the corresponding photon curve.

Given a curve showing the photon distributions for a black body at one temperature, relations (5') and (6') may be used just as the corresponding Wien laws are used, to obtain distributions for other temperatures.

PHOTON SPECTRAL DISTRIBUTION LAWS

As derived by Planck, the law which bears his name was deduced on a basis of counting photons. This applies also to the constants $8\pi hc$

and $8\pi h/c^3$ of (9) and (10) which appear in their exact forms as a result of the requirement that the equation should reduce, for conditions where λT is large in comparison with hc/k, to the Rayleigh-Jeans equation which also was built up on concepts of wave trains or photons. Most, if not all, derivations of the Planck equations, (9) to (12) normally lead first to the corresponding photon relations (9′) to (12′),—the connecting link being Eq. (1). As with the relations already considered, we have here similar corresponding photon and radiant energy equations which differ chiefly by a power of one, this time in the corresponding powers of λ or ν but not T.

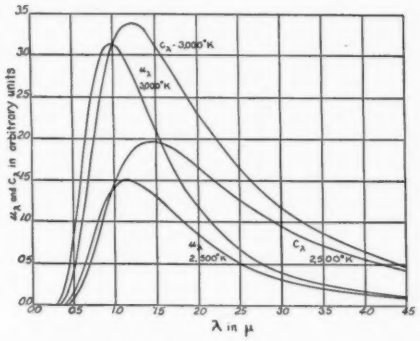

FIG. 1. Curves showing, for black body cavities at 3000°K and 2500°K, spectral energy density, u_λ, and spectral photon concentration, C_λ, distributions as functions of wave-length.

SPECTRAL PHOTON DISTRIBUTION CURVES

Data for curves of this type may be rather easily obtained from published data[3] which are normally intended for the construction of similar spectral distribution curves for radiant energy. Appropriate pairs of equations from (9) to (12)

[3] *International Critical Tables*, Vol. 5.

TABLE II. *Equations and values for the collective groups of constants enclosed in* [ ].

No.	EQUATION	VALUE OF GROUP OF CONSTANTS
	c	*2.99776×10¹⁰ cm/sec.
	$\sigma=[2\pi^5k^4/15c^2h^3]$	*5.735×10⁻⁵ erg/(cm² sec. K°⁴)
	$c_2=[hc/k]$	*1.4320 cm K°
	h	6.577×10⁻²⁷ erg sec.
	k	1.377×10⁻¹⁶ erg/(molecule K°)
	RADIANT ENERGY LAWS	
2	$u=aT^4=[8\pi^5k^4/15c^3h^3]T^4$	7.652×10⁻¹⁵ erg/(cm³ K°⁴)
3	$\mathfrak{R}=\sigma T^4=[2\pi^5k^4/15c^2h^3]T^4$	5.735×10⁻⁵ erg/(cm² sec. K°⁴)
4	$s=[32\pi^5k^4/45c^3h^3]T^3$	1.0203×10⁻¹⁴ erg/(cm³ K°⁴)
5	$u_\lambda=T^5f_1(\lambda T)$	
6	$u_\nu=T^3f_2(\lambda T)$	
7	$\lambda_mT=[(hc/k)/4.965]$	2884 μ K°
8	$\nu_m/T=[2.8214k/h]$	5.906×10¹⁰ 1/(sec. K°)
9	$u_\lambda=[8\pi hc]1/\lambda^5(e^{hc/\lambda kT}-1)^{-1}$	4.955×10⁻¹⁵ erg cm
10	$u_\nu=[8\pi h/c^3]\nu^3(e^{h\nu/kT}-1)^{-1}$	6.136×10⁻⁵⁷ erg sec.⁴/cm³
11	$\mathfrak{R}_\lambda=[2\pi hc^2]1/\lambda^5(e^{hc/\lambda kT}-1)^{-1}$	3.714×10⁻⁵ erg cm²/sec.
12	$\mathfrak{R}_\nu=[2\pi h/c^2]\nu^3(e^{h\nu/kT}-1)^{-1}$	4.598×10⁻⁴⁷ erg sec.³/cm²
18	$\lambda T_m=\lambda_eT=[hc/3.9207k]$	3652 μ K°
	PHOTON LAWS	
2′	$C=a'T^3=[16\pi k^3/1.2021c^3h^3]T^3$	20.58 1/(cm³ K°³)
3′	$N=\sigma'T^3=[4\pi k^3/1.2021c^2h^3]T^3$	1.542×10¹¹ 1/(cm² sec. K°³)
5′	$C_\lambda=T^4f_1'(\lambda T)$	
6′	$C_\nu=T^2f_2'(\nu T)$	
7′	$\lambda_m'T=[(hc/k)/3.9207]$	3652 μ K°
8′	$\nu_m'/T=[1.5936h/k]$	3.300×10¹⁰ 1/(sec. K°)
9′	$C_\lambda=[8\pi]1/\lambda^4(e^{hc/\lambda kT}-1)^{-1}$	25.133
10′	$C_\nu=[8\pi/c^3]\nu^2(e^{h\nu/kT}-1)^{-1}$	9.3290×10⁻³¹ sec.³/cm³
11′	$N_\lambda=[2\pi c]1/\lambda^4(e^{hc/\lambda kT}-1)^{-1}$	1.8836×10¹¹ cm/sec.
12′	$N_\nu=[2\pi/c^2]\nu^2(e^{h\nu/kT}-1)^{-1}$	6.9917×10⁻²¹ sec.²/cm²
18′	$\lambda T_m'=[hc/(3.9207k)]$	3652 μ K°

* These experimentally determined values taken together form the basis for the other, computed constants. Unfortunately, the values for σ and c_2 vary somewhat from those obtained with the aid of generally accepted formulae using other observed data. While in the table the number of places used in expressing the values for the bracketed constants are those to be expected, were the values given for c_2 and σ accepted, it is understood that they possess actual uncertainties of the order of ½ to 1 percent. How to shift from the values reported here to others based on other values for σ and c_2 will be apparent to the user.

and (9′) to (12′) yield

$$N_\lambda = (\lambda/hc)\mathcal{R}_\lambda \tag{15}$$

or

$$N_\nu = (1/h\nu)\mathcal{R}_\nu. \tag{16}$$

Using listed values of $\mathcal{R}_\lambda = f(\lambda)$ for 3000°K, for instance, one merely multiplies each value of $\mathcal{R}_\lambda$ by λ/hc, or by λ, if only relative values are desired, to obtain the desired N_λ for 3000°K.

Given the photon distribution curve for temperature T_0, one readily obtains a similar curve for temperature T with the aid of the displacement laws. Thus at corresponding λ's given by

$$\lambda = (T_0/T)\lambda_0, \tag{17}$$

we have

$$\frac{C_\lambda}{C_{\lambda 0}} = \frac{N_\lambda}{N_{\lambda 0}} = \left(\frac{T}{T_0}\right)^4. \tag{17′}$$

In Fig. 1, spectral radiant energy and photon distributions for 2500°K and 3000°K are given. They show in what ways the two systems of curves are alike and also different.

A curve showing $\int_0^\lambda N d\lambda = f(\lambda T)$ would seem to be quite helpful in the application of photon laws. It is hoped that such a curve or better a table giving values of the integral for various combinations of λ and T may be published in this journal under other auspices in the near future.

New λT Relations for Black Body Radiation*

A. G. WORTHING
Physical Laboratory, University of Pittsburgh, Pittsburgh, Pennsylvania
(Received November 7, 1938)

When the temperature of a black body is such that the maximum spectral efficiency of production of radiant energy occurs at a given wave-length there also occurs at that wave-length, both the maximum spectral rate of production and the maximum spectral efficiency of production of photons. The particular wave-length involved is the effective wave-length for the total radiation, which is defined as the wave-length at which, for a given temperature, the percentage rate of increase in spectral radiancy with temperature is the same as for the total radiation from the black body source.

BENFORD[1] has pointed out a new relation embodied in Wien's generalized displacement law, which has special interest for those concerned with the utilization of radiation. It is similar† to (7). But whereas (7) specifies the wave-length-temperature relation for which the spectral radiancy is a maximum, Benford's relation,

$$\lambda T_m = 3652\mu\text{K}^\circ, \tag{18}$$

specifies the condition for which the spectral efficiency of production, $\mathcal{R}_\lambda/\mathcal{R}$, is a maximum, and is obtained by equating to zero the derivative $d/dT(\mathcal{R}_\lambda/\mathcal{R})$. In practice it is likely to be used to determine the temperature T_m for a radiator at which, for a given total energy input and a given region, there will be a maximum output of radiation.

An exactly similar relation for photon emission is obtained from a similar process of maximizing the corresponding ratio $N_\lambda/\mathcal{R}$, thus

$$d/dT[A/T^4(e^x-1)]=0, \tag{19}$$

where A is made up of those parts of the right-hand members of (3) and (11′) which do not involve T, and x is the ratio $hc/\lambda kT$. Following standard procedure this yields

$$1-x/4-e^{-x}=0, \tag{20}$$

whence $x=3.9207$ (21)

and $\lambda T_m'=hc/(3.9207k)=3652\mu\text{K}^\circ.$ (18′)

This equation likewise specifies the wave-length-temperature relation associated with a maximum spectral efficiency of photon production. It turns out, somewhat surprisingly, that the constant of (18′) is the same as the constants of (7′) and (18). Consideration, however, of another λT relation, shows why this is true for the relations involving spectral efficiencies of production. This other relation is

$$\lambda_e T=hc/(3.9207k)=\lambda T_m \tag{18}$$

and is obtained by straightforward procedure from the following relation

$$\left[\frac{T}{\mathcal{R}_\lambda}\frac{dR_\lambda}{dT}\right]_{\lambda_e}=\frac{T}{\mathcal{R}}\frac{d\mathcal{R}}{dT}=4, \tag{22}$$

which is the defining equation for the effective wave-length for the total radiation from a black body, λ_e, that is, the wave-length at which the spectral radiancy experiences the same percentage change with temperature as is experienced by the total radiation. Now, with a spectral radiancy curve such as one of those of Fig. 1 in mind, consider for different wave-lengths the effect of a change in temperature. At wave-lengths less than λ_e, $[T/R_\lambda \times dR_\lambda/dT]_\lambda$ is greater than 4 and something is to be gained in the efficiency of radiant energy or of photon production by an increase in temperature. Evidently at wave-lengths greater than λ_e, the reverse holds true. Only at wave-length λ_e are there no gains or losses in these efficiencies by changes in tem-

* This paper has so much in common with the same author's preceding paper in this journal, entitled, "Radiation Laws Describing the Emission of Photons by Black Bodies," that the equations used here are numbered to follow those in the preceding paper. References to the equations and tables of that paper are made as though together the two formed a single paper. Ed.

[1] Frank Benford, "Laws and Corollaries of the Black Body," J. Opt. Soc. Am. **29**, 92 (1939).

† For the symbols and terminology in this equation and elsewhere throughout the paper, see Tables I and II of the previous paper.

peratures. Hence the expected agreement with regard to the constants of (18) and (18′). That the constant of (7′) should be the same is not so apparent.

Treatment of $N_\nu/\mathfrak{R}$, in the manner suggested above for $N_\lambda/\mathfrak{R}$, to obtain the maximum efficiency of photon production for a given frequency leads to

$$\nu/T_m' = 3.9207k/h = 8.2077\times10^{10}1/(\text{sec. K}^\circ). \quad (23)$$

The frequency ν associated with a given T_m', as indicated by the numeric 3.9207 is just that for which the wave-length is the λ of (18′).

The ratio N_λ/N might be treated in a manner similar to that given $N_\lambda/\mathfrak{R}$, but there seems to be no particular advantage in so doing.

Book Review

Charles Fabry: Oeuvres Choisies Publiées à L'Occasion de Son Jubilé Scientifique. Pp. 689+vi. Gauthier-Villars, Paris, France, 1938.

In 1937, a committee was appointed to prepare the program of a scientific jubilee in honor of M. Charles Fabry, who had reached the age of seventy and was retiring from his professorship at the University of Paris. The celebration was held December 3, 1937, at the Sorbonne under the chairmanship of M. Emile Picard, Permanent Secretary of the French Academy of Sciences. It was attended by a large number of Professor Fabry's colleagues, friends and former students. Congratulatory addresses were presented by numerous men of science and of affairs in France, as well as from various scientific bodies throughout the world. These addresses are collected in a little volume of 96 pages published by Gauthier-Villars.

At the conclusion of the celebration, it was announced that through the generosity of Professor Fabry's friends, and with the aid of contributions from certain national research funds, a volume would be prepared under Professor Fabry's editorship, which would bring together a selected list of his more important publications during his fifty years of activity as a scientist. The present volume is the result.

In a brief preface, Professor Fabry states that he has taken occasion to correct a few mistakes in the original papers, to make some condensations and here and there to add a short explanatory comment.

The papers are arranged in seven sections as follows. I. Interference and Its Applications. II. Miscellaneous Problems in Optics. III. Electricity. IV. Photometry and the Measurement of Radiation. V. Astrophysics and Geophysics. VI. General Papers. VII. Complete list of publications (301 titles).

Professor Fabry's contributions to the science of physics during the last half century, particularly to optics and its various branches, are so well known that there is no need to comment at length on the fundamental nature of the papers and subjects reproduced in this volume. The first paper on "Interference and Its Applications" was published in the *Journal de Physique*, January, 1891, in collaboration with MM. J. Macé de Lépinay, under the title, "Théorie Générale de la Visibilité des Franges D'Interférence." The last paper, selected for inclusion in this section, was published in *Comptes rendus de l'Académie des Sciences*, Volume 193, page 99 (1931), under the title "Sur un Niveau Interférentiel sans Bulle d'Air." In this space of forty years, Professor Fabry's contributions to this subject may be designated as almost monumental. Although they represent researches published in sequence as they were completed, they nevertheless, as collected and edited in this volume, provide an extremely lucid and complete text for those who wish to familiarize themselves with this fascinating branch of physical optics.

The section on Photometry and the Measurement of Radiation begins with "A Practical Solution of the Problem of Heterochromatic Photometry" (1903) and concludes with a paper on "Photometric Nomenclature" (1932). While this section of the book does not contain as many pages as the section on interference, Professor Fabry's contributions to this subject have laid much of the foundation for its future development.

The many friends and scientific colleagues of Professor Fabry in America will welcome the appearance of this volume, not only for its scientific worth but because of our high regard for him as a man and a scientist. He has been a member of the Optical Society of America almost since its organization. He was elected honorary member of the Society, October 19, 1933. He was guest of honor at the Ninth Annual Meeting of the Society held in Cambridge, Massachusetts, October 23–25, 1924, at which time he presented before the Society a paper on "Heterochromatic Photometry."[1] He is also a member of the Illuminating Engineering Society.

This volume is destined to become one of the treasured classics in the literature of science for, as Sir William Bragg said in his congratulatory address on behalf of the Royal Society of London, Professor Fabry's researches are "not only of the greatest value to students of pure science; they have had a profound effect over a much wider field and have contributed in no small measure to national efficiency and prosperity."

F. K. RICHTMYER

[1] C. Fabry, J. Opt. Soc. Am. and Rev. Sci. Inst. **10**, 521 (1925).